Study of pump-delivered insulin propagation into the subcutaneous tissue

Pauline Jacquemier

Sorbonne Université

Ecole doctorale ED394

Centre Explor! Air Liquide Healthcare

IMMEDIAB - Institut Necker Enfants Malades INSERM U1151

Study of pump-delivered insulin propagation into the subcutaneous tissue

Etude de la propagation sous-cutanée d'insuline délivrée par pompe

Par Pauline Jacquemier

Thèse de doctorat

Direction : Pr Jean-Pierre Riveline

Présentée et soutenue publiquement le 13 juin 2023

Devant un jury composé de :
Pr Bertrand Blondeau, Président du jury
Pr Laurent Navarro, Rapporteur
Pr Yves Reznik, Rapporteur
Dr Ghislaine Guillemain, Examinatrice
Pr Hélène Hanaire, Examinatrice
Dr Clara Virbel-Fleischman, Superviseure industrielle, (membre invité)
Pr Jean-Pierre Riveline, Directeur de thèse

Outline

Acknowledgments

Je remercie chacun des membres du jury, dont je suis honorée qu'ils aient accepté de consacrer du temps à ce travail.

Je suis reconnaissante à chacune des personnes qui ont participé à encadrer ce travail de thèse. Merci à Sylvain G. pour son goût à partager son travail, pour les premiers mois passés à travailler sur les pompes à insuline ensemble, ainsi que pour son désir d'être facilitateur de ma thèse, en partageant avec honnêteté et simplicité son propre vécu de doctorat. Merci à Sébastien H. pour son discernement, sa grande confiance, son accompagnement initial formateur et responsabilisant. Merci à Yann R., qui a pris la relève de cet accompagnement industriel de thèse avec brio, bienveillance, créativité et un brin de folie, alors même qu'il ne s'agissait pas de son sujet d'expertise. Merci à Clara V-F. d'avoir achevé cet accompagnement industriel avec sérieux, précision et bienveillance.

Enfin, merci beaucoup à Jean-Pierre R., pour la confiance initiale et celle renouvelée au fil de la thèse, appuyée et persistante, qui m'a été précieuse. Je suis reconnaissante pour son souci sincère, ses encouragements, son soutien dans les différentes phases de ce travail. Pour son respect, sa pédagogie et son humilité. Merci également à lui, pour la bienveillance manifestée lors des évènements personnels vécus au cours de ces quelques années de travail.

Merci à Baptiste R. d'avoir partagé la route de doctorant au centre Explor!, entre partages des avancées et des difficultés de nos projets de thèse respectifs, ponts interdisciplinaires entre apnée du sommeil et diabète, et les astuces partagées, de la mécanique de la peau à l'Arduino et au code Python. Merci à Clara V-F. pour la grande disponibilité d'écoute, les échanges et encouragements personnels et professionnels, bien avant qu'elle participe à l'accompagnement de cette thèse.
Merci à Carine R. pour son écoute attentive et paisible, particulièrement dans les moments d'agacement ou de découragement ! Et pour sa curiosité des actualités de cette thèse, très régulièrement manifestée. Merci à Yann R. pour toutes les belles excursions intellectuelles interdisciplinaires imaginatives (ça fait beaucoup de qualificatifs). Merci à Flavien M. pour les partages de connaissances enthousiastes, et de ne jamais s'être agacé de mes plaintes quant à son débit de parole. Mes excuses à lui pour la partie de ce travail réalisée en Matlab. Merci à Eugénie B. pour son optimisme et ses joyeuses onomatopées qui ont ponctué ces quelques années. Merci à Charles-Philippe T. pour sa bienveillance et sa simplicité, ses anecdotes, ses récits historiques animés, et ses tirades percutantes ! Merci à Kaixian Z. pour les discussions médicales et musicales, à Manon pour la bienveillance, et pour la relecture de portions de ce manuscrit ! Merci pour les chouettes échanges aux nouvellement arrivés à Explor, Stéline S., Johan T., Carine P, Isabelle D., qui parlent d'une jolie suite pour le centre Explor ! Merci à Alexandra S. pour sa confiance et ses conseils professionnels, et à la PMT pour l'intérêt manifeste répété.

Un grand merci à Jean-Baptiste J. pour son enthousiasme au sujet de ce travail, ses suggestions et questions régulières au fil de la thèse, ainsi que pour son aide et sa participation indispensable sur l'étude IMPLIQUE-KT.

Je remercie vivement le laboratoire IMMEDIAB pour son accompagnement sur des sujets que je maîtrisais peu ou pas. Merci à Tina E., Rafaëlle B., Joy C., Akila H., Fawaz A., pour leur conseils et aides dans mon apprentissage en immunofluorescence et de l'utilisation de tout le matériel associé qui m'était si peu familier. Merci d'avoir répondu à toutes mes questions bêtes ! Merci à Amélie G., Diane G., Ronan T., Aude J., Ray B. pour leur joyeuse camaraderie malgré ma présence irrégulière au labo. Je remercie Charline P., Charline G., Kennan K., Zaineb M., Claire L., Elena C., Bao V. pour les échanges lors de mes passages au labo. Merci aux PI, Jean-François G., Louis P., Marc D., Fawaz A., Elise D., Camille B., Claire V., Gilberto V., Frédéric F., Nicolas V. pour leurs conseils lors des présentations réalisées au fil de la thèse. Merci à Nicolas V. d'avoir accepté d'héberger cette thèse dans son laboratoire.

Merci à Elian L. et Caroline D., des laboratoires Bio-EC, qui ont été très disponibles. Leur désir de répondre aux besoins de cette thèse et leur compréhension et flexibilité ont été déterminants dans ce travail. Merci à Martine C-S. et à Agnès O. pour leur aide très précieuse concernant l'accès et l'utilisation du µCT scanner et des outils logiciels associés. Merci au laboratoire BIOSCAR et à Christine C. pour la mise à disposition du scanner et l'aide lors des dysfonctionnements. Merci à Loïc A. pour l'aide critique apportée quant à l'optimisation des paramètres du scanner.
Merci à Bertrand B. et Ghislaine G. pour le déblocage apporté dans le marquage en immunofluorescence des dépôts d'insuline sous-cutanée. Merci à Mihalea M., Eric L., et à tout le board scientifique de l'étude IMPLIQUE qui ont nous ont accepté de nous suivre et accompagné dans la rédaction, en une semaine, du protocole ancillaire IMPLIQUE-KT. Merci à Vitalaire d'avoir permis cet ajout. Merci à Cécile C. pour l'accompagnement du projet, et à Qualees et Mydiabby qui par leur travail, ont largement contribué à une collecte de données de cette qualité.

Merci enfin, à ceux qui m'ont permis de tenir la distance sur ces quelques années de travail ! Elise C., colocataire courageuse, codeuse de robots qui cliquent, qui a assisté aux nombreux épisodes frustrants des 2 premières années de thèse et avec qui nous avons pu rire de la situation ! Joël et Patricia R., pour leur affection, et le logement et les partages à des moments importants de ces quelques années. Claude L. pour son amitié, pour les longs coups de fil enthousiastes, remplis de témoignages et clins d'yeux, qui m'ont souvent sortie de la "maroquinerie" ! Et plus largement, le coquelicot et l'hysope qui ont accompagné ces quelques années. Merci à mes parents, Claire et Jean-Pierre J., pour leur fierté et leurs encouragements, leur confiance, leur soutien. Merci à Michel et Jocelyne J. pour les discussions sur l'anatomopathologie de la peau. Merci à Etienne A., d'avoir trouvé bonne l'idée de m'épouser pendant cette thèse. Ainsi que pour sa fierté, et le paisible soutien moral et culinaire dans l'aboutissement de ce travail.

Merci à Celui dont j'ai pu mesurer, de nouveau, la fidélité au cours de ces quelques années.

List of abbreviations

- T1D: Type 1 diabetes
- CSII: Continuous subcutaneous insulin infusion
- IP: insulin pump
- BR: Basal rate
- GV: glycemic variability
- CGM: continuous glucose measurement
- UI: unit of insulin (1UI = 10µL of insulin for the standard insulin concentration "U100")
- PK/PD: pharmacokinetics / pharmacodynamics
- GIR: Glucose infusion rate (in clamp studies)
- STVR: surface-to-volume ratio
- CA: Contrast agent
- e-CRF: electronic case report form
- HbA1c: Glycated haemoglobin
- BMI: Body mass index
- KT: catheter
- OL: open-loop
- CL: closed-loop
- %TA180: percentage of time spent with a glycemia above 180 mg/dL
- TIR: time spent in the target glycemic range ("Time in range")

List of Figures

List of Tables

Abstract

Type 1 diabetes results from the total destruction of the beta cell function of insulin secretion in the pancreas. Treatment consists in providing exogenous insulin to the patient for glucose control, in order to prevent acute and chronic complications. This is achieved by a subcutaneous multiple daily injection or by the use of a pump that continuously administers insulin in the patient's subcutaneous tissue through a catheter (KT) which is changed every 3 days. Pump therapy is now being improved by control algorithms that automatically adapt delivery in real-time, according to interstitial glucose measurements. These are called closed-loop systems.

Despite the significant improvement in glucose control in pump users, metabolic targets are often not reached and some glycemic variability remains in many patients. The etiopathogeny of this glucose variability remains mainly unexplained. A heterogeneous and unpredictable absorption of insulin in the subcutaneous tissue is suspected to cause this but requires further demonstration and description. Additionally, many factors could bring variability to absorption, such as age, sex, physical activity, but also lipodystrophies, or KT characteristics. However, this question is largely unsolved because ex vivo models are scarce.

This work aims at studying insulin subcutaneous propagation and absorption in the specific case of an insulin pump at basal rate delivery.

This project first develops the proof-of-concept of a dynamic follow-up method of subcutaneous infusion in ex-vivo human skin explants, by micro-computed tomography and pressure measurement. Then, this method was applied to study propagation for two pump models and two basal rates. Finally, a real-life observational study was performed to explore the clinical implications of one potential source of absorption variability: KT change (KTC). In that context, glycemia was compared in the hours after KTC to the following days, both in open-loop and in closed-loop systems.

3D imaging was performed every 5 min in the ex-vivo experiments on 24 explants from 4 different donors during 3h infusion of insulin at 1UI/h with a t:slim x2 pump (Tandem) and pressure inside the tubing was recorded. An interpretable dispersion index (DI) was introduced to describe insulin propagation. 14/24 infusions did reach the targeted hypodermis while other infusions reached alternative skin structures. DI increases with time reaching a mean value of 6.64 after 3h, and its evolution is reproducible for hypodermal infusion. Insulin was found to propagate preferably along the interlobular septum. Momentaneous pressure elevations in the tubing were associated with air bubble infusions.

Application of this follow-up method shows DI is independent from delivered volume. All insertions and infusions performed with the Medtronic 780G did reach the target tissue. Large air volumes were observed at the start of the infusions, probably due to insertion technique. DI

evolution appears to be otherwise comparable between the two pumps, although more tests are required for confirmation.

In the clinical study, significant time above target glycemic range was observed after KTC compared to the same time of day 24h and 48h later, both in open and closed loop, suggesting a slower absorption in naive infusion sites. When boluses were infused prior to KTC, no such event was observed. Confirmation of this in a randomised control trial may allow to include timing the KTC after boluses into patient education.

To summarise, the ex-vivo study was the opportunity to introduce a new interpretable metric to describe insulin propagation. This method can be used to further investigate the impact of the many parameters likely to affect insulin absorption. Finally, KTC was identified as a critical moment in the insulin treatment. This may be solved by bolusing before KTC. Confirmation of this may allow to significantly improve time in range of patients using open and closed loop systems.

Résumé

Le diabète de type 1 résulte d'une destruction totale de la fonction de sécrétion d'insuline des cellules bêta du pancréas. Il en résulte une hyperglycémie chronique et une variabilité glycémique, associées à des complications à court et long terme. Une insulinothérapie est nécessaire et peut être effectuée par un schéma de multiples injections quotidiennes, ou via une pompe qui délivre l'insuline de façon continue dans le tissu sous-cutané à travers un cathéter (KT) renouvelé tous les 3 jours. Ces pompes sont désormais améliorées par un algorithme de contrôle qui permet une adaptation en temps réel le débit d'insuline en fonction de la glycémie interstitielle mesurée par un capteur, au sein de systèmes communément appelés boucle fermée.

Malgré une amélioration significative de l'équilibre glycémique des patients équipés de pompes, une variabilité glycémique subsiste chez certains d'entre eux. Une absorption hétérogène de l'insuline dans le tissu sous-cutané est une des causes fréquemment suspectées, mais a peu été décrite. Par ailleurs, de nombreux facteurs sont susceptibles d'apporter une variabilité supplémentaire : l'âge, le sexe du patient, ses activités physiques, des lypodystrophies, ou les caractéristiques du KT.

Ce projet se propose d'étudier la propagation et l'absorption sous-cutanée d'insuline dans le cas spécifique d'une délivrance par pompe en débit basal.

Il développe d'abord une méthode ex-vivo dynamique de suivi de la propagation d'insuline dans des explants de peau humaine via un micro-scanner et des mesures de pression dans la tubulure. Cette méthode est ensuite employée pour comparer l'infusion pour deux pompes et deux débits différents. Enfin, une étude observationnelle en vie réelle étudie l'impact des changements de KT (KTC) sur la glycémie dans les heures qui suivent ce KTC, en boucle ouverte et fermée.

Lors des essais ex-vivo, une image 3D a été prise toutes les 5 min pendant 3h d'infusion à 1UI/h avec une Tandem t:slim x2, pour 24 explants. Un indicateur de dispersion (DI), interprétable, a été élaboré pour décrire la propagation d'insuline. 14/24 infusions ont atteint l'hypoderme, tissu cible, les autres ont atteint d'autres structures dermiques. Le DI croît progressivement et atteint une moyenne de 6.64 à 3h. Son évolution est reproductible pour les infusions hypodermiques. L'insuline s'est propagée préférentiellement dans le septum interlobulaire. De courtes élévations de pression de tubulure ont été associées à l'infusion de bulles d'air.

La comparaison de deux débits basaux confirme que le DI est indépendant du volume infusé. Les injections avec la pompe Medtronic 780G ont atteint l'hypoderme, et des volumes d'air importants ont été observés en début d'essai, probablement liés à la technique d'insertion du KT. L'évolution du DI est comparable entre les deux pompes. Cela doit être confirmé par plus d'essais.

Enfin, l’étude clinique montre un temps significativement plus élevé au-dessus de 1.80mg/dL après KTC, par rapport à 24 ou 48h plus tard, en boucle ouverte comme fermée. Ceci n’est pas observé lorsque des bolus sont délivrés avant KTC. La causalité entre ces événements nécessite d’être confirmée par essai contrôlé randomisé, ce qui pourrait conduire à inclure dans l’éducation des patients le fait d’effectuer le KTC après bolus.

Ainsi, notre étude ex-vivo a permis d'introduire un nouvel indicateur interprétable pour décrire la propagation sous-cutanée d’insuline. Cette méthode peut désormais être employée pour explorer l’impact de nombreux paramètres sur l’infusion. Notre étude clinique a permis d’identifier les KTC comme un moment critique de l’insulinothérapie, ce qui pourrait être résolu en positionnant les KTC après bolus, améliorant ainsi le temps dans la cible tant chez les patients en boucle ouverte que fermée.

Introduction

Type 1 diabetes (T1D) results from an absolute defect in insulin secretion due to autoimmune beta cell destruction in the pancreas. Insulin is a hormone that both triggers glucose uptake by the cells and inhibits glucose hepatic production and therefore reduces blood glucose. This absence of insulin secretion in patients with T1D leads to a hyperglycemia and is lethal in the absence of a treatment.

Diabetes short and long-term complication: what makes glycemic control essential?

The ideal glycemic range (euglycemia) is between 0.70 mg/dL and 1.80 mg/dL. The disease exposes patients to chronic hyperglycemia leading to long-term consequences among which cardiovascular complications, retinopathy leading sometimes to a definitive vision impairment or blindness, or neuropathy with amputations.
On the other hand, patients are also exposed to risks of short term complications. Among them, acute hyperglycemia (above 2.50 mg/dL) can lead to ketoacidosis, a life-threatening event that requires hospitalisation. Hypoglycemic events (glycemia below 0.70 mg/dL) is another short term complication that can strongly affect daily life, from lack of concentration, headache, blurred vision to speech disturbances or loss of consciousness [1].

Finally, glycemic variability refers to both intra- and inter-day glycemic excursions. It is particularly frequent in T1D [2,3]. It increases the risk for hypoglycemic events and is suspected to be a specific cause for diabetes long-term complications [3,4].

Several randomised control studies such as the Diabetes Control and Complications Trial (DCCT) [5] and UK Prospective Diabetes Study (UKPDS) [6] showed that a good glycaemic control is able to prevent some of these complications. It is then critical to ensure that blood glucose of patients with T1D stay within the target glycemic range.

The existing treatments

Since the discovery of insulin in 1921[7], the treatment has consisted in providing exogenous insulin to the patient for glucose regulation. Nowadays, various insulin analogs are provided. They present slight amino-acid modifications compared to the original insulin, that allow to modulate their pharmacodynamics, leading to designations such as rapid insulin, or long-acting insulin [8].

Today, these insulin analogs can be delivered to the patient in two main different ways:

- multiple daily injection (MDI) schemes, with subcutaneous injections of both rapid and long-acting insulin using syringes or insulin pens
- Continuous subcutaneous insulin infusion (CSII) using insulin pumps (Figure 1).

Insulin pumps

Insulin pumps are electromechanical devices that continuously deliver very small amounts of rapid insulin into the subcutaneous tissue of patients. Although such delivery is also called "continuous subcutaneous insulin infusion" (CSII), pumps do not deliver a strictly continuous flow, but rather regular micro-impulsions [9].

CSII present two main delivery modes: one is called "basal delivery". The basal rate (BR) is the constant flowrate applied by the pump, mimicking the continuous background secretion of insulin, which aims to control glucose hepatic production. Various basal rates can be applied in different time-windows during the day to adapt to the patient's needs. The other delivery mode is a patient-triggered "bolus": a one-off volume of insulin destined to control postprandial glycemia, or any other temporary elevation of glycemia.

Figure 1 : A few examples of insulin pumps (from left to right and from top to bottom: a t:slim x2 (Tandem), a Medtronic 780G (Medtronic), an Ypsopump (Ypsomed), a Dana i (Dana), and an Accu-Chek Insight (Roche Diabetes).

CSII use in patients has contributed to improve glycemic control [10], as shown by several meta-analyses of randomised studies comparing MDI to CSII [11–15]. The studies included within these meta-analyses mostly compare glycated haemoglobin (HbA1c) in both insulin therapies. HbA1c is a type of haemoglobin for which an elevation concentration mirrors a poor glycemic control over the 3 previous months.

Contrary to MDI delivery, CSII offers the possibility to set various BR defined per time-windows in the day, thus adjusting to the specific needs and lifestyle of a patient. Insulin consumption was also reported to be weaker for insulin pump users compared to insulin delivered by MDI, for identical glycemic targets.

Struggle to reach stable glycemia even for pump users

Despite this clear efficiency of CSII in regulating blood glucose, a certain population of patients with T1D struggles to maintain its glycemia within the target range, and is subject to frequent hypoglycemic events and high glucose variability (GV) [2]. An illustration of a glycemic profile from a patient treated with a pump, with high GV can be found in Figure 2. Each coloured line displays glycemic evolution through one day. Great variations from day-to-day can be observed on this graph.

In addition to the complications associated with high GV and frequent hypoglycemia, they constitute a heavy psychological burden which was thoroughly documented [16].

In such patients, the most often suspected causes for high GV are either co-pathologies associated with T1D [17,18], or patient behaviour such as irregular food intakes, poor pump management, or difficulties in estimating the carbohydrates they eat [19,20]. However, in some cases, none of these suspected causes are sufficient in explaining GV.

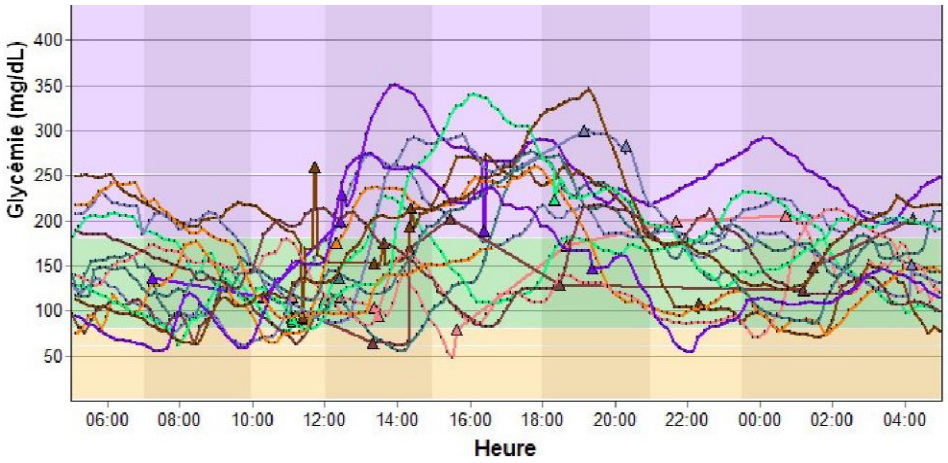

Figure 2: 14-days glycemic profile of a patient treated with CSII. Target glycemic range delimited with a green background. Source: personal data from Pr Riveline.

It is especially critical to identify sources for GV in pump users as pumps are now being associated with continuous glucose measurement (CGM) and control algorithms into systems called “closed loop systems”, or “hybrid closed loop systems”, which enable constant adjustment of the insulin delivery according to the patient’s current needs. Any source of variability in insulin delivery performance is likely to alter the proper function of the closed loop algorithm and therefore of insulin administration.

Looking for more causes for GV in patients treated with pumps

Pumps infuse insulin into the subcutaneous tissue through a catheter (Figure 3) which should be changed every 3 days according to international recommendations [21,22] . Insulin therapy relies on a reproducible absorption of insulin from this subcutaneous tissue [23]. However, many parameters can affect insulin absorption, and the insulin infusion site and infusion set was especially referred to as the "Achilles heel off insulin pump delivery" [24] by Heinemann and Krinelke.

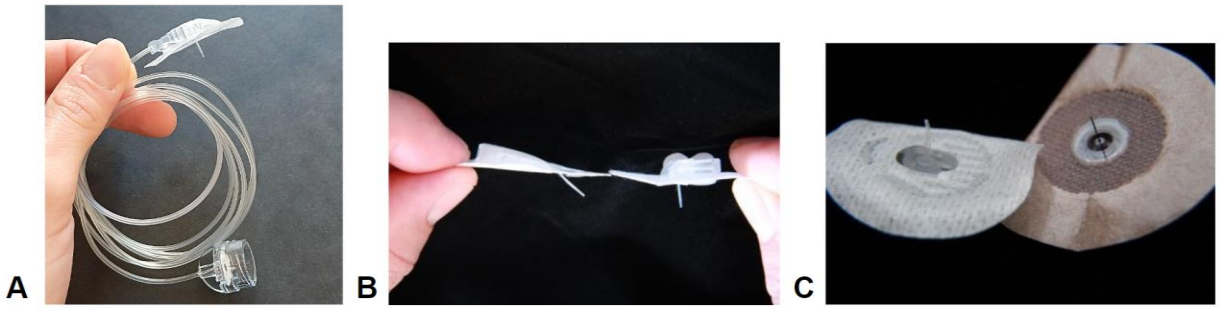

Figure 3: CSII catheters with various cannula length, material, or insertion angle. (Sources: A: personal picture. B, C: https://waltzingthedragon.ca/diabetes/insulin-pumps-cgm/using-insulin-pump-choosing-infusion-set-brands-features/)

A few studies have explored insulin subcutaneous depot and absorption [25–32]. However, the vast majority concentrates on one-off injections with pens or syringes such as those of MDI. Those who do study CSII also concentrate on bolus injections, which are infusions of large amounts of insulin, comparable with those of MDI.

However, to our knowledge, none studied subcutaneous absorption in BR delivery, which is the very specificity of CSII, although many parameters are likely to introduce variability in BR delivered insulin. Indeed, Luijf et al have observed that postprandial glycemic excursions are higher on day 1 of catheter wear than it is on day 3 of wear [33], suggesting that insulin absorption varies according to catheter age. The effect of the various delivery patterns of insulin pumps [9], and of the different basal rates, is also unknown. In addition, multiple infusion sites are recommended to patients, namely abdomen, thighs and arms, and the impact of those various locations on propagation is still unknown. A rotation between these possible infusion sites is recommended to prevent the occurrence of lipodystrophies, which are a cause for disturbed insulin propagation, and therefore disturbed insulin absorption [21,23]. Catheter and cannula length, material, or cannula angle of insertion, the type of insulin analog, are also all potential parameters affecting diffusion [25,34], along with air bubbles in the tubing and obstructions due to insulin precipitation [35–37].

Objective for this work

This work aims at **studying insulin subcutaneous propagation and absorption in the specific case of an insulin pump, basal rate delivery**.

- Insulin absorption increases with the surface of the insulin subcutaneous depot [38]. No method was developed yet to describe basal infusion of insulin to characterise subcutaneous depot surface evolution. This project **develops a follow-up method of subcutaneous infusion in ex-vivo human explants by micro-computed tomography and pressure measurement**.

- Implementation of this method allows to start exploring **the impact of various basal rates and CSII delivery patterns on insulin subcutaneous propagation.**

- Finally, due to the postprandial excursions after catheter changes observed in supervised clinical settings, a **clinical section of this work looks at catheter change impact on patient glycemia in the hours following catheter change compared to other days of CSII wear**, both in **open-loop CSII setting** and in the **context of a hybrid closed-loop system**.

Chapter 1: A diverse and heterogeneous set of endpoints to describe insulin absorption

1.1 A few words on skin structure and the subcutaneous tissue

The skin tissue is composed of three layers (Figure 4). The most superficial, the epidermis (0.1mm) is mostly formed of keratinocytes, and the dermis (1-2mm) is mainly composed of fibroblasts and extracellular matrix [39]. Both are very rich in collagen [40]. The third layer, the subcutaneous tissue or hypodermis, is adipose tissue [41]. It is the target tissue for CSII delivery and our main interest here.

The adipose tissue in the hypodermis is therefore composed of adipocytes, which are organised into lobules [42]. These lobules are visible to the naked eye (Figure 5), and are separated by an interlobular septum mostly formed of collagen [43] (Figure 6). The hypodermis is **vascularized** [44–46] by a network of capillaries of progressively decreasing diameter [47]**.** Its thickness varies according to body location and fat mass.

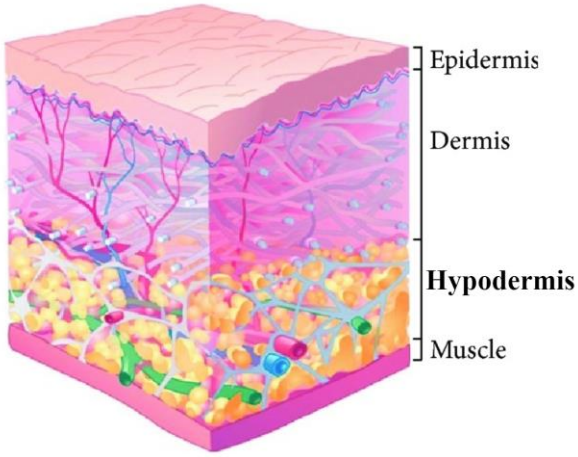

Figure 4: Skin structure schematics (adapted from Gradel et. al, 2018)

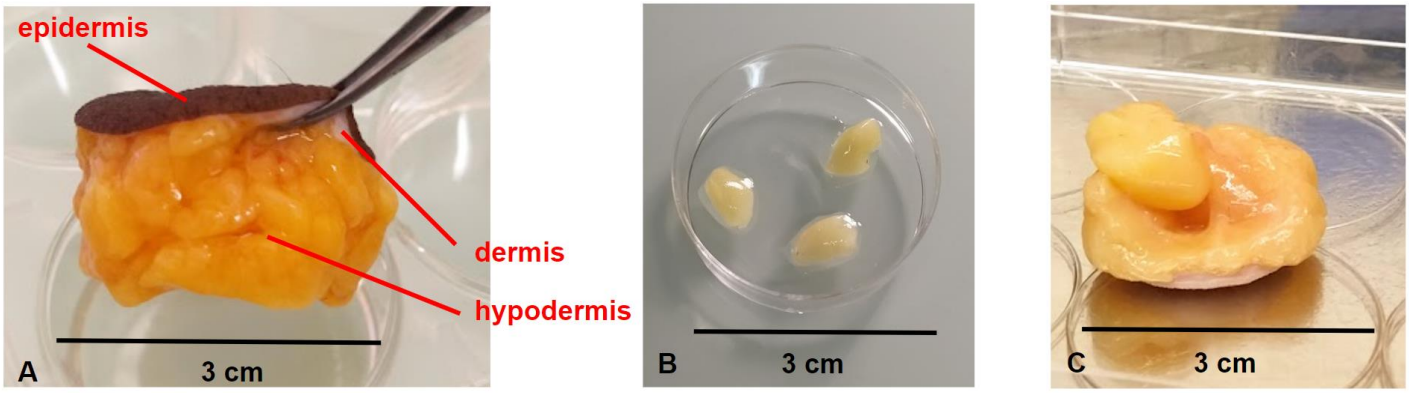

Figure 5: Pictures from handling of explants. A. Skin explant from post-bariatric surgery with all three layers of the skin visible. B. Three isolated fat lobules from a skin explant. C. Extraction of a group of lobules from an explant.

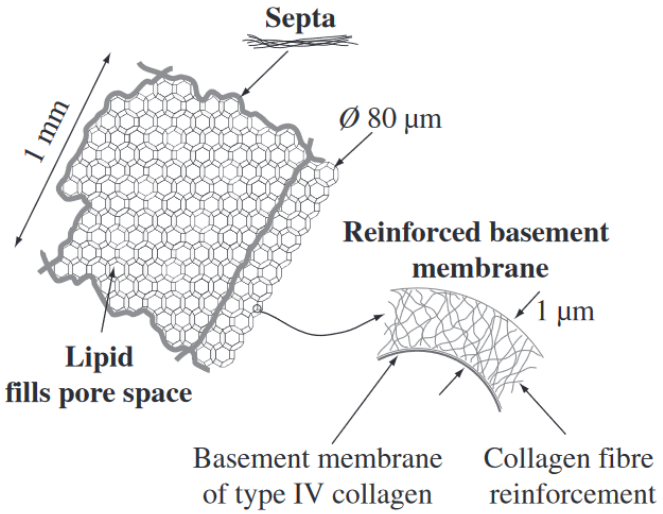

Figure 6: A sketch of a lobule of adipose tissue. Source: Comley and Fleck (2010)

1.2 Processes at subcutaneous infusion sites - contribution of pharmacokinetics on vocabulary

In subcutaneous delivery, insulin should be deposited in the hypodermis at a depth that depends on the choice of catheter (usually between 4 and 9 mm below the skin surface, according to catheter length and angle). However the ultimate target that insulin must reach is the vascular system.
In a pharmacokinetics - pharmacodynamics (PK-PD) point of view, the subcutaneous tissue is the first compartment, and the plasma is the target compartment [48]. Many models have been suggested by various authors as possible approximations of how insulin exits that first compartment. A few examples of these, models from several to no compartments in between the subcutaneous tissue and the plasma, are presented in Figure 7.

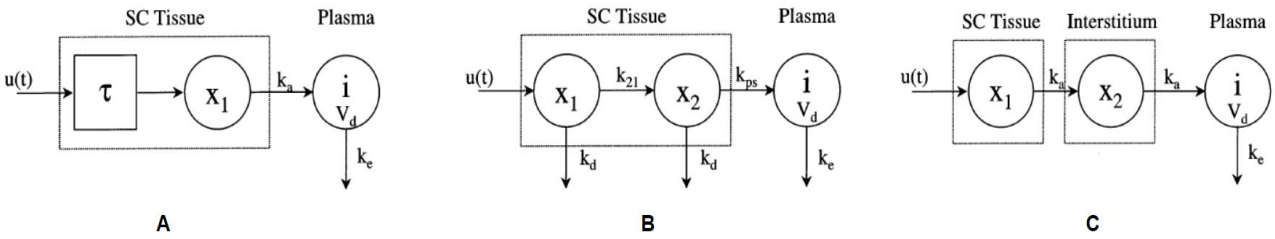

Figure 7: A few examples from various PK-PD models for insulin absorption. Source: Nucci and Cobelli, 2000. A. Single-compartment model by Kobayashi et. al, 1983. B. Two-compartment model by Kraegen et. al, 1984. C. Two-compartment model by Puckett et. al 1995.

We will not detail these models. However, although these are not descriptions of the mechanisms happening in the subcutaneous tissue but models allowing to provide predictions best fitting experimental data, these models provide a useful opportunity to precise both the vocabulary we will be using, and also the parts of mechanism we are, or not, able to study.

Indeed, an extremely basic key distinction derives from these: it is not the same thing for the insulin to expand into the subcutaneous tissue than for insulin to enter plasma.

Therefore, we will further call **propagation** the evolution of the volume of subcutaneous tissue infused with insulin, whatever phenomenon drives this extension: whether active (pushed by pump administration pressure for example), or passive. We will call **diffusion**, passive propagation only (for instance resulting from a local concentration gradient).
We will call **dispersion** the state of propagation at a given time-point.
Insulin entering the plasma is the phenomenon we will call **absorption**. On the models presented in Figure 7, this would correspond to the last arrow pointed to the plasma.

Quantifying absorption would be our ideal endpoint. However, it cannot be measured directly and **all quantifications are partial and indirect**. For indeed, insulinemia (insulin concentration in the patient's blood) measurement, apart from being an invasive in vivo measurement requiring regular blood sampling, does not take into account the insulin that has had an immediate effect and was consumed already.

Other endpoints can help us understand insulin absorption. Some are upstream from absorption itself, describing insulin depot shape and morphological characteristics mainly, others are downstream, providing data on the pharmacokinetics of the insulin effect.
Yet, before we look into these possible indirect endpoints, let us introduce a few exceptions in the literature, which **did achieve to approximate absorption itself**, although such studies would nowadays no longer be reproduced for ethical reasons.

1.3 A first study - Lauritzen et. al

A pioneering 1983 study from Lauritzen et al [49] started investigations on insulin absorption in the context of CSII use, at a time where CSII adoption was in its early stages and therefore incipient. Lauritzen used radioactive ^{125}I-labelled insulin. 8 patients were included and equipped with pumps infusing radioactive insulin in basal delivery. Radioactive counting was then performed to quantify insulin in the subcutaneous tissue, and blood glucose and serum free insulin measurements were conducted on blood sampling on regular time intervals prior and after a bolus injection, on two consecutive days.
Gathering this data allowed them to estimate insulin absorption rate. Indeed, as the instantaneous increase in radioactive counts per min (cpm) at the subcutaneous depot at the time of bolus

injection had to match with the bolus injection volume, they obtained an equivalence between cpm and UI.
This allowed them to compute the volume of insulin absorbed between any two time points t_1 and t_2 as the difference in insulin volume at the infusion site, to which is added the amount of insulin delivered by the pump in that time.
In short, they were able to compute the **insulin absorption rate** A_r.

$$A_r = \frac{V_{depot}(t_2) - V_{depot}(t_1) + V_{infused}}{t_2 - t_1}$$

This study was performed using means which do not match the current ethical standards, exposing patients to doses of radioactivity above reasonable levels, with no direct therapeutic goal associated with the radioactivity.
This direct measure of the absorption rate did allow the authors to compare intrapatient day-to-day variability in absorption, although the insulin infused (purified porcine insulin) is different from the currently available human insulin analogs. The observed coefficient of variation for the day-to-day intrapatient variability (upon 2 days) varied from 11 to 35%.

A few studies have followed using similar endpoints, looking at the effect of lipohypertrophy on insulin absorption with ^{125}I-labelled insulin [50] for instance in 1984, or the impact of various patient phenotypes on the rate of insulin absorption [51] in 1993. This last study demonstrates a negative correlation between adiposity (whether measured by skinfold thickness or BMI) and absorption rate, and a positive correlation between insulin absorption and subcutaneous blood flow. It also observed significantly quicker absorption in the abdomen and arm than in the thigh.

Although they provide interesting results, it is good news that such methods are no longer available, and we must make the most of more indirect methods to describe absorption. Therefore, let us now look into other endpoints that can help improve our understanding of insulin subcutaneous absorption.

1.4 Upstream measurements: describing insulin propagation or insulin infusion site state

a. Studying the morphology of large subcutaneous depots

Various studies describe the morphology of the subcutaneous depot after injections of large amounts of insulin similar to those of MDI schemes or CSII bolus delivery. Most of them use swine skin tissue, which presents a close structure to human skin. Thomsen et al. along with Kim et al. have looked at indicators such as the average size of insulin depots in the horizontal or vertical directions, relying on X-ray imaging, sometimes associated with computed tomography [25,28,29]. This was their endpoint to study the effect of infusion speed on insulin depot shape for syringe

injections. Effect of injection volume, of needle length [29] or nature of injected tissue (whether adipose or muscle tissue is reached) [25] was also considered. All of them agree that insulin appears to spread preferably along a path of least resistance [25,26], first along a plane parallel to the skin surface, before spreading along a vertical axis. Such studies also look at spatial concentration of contrast agent in the depot, namely the decrease in concentration when radial distance from the tip of the cannula increases.

Most of these studies focus on the morphology of the injected volume of insulin once it has been delivered. Only one study introduces a dynamic follow-up of insulin propagation in swine tissue [25], but upon volumes and delivery rates which sharply exceed the common volumes and delivery rates of insulin a patient would receive in a whole day : the smallest rate of delivery they study is of 25 units of insulin per minutes (UI/min), up to 600 UI/min, when standard rates of delivery for insulin pumps are of 1 - 2 units of insulin **per hour** (UI/h). Moreover, it only captures 2D-spatial evolution and therefore displays limited information.

b. A few other endpoints from the literature describing CSII subcutaneous delivery upstream from absorption.

Patte et al. have looked at conditions closer to our interest, for they measured the evolution of tissue resistance pressure against various infusion rates of similar order of magnitude to those of CSII bolus delivery [52]. This was achieved using a pressure transducer placed upstream from the infusion set. They conclude that tissue resistance pressure increases significantly with higher infusion rates. Regittnig et al. also conducted pressure measurements, noticing that tissue resistance pressure increases with catheter wear-time [53]. Both of these studies were performed in vivo, in humans.

Others have looked to conditions close to CSII delivery. Hauzenberger et al. perform in vivo pump delivery in swine and histopathology on biopsies show that inflammation of the infusion site increases with wear time and changes according to catheter type [30–32].

1.5 Downstream measurements: glycemia and interstitial glucose

Two possible downstream endpoints partly result from insulin absorption, namely glycemia (blood glucose) and interstitial glucose (glucose level in the interstitial fluid, measured by continuous glucose monitoring systems). But both are also subject to many other phenomena and are not just the result of insulin absorption, but also physical activity, food intake, metabolism, sleep or emotions [54].

The principle of clamp studies does allow to partially bypass this issue by maintaining patients in euglycemia under glucose perfusion [55]. Indeed, one then measures the glucose infusion rate (GIR) that must be delivered to maintain the patient at a stable glycemia. This mirrors the insulin metabolism, if the patient is healthy, or efficiency in insulin delivery, if the patient is under exogenous insulin. Yet this measure still depends on the insulin sensitivity that varies according to the patient.

a. Using standard pharmacokinetics variables to describe insulin absorption

Several works study insulin absorption according to various parameters, in the context of CSII, making use of such endpoint and the classical variables associated with pharmacokinetics studies:

- the maximum concentration (either of glucose or of plasma insulin) upon a given time window (C_{max}),
- the time t_{max} to reach C_{max} (or $t_{50\%max}$ to reach 50% of C_{max})
- the half-life $t_{1/2}$ of a substance (either insulin or glucose)
- the area under the curve (AUC) of the concentration evolution through time of a substance (insulin or glucose)

Rini et al. [56] for instance, particularly use $t_{50\%max}$ in a randomised study comparing infusion using an CSII delivering in the standard way to the subcutaneous tissue, and delivering through a microneedle into the dermis. They found a significantly shorter $t_{50\%max}$ for dermal infusion which allows them to deduce a quicker absorption in the case of dermal delivery in their cohort.

Another example of such metric deployed to obtain data on insulin absorption can be found in a randomised study from Raz et al. [57], who used t_{max} and the insulin AUC to see the impact on insulin absorption of a heating patch placed on the infusion site compared to a control group with no heating patch.

b. Studying insulin absorption using glucose clamp studies

Euglycemic clamp studies have also been used to get data upon absorption. We will provide a few examples. Just as Raz et al, Cengiz et. al [58] have looked into impacts of an infusion site warming device on the time to reach the maximum GIR, t_{GIRmax}, observing a significant reduction of t_{GIRmax} with the device [59].
In another study, efficiency of an innovative anti-occlusion infusion set (with additional openings on the sides) was tested upon 7 days, among which 3 under euglycemic clamp. T_{GIRmax} reduced with time between day 1 and 7, suggesting quicker absorption rate as wear time increased. However AUC_{GIR} upon the various days showed the total absorbed amount of insulin decreased with wear time.

Finally such studies were also used to compare absorption rates for various insulin analogs [60].

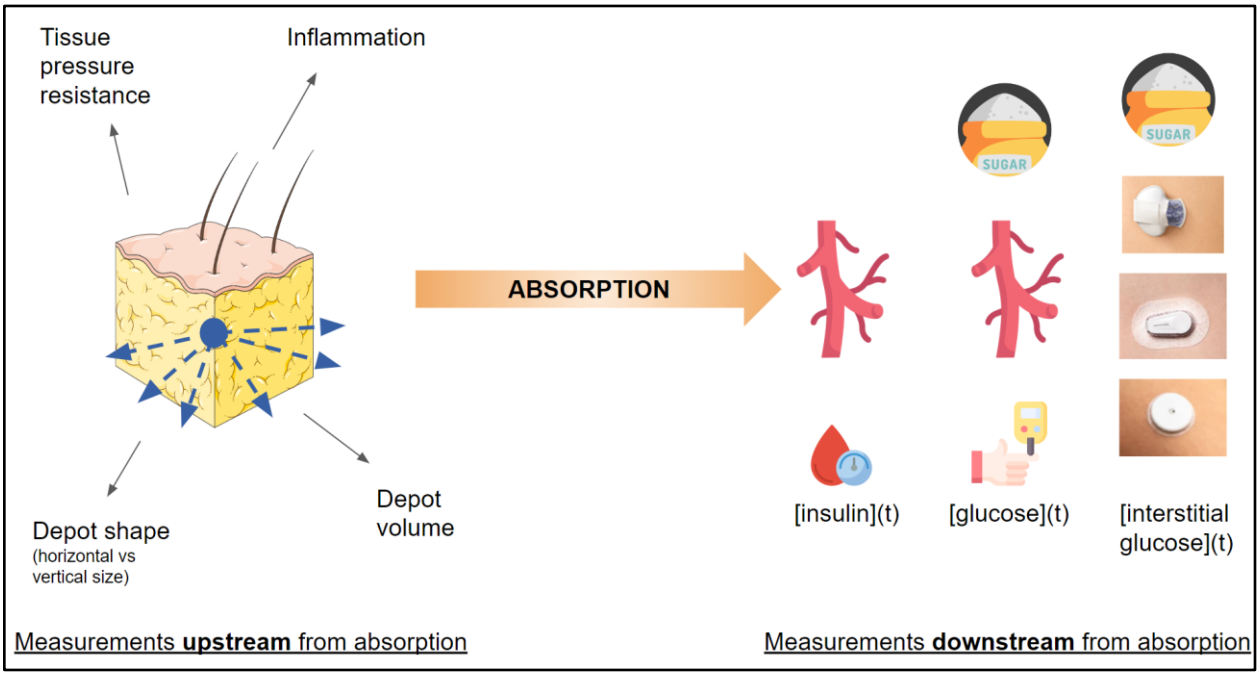

Figure 8: graphical summary of the various metrics to approach insulin absorption

Up to this point, several approaches to indirectly describe insulin absorption have been made, either upstream from the absorption phenomenon itself, or downstream from the absorption. These approaches are graphically summed up in Figure 8.

1.6 One link between upstream and downstream measurements: Mader et al.

Upon these different studies, one work from Mader et al. [38] builds a bridge between morphological analysis of insulin depot in the tissue and insulin absorption via a clamp study and glucose infusion rate (GIR) measurement. Indeed, they compare two administration strategies for a given volume of bolus. They show that increasing the surface-to-volume ratio (STVR) using a dispersed injection strategy (one volume delivered via 9 infusion spots VS the same volume delivered in one single spot, see Figure 9) decreases the time to reach maximum GIR, and therefore the insulin absorption speed.

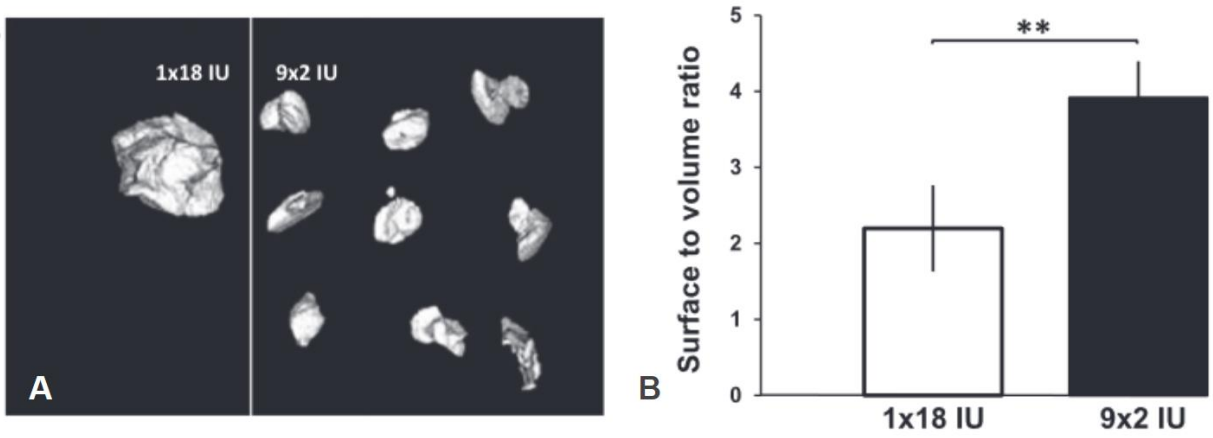

Figure 9: A. 3D reconstruction of the micro-computed tomography measurements of the two injection strategies performed ex-vivo. B. Mean surface-to-volume ratios comparing two injection strategies (1 x 18 UI vs. 9 x 2 UI). **P < 0.01. Source: Mader et al, 2013.

Although this result is rather intuitive, for increasing the STVR of an insulin depot increases the interface with the tissue microvascularisation, thus facilitating absorption, such demonstration was lacking in the literature until 2013. It provides a link between upstream and downstream measurements, showing that morphological study of the depot is a meaningful and valid choice, as it directly impacts the absorption rate of insulin.

Chapter 2: Sources of variability in insulin absorption

Last section clarified that insulin absorption is dependent on insulin depot morphology, and therefore, on insulin propagation in the tissue. This propagation is itself dependent on many factors such as the mechanical and biological characteristics of the tissue, or various aspects of the infusion system. A brief overview of these factors will be introduced in this chapter. When the exact effect of these factors on skin mechanics and on subcutaneously delivered drugs is known, it will be detailed. However for several factors, the specific consequence on drug propagation is only suspected but not described.

We will discuss the impact of patient phenotype, of infusion site location, catheter wear-time and inflammation at the infusion site. We will mention hypodermis microvascularisation variability, external mechanical actions applied to the infusion site, and lipodystrophies. We will finish on the variability which the pump itself can cause.

2.1 Patient phenotype

Many aspects of patient phenotype are likely to affect insulin absorption. Both age and gender majorly influence skin mechanics: age is associated with elasticity loss [61–63], and female skin was shown to be thinner and more elastic than male [64,65]. Pigmentation is sometimes suspected to have an effect on epidermal and dermal thickness, but there are very few studies on the matter, and those which do exist only cover a limited range of the world population [61]. Moreover, no data was found on phototype influencing the mechanics of the subcutaneous adipose tissue [66], thus potentially affecting insulin propagation.

Finally, smoking habits have been demonstrated to trigger a loss in elasticity and thickness modifications [61,67,68], which could modify insulin propagation in the tissue, but also, was associated with a reduced insulin subcutaneous absorption speed [69].

All of these patient-dependent parameters add up in intra-individual variability in insulin absorption.

2.2 Impact of infusion site location

Recommended body locations for insulin infusion are the abdomen, outside fonts of thighs, upper buttock and lower back, and the back of the arm [21] (Figure 10). The impact of those various locations of insulin absorption itself is scarcely known [24]. Epidermal and dermal thickness and elasticity vary according to body location [70], but not much data is available on the subcutaneous tissue mechanical variations according to body location. In a 1981 study,

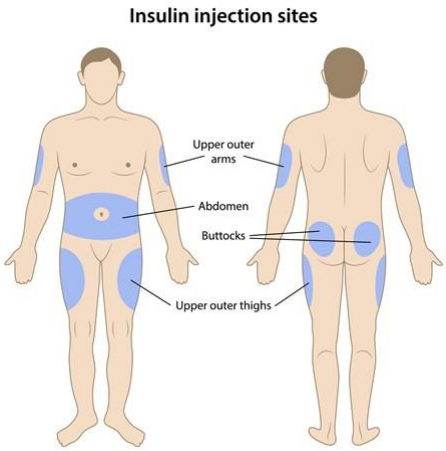

Figure 10: Recommended insulin infusion sites. Source: diabetesmyway.nhs.uk, NHS.

a plasma insulin follow-up was performed after various injections and suggested quicker absorption in the abdomen than in the thighs [71] but these data were obtained under long-acting non-human insulins, not delivered through CSII. A few slightly more recent studies confirm that tendency [72,73] but still not with CSII.

Furthermore, failure to change infusion site every 3 days when renewing the catheter (often called "rotating infusion site" in the literature), could lead to an increased intra-individual variability of absorption, according to data obtained with radiolabelled insulin [74].

2.3 Impact of catheter wear-time

Several studies demonstrate the effect of the CSII catheter wear-time on the resulting glycemia. Set aside the release of a new extended wear-time catheter designed to be changed every 7 days by Medtronic (™) in 2021 [75], catheters should be changed every 3 days according to recommendations and this change should be associated with an infusion site rotation [76]. Yet, many patients keep their catheters for longer periods of time, either out of comfort reasons or sometimes, for economic reasons [22].

Several observations in the literature are to be noted. Luijf et. al [33] noticed in 2013 higher postprandial glucose excursions following initiation of a new infusion site, compared to the postprandial glucose excursions 72h later (Figure 11). These results were obtained by follow-up of plasma insulin and glycemia constants by blood sampling following test meals, in a randomised study. They could suggest insulin absorption is less efficient (more laborious) on the first day of catheter wear. Yet no difference in the AUC_{GIR} and $AUC_{plasma\ insulin}$ between day 1 and 3 were found, which rather points towards a slower absorption (lower absorption rate) on day 1 but no difference in overall insulin absorption.

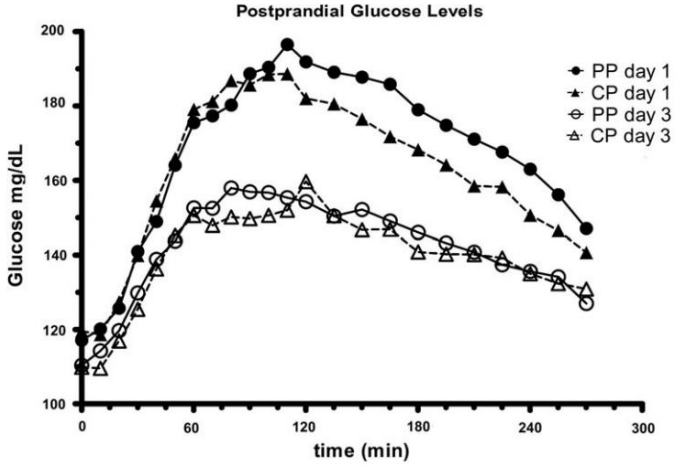

Figure 11: Mean postprandial glucose excursions for Day 1 and Day 3 of patch pump (PP) and catheter-based conventional pump (CP) use, upon 20 patients. Source: Luijf et. al, 2013

Looking at timings a little further away from day 1, Swan et. al [77] had already been comparing bolus effect on day 1 and 84h after infusion site initiation, using a clamp study, in youth treated with CSII. They found a significantly shorter t_{GIRmax} on day 4 compared to day 1, but similar AUC_{GIR}, which in other words corresponds to a quicker absorption rate on day 4 but no difference in the total absorption. These results are therefore consistent with those of Luijf.

Despite these results, Karlin et al. [78] describe an increase in fasting blood glucose, and therefore potentially in basal insulin absorption, after day 3 of catheter wear, and an online study upon the T1D exchange community suggests mean fasting blood glucose increase with each day of catheter use [79].

2.4 Inflammation at the infusion site

Increasing inflammation with wear-time is observed at the infusion site by several authors [30–32]. This inflammation is likely to affect the local mechanical characteristics of the subcutaneous tissue, increasing its stiffness. In line with that hypothesis, Regittnig et. al [53] observes a progressive increase in tissue pressure resistance with wear-time of catheter at the infusion site up to 7 days of catheter wear. They hypothesise that this increased resistance of the tissue may be due to inflammation, and thus to the accumulation of collagen fibrils and cells such as fibroblasts at the infusion site, increasing stiffness and "increasing the path length to fluid flow by imposing a tortuous pathway [to the infused insulin]" [53]. Another potential effect of inflammation is an increased blood flow with the recruitment of blood vessels to the inflamed tissue. This, on the contrary, would have an opposite effect to stiffening of the tissue as the increase in blood flow is likely to improve absorption.
Finally, according to Hauzenberger et al, who have noticed high PK-PD intra-individual standard deviations in their swine study [31], this inflammation could also favour a high intra-individual variability of absorption.

2.5 Hypodermis microvascularisation variability

Studies using radiolabelled insulin have demonstrated a positive relationship between subcutaneous blood flow and insulin absorption rate [80,81]. And we know subcutaneous blood flow increases with temperature [82,83], and varies according to physical exercise, smoking, metabolism and hormonal cycles [84,85]. Interestingly, there is also some suspicion that diabetes itself alters skin blood flow [86].

2.6 External actions on infusion site

Several studies show shorter time to maximum insulinemia when a warming device is being used upon the infusion site, which is consistent with the previously mentioned studies [57,58]. Such an effect has also been reported when a mechanical action is exerted upon the skin, typically when

patients massage their infusion site [87]. This however is probably due to an increased STVR of the insulin depot rather than to an increase in blood flow [85].

2.7 Lipodystrophies

Lipodystrophies (hypertrophies or atrophies) are a misbehaviour occurring in the adipocytes undergoing frequent contact with insulin [88,89]. They can therefore occur at / around infusion sites, especially when patients fail to rotate their infusion site as recommended [90]. Pain at infusion sites can sometimes be belittled upon lipodystrophies, which does encourage some patients to repeatedly use dystrophic tissues for infusion [23].

Lipodystrophies are known to be deleterious for insulin absorption:

- Lipohypertrophies were shown to delay insulin absorption [50]
- Changing injection site from a lipodystrophic area to a healthy one was shown to improve glycemic control significantly [34,91]
- Some authors even suspect insulin to degrade locally in lipodystrophic areas, leading to an even less efficient and more erratic effect on glycemia [92]

2.8 Impact of the insulin pump infusion profile, pump model and basal rate

Although it was only documented upon these last 4 years, CSII do not all deliver the same way [9,93]. From one manufacturer to the other, the engineering choices that were made affect the flowrate pattern of the pump. This was extensively described by Girardot et al [9,93,94]. One observation is that the strategies of delivery can differ from one model to the other, and some pumps increase the frequency of single-volume impulsions to modulate their pump's basal rate, while others deliver impulsions of various volumes at a fixed frequency to achieve that [9].
But another important observation is that some insulin impulsions are sharp, others are smooth and some have their flowrate in triangular patterns (Figure 12). The instantaneous flowrate measurements which were enabled in the context of Girardot's work, display a wide range of instantaneous flowrate values according to the CSII model. The mechanical response of the tissue to such different delivery patterns and signals has not been at all explored yet, but is likely to affect the formation of the insulin depot and therefore, its absorption.

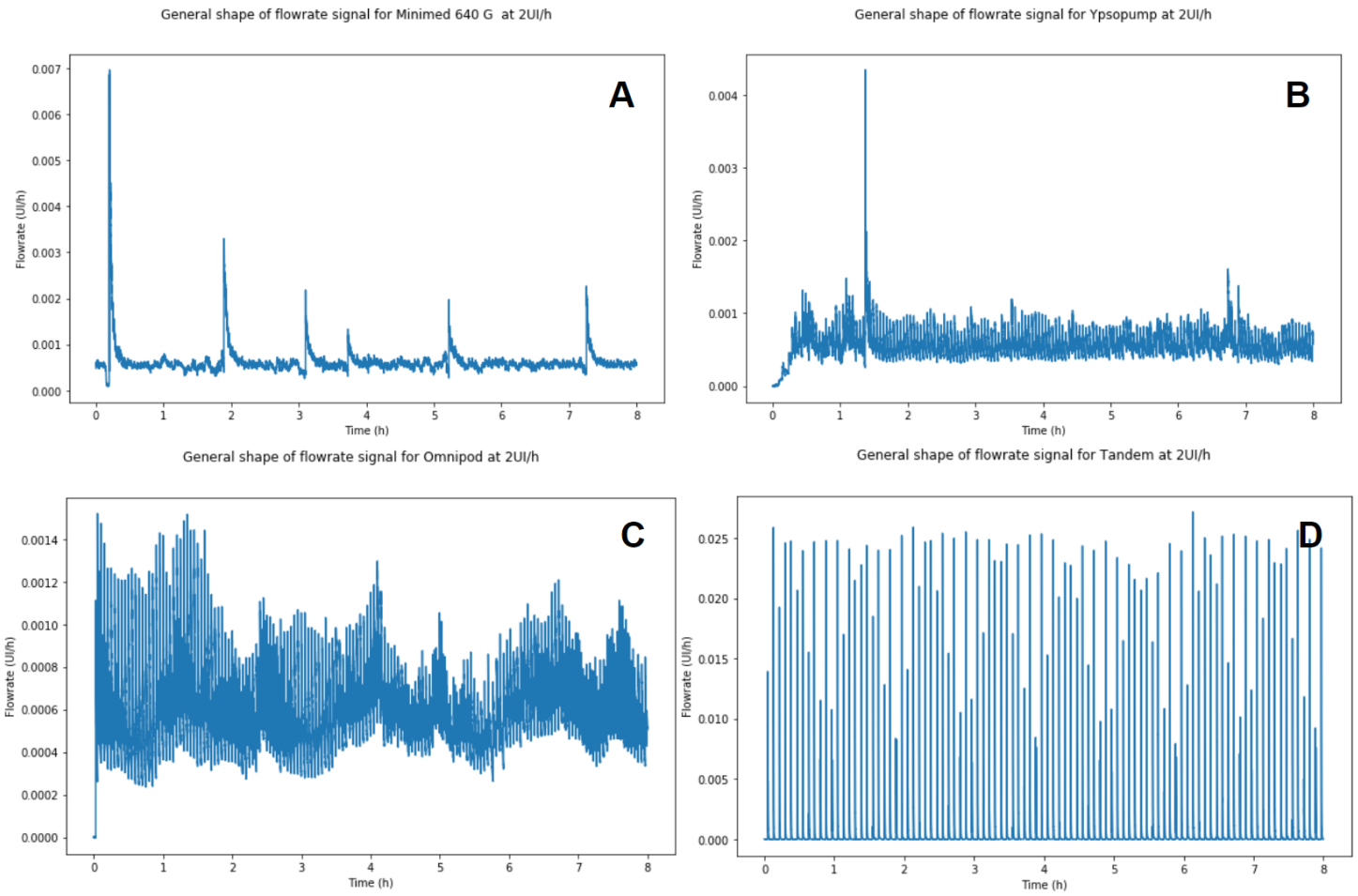

Figure 12: Basal infusion profile of 4 different pump models during 8h at 2UI/h. Vertical scales are different between the four graphs. Source: Unpublished data from Dr Girardot. Profiles for: A. A Minimed 640G. B. An Ypsopump. C. An Omnipod. D. A t:slim x2.

A 2023 paper by Kalus et. al, describes the level of inflammation on skin biopsies from infusion sites in patients with T1D [95]. Patients were equipped from various pump models. Differences in inflammation and especially in the number of eosinophils found at the infusion site, were observed between pump models. Considering the small number of patients using each pump, no statistical significance could be found. The hypothesis for that phenomenon provided by the authors is the existence of undocumented differences in insulin reservoir material between pump models, which could explain these different biological responses once insulin is infused. However, the observation could also nurture the hypothesis of various inflammation levels triggered in the tissue by the different delivery patterns of the pumps and therefore, to the differences in amplitude of the mechanical stress repeatedly applied to the tissue according to pump model.

To conclude, many parameters are likely to greatly impact insulin propagation and absorption in the tissue, most of them are partially documented only. Building a method that allows to describe insulin propagation in the tissue in the specific case of basal delivery, which is the delivery mode patients spend the most of their time in, is a necessary step to achieve comparison of these parameters on the propagation (and therefore indirectly on the absorption) of insulin in the subcutaneous tissue.

Chapter 3: Building the method for the analysis of subcutaneous propagation of insulin, including home-based preliminary experimentations (lockdown)

Summary of the literature review

A brief summary of the literature review in the perspective of our problem:

- ➔ It is suggested that subcutaneous insulin absorption could be involved in glucose variability in patients living with type 1 diabetes
- ➔ No direct means are available to measure insulin absorption. Only a few techniques exist to indirectly evaluate insulin absorption in various conditions, by quantifying either the phenomena occurring before, or after absorption (Chapter 1).
- ➔ The insulin spread in the tissue can be quantified and a high surface-to-volume ratio was associated with an increased rate of insulin absorption [38].
- ➔ Insulin spatial propagation in the tissue is therefore critical to an efficient absorption.
- ➔ Very little data is available on insulin propagation in the tissue. Existing studies all present at least one, and often two of these main limits :
    - ◆ They are swine-based studies, rather than human ones [25–32]
    - ◆ They focus on large amounts of insulin delivered, such as those of bolus delivery, rather than the small rates of basal delivery, which is the one delivery mode patients spend most of their time in [25–30].
    - ◆ They are not time-dependent studies, but centred on a single time-point after delivery [26–29].

Our intent was to build an ex-vivo method which would address these three limits and describe insulin propagation in the tissue. This, in order to compare various infusion parameters among which principally:

- Pump delivery pattern
- Basal rate of delivery
- Shape of cannula

3.1 Choosing the infusion medium

A few options were available as to which medium should be chosen to perform an ex-vivo assessment of insulin infusion. Since 2013, animal dermatological testing is no longer allowed for the cosmetic industry [96]. As a consequence, many testing alternatives have been developed to further perform tests prior to cosmetic products being dispatched unto the market. These alternatives provide interesting possibilities for infusion and injections evaluation.

a. Skin cells culture and skin cells bioprinting?

Skin cell culture of epidermal or dermal cells have been increasingly used to test cosmetics and substances [97,98]. Some laboratories even use 3D printing to perform printing of gels with embedded skin cells to create a 3D structure of skin cells [99].
Although these models do reproduce part of the biological response and metabolism of the cells, they do not present the mechanical properties of natural human skin which is a critical aspect for the experimental relevance of the injections intended in this project.

b. Skin explants from post-bariatric surgery

A few companies have developed solutions to maintain skin from post-bariatric surgery in survival for a few days. They show good survival for 7 to 10 days post-surgery. The content of their solutions is patented and undisclosed.
We chose to work with Bio-EC laboratories, who provided the survival Medium (BEMc - Bio-EC Explant Medium, Bio-EC, Longjumeau) [100] and adapted the dimensions of the explants to the dimensions required for our project.

Explants provided were cylindrical, with a 3 cm diameter and a thickness comprised within 1.5 and 2cm. Such dimensions allow the adhesive part to be fully placed upon the explant and the inserted cannula length to be within the depth of the adipose tissue (Figure 13: Explants from post bariatric surgery. A. 3 explants from one batch, in their survival medium. B. One explant, out of survival medium. C. Another explant with catheter and cannula inserted.).

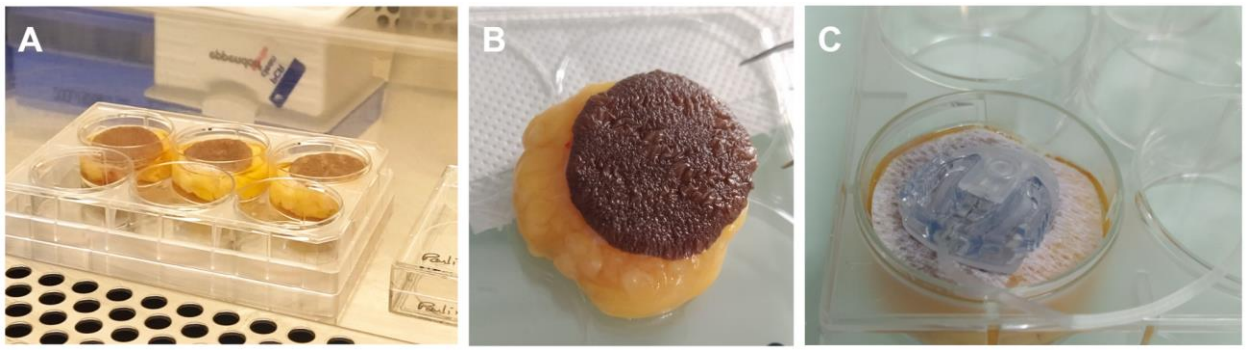

Figure 13: Explants from post bariatric surgery. A. 3 explants from one batch, in their survival medium. B. One explant, out of survival medium. C. Another explant with catheter and cannula inserted.

Such explants were provided in batches of 6, coming from the same donor. The only data available about the donors were their age, sex and phototype upon the Fitzpatrick scale [101] (Table 1:

Fitzpatrick Classification of Skin Types I through VI. Source: Ward WH, Lambreton F, Goel N, et al. Clinical Presentation and Staging of Melanoma, 2017).

Type I	Type II	Type III	Type IV	Type V	Type VI
White skin. Always burns, never tans.	Fair skin. Always burns, tans with difficulty.	Average skin color. Sometimes mild burn, tan about average.	Light-brown skin. Rarely burns. Tans easily.	Brown skin. Never burns. Tans very easily.	Black skin. Heavily pigmented. Never burns, tans very easily.
					

Table 1: Fitzpatrick Classification of Skin Types I through VI. Source: Ward WH, Lambreton F, Goel N, et al. Clinical Presentation and Staging of Melanoma, 2017

Overall this project, 13 batches of 6 explants were collected (Table 2). One donor was male. All samples were collected from **abdominal** surgery.

	Age	Sexe	Phototype (Fitzpatrick)
Donor 1	48	F	5
Donor 2	46	F	6
Donor 3	33	F	2
Donor 4	39	F	5
Donor 5	45	F	3
Donor 6	55	F	3
Donor 7	57	F	2
Donor 8	43	F	5
Donor 9	51	F	2
Donor 10	33	F	3
Donor 11	52	F	2
Donor 12	47	M	2
Donor 13	39	F	3
Mean age:	**45.23**		

Table 2: Available patient data: age, sex, skin Fitzpatrick scale

Before infusions were performed, explants were stored at 37°C in an incubator (95% humidity, 5% CO_2). The adipose tissue was immersed in the BEMc survival medium which was renewed every 2 days. All infusions were performed between 2 and 8 days after surgery.

Unlike a large number of studies [25–29,31], these explants are of human origin, rather than swine, which constitutes a big step towards clinical relevance. Yet these tissues come from patients who underwent post-bariatric surgery, and therefore who were once obese. High weight variations are known to increase fibrosis in the tissue and the amount of collagen in the interlobular septum [102]. Such a change is likely to increase the stiffness of the tissue [43], compared to tissue from non-obese patients, as are most patients with type 1 diabetes.
However, surgical tissue from non-obese patients, sourced from aesthetic surgery, is much rarer. Also, it is available in smaller amounts for one individual patient, for indeed less skin being removed: this provides less opportunity to explore intra-individual variability.
Although the possibility of collecting such non-obese tissue was discussed with Bio-EC, it did not occur during the scope of this project.

3.2 Covid 19 and confinement: waiting for human skin to be available, performing tests on pork tails

The Covid-19 crisis occurred just before the planned reception of the first human explants. Suddenly and for an undefined period of time, post-bariatric surgeries were not prioritized, therefore no longer happening. As a consequence, no human explant was available. Additionally, one had to stay home and no part of the project could start the way it had previously been defined.

At disposal were two pressure sensors (Elvesys MPS0), a flowmeter (Bronkhorst™ ML120), and insulin pumps (Tandem t:slim x2, Medtronic 640G, Ypsomed Ypsopump), which were temporarily retrieved from the lab and brought home.

A home test bench was constituted with pressure sensors, the flowmeter, and alternatively the Tandem and the Medtronic pumps (Figure 14). The following infusion mediums were used with water and blue staining (destined to food consumption) injected as continuous flow or boluses:

- Pork tail (destined to food consumption) bought from local butcher
- Gels made from various concentrations of gelatine, agar-agar and colza oil (all destined for food consumption). Concentrations of gelatine, agar-agar and oil were measured from home with no material other than teaspoons and are not reported later.

Infusions in pork tails were intended for follow up of infusion pressure and flowrate only. Due to the transparency of the gels, a visual, camera-based follow up of the insulin spread in the medium was also possible in addition to pressure and flowrate (Figure 15).

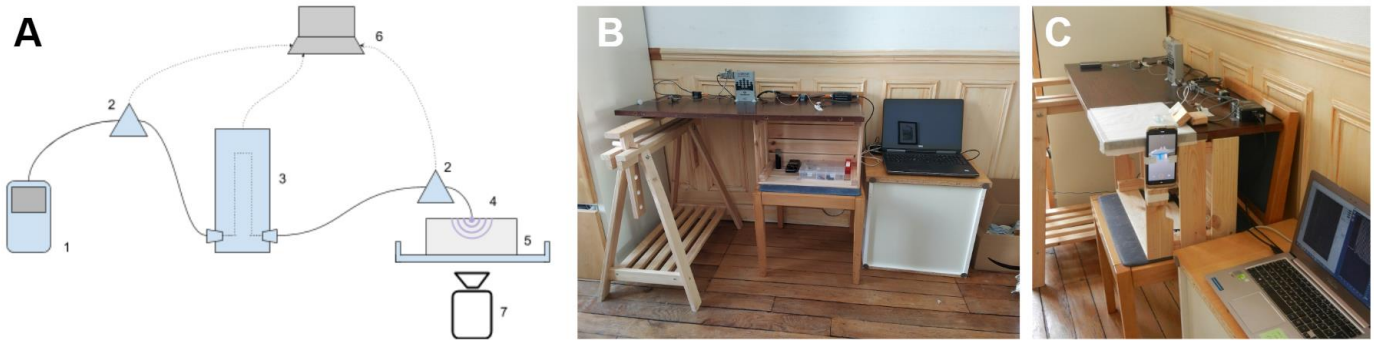

Figure 14: A. Home infusion bench setup: 1 - Insulin Pump. 2 - Pressure Sensors (upstream and downstream from flowmeter). 3 - Bronkhorst ML120 Flowmeter. 4 - Injection site. 5 - Agar gel. 6 - Real-time data collection. 7 - Camera (phone). B, C. Bench pictures.

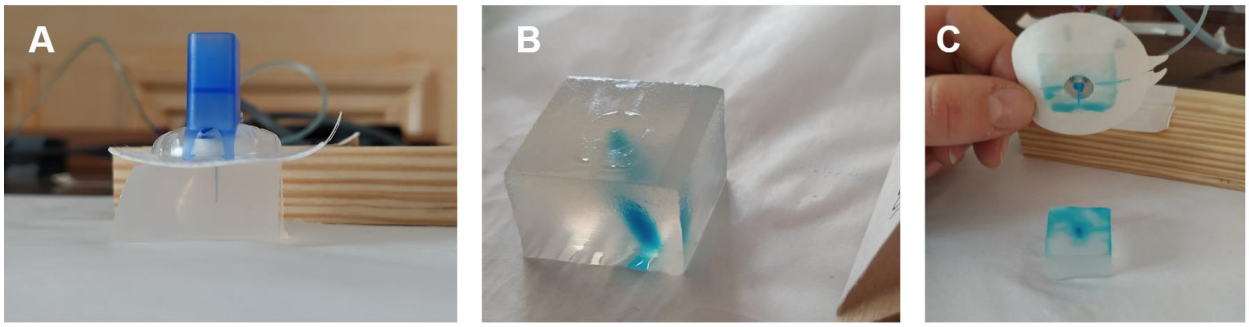

Figure 15: Infusing blue stained water into gel. A. A gel during cannula insertion. B. Blue stained water that spread along a plane inside the gel. C. Blue stained water on top of the gel at the end of infusion.

a. Pork tails infusions

18 basal infusions of at least 3h were performed in pork tails, at 2, 1, 0.5 and 0.1UI/h (Table 3: Durations observed before a pressure drop occurred in the tubing for 18 infusions performed in pork tails.). Observations of pressure during basal infusion in pork tail tissue showed on several occasions, pressure build-ups upon several minutes, sometimes hours, before an abrupt pressure drop (Figure 16).
This phenomenon happened in 78% of the infusions. In the other infusion situation, no pressure build-up was observed.

Basal rate (UI/h)	2	1	0.5	0.1
Duration before pressure drop (min)	15	20	35	105
	8	15	0	
	20	20	30	
	0	25		
	7	107		
	0	0		
	10			
	11			

Table 3: Durations observed before a pressure drop occurred in the tubing for 18 infusions performed in pork tails.

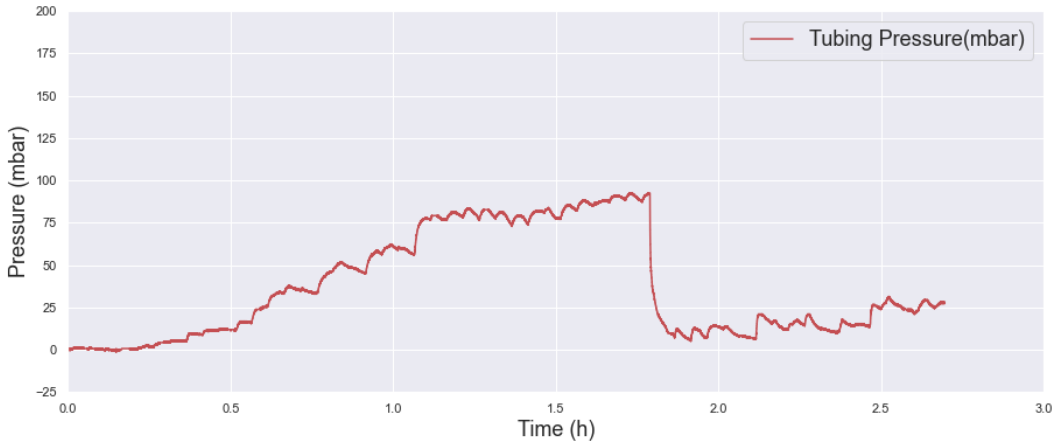

Figure 16: Pressure evolution inside the tubing during 1UI/h basal infusion in pork tail.

In bolus delivery, similar phenomena did occur. As for basal delivery, it did not happen in all the injected boluses. Also, it only happened on the first bolus infused in new infusion sites. For instance, in series of bolus of 2UI (Figure 17 A), only the first was preceded by a pressure peak (Figure 17 B). During the pressure build-up, the flowrate of delivery was lower than after the pressure drop (Figure 17 C).

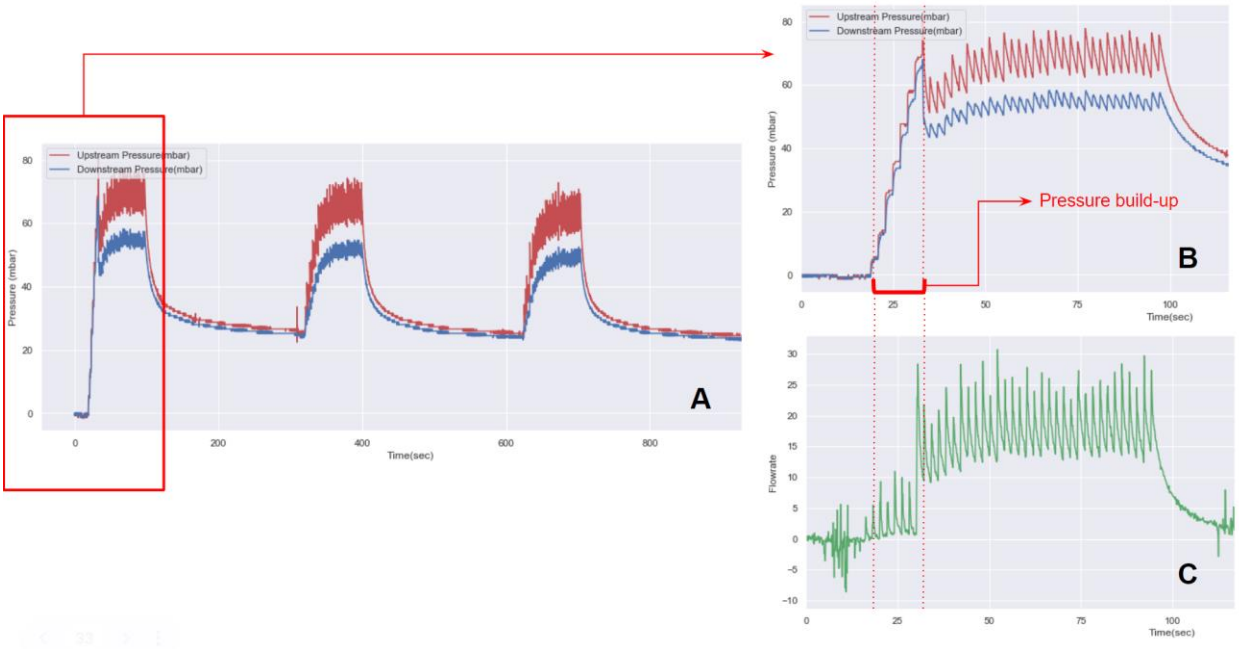

Figure 17: Pressure record of three successive 2UI boluses. Blue and red lines represent pressure upstream and downstream from the flowmeter respectively. A. Full test (800 seconds) with all three boluses. B. Extract of the pressure measurement during the first out of three bolus. C. Extract of flowrate measurement during the first out of three bolus.

b. Gelatine and agar-agar gels infusion

On the opposite, independently from the doses of gelling agents involved, none of the infusions performed in gels were associated with pressure elevations. Visual observation of the blue stained water infused inside the transparent gel (Figure 15) did allow to make the following observations:

- As soon as the infusion had started, blue-stained water spread inside the gel along a determined plane (Figure 15 B). The likely hypothesis is that the gel is too brittle and the infusion creates a mechanical constraint that splits the gel along a plane from the very initiation of the infusion.

- On some infusions, the blue stained water flowed back along the inserted cannula and went onto the surface of the gel (Figure 15 C). Such phenomena do exist in human insulin CSII delivery, with insulin accumulating at the surface of the skin (easily detectable by patients as humidity can be felt upon the skin, and insulin can be smelled).

The absence of pressure variation in the gels can probably be explained by the fact that blue-stained water spreads along a plane split open in the infusion medium. However, it appears to us that no

more information than this can be extracted from gel infusion: the absence of pressure build-up demonstrates that it cannot be compared to tissue infusion.

On the other hand, pork tails infusions provide two notable facts. Indeed, in our tests:

- **Pressure build-ups occur**, and can last for various lengths of time from 25 min to 2h30, on **new infusion sites only.**
- There is a **binary behaviour**: such build-ups on new infusion sites do not always occur. Either such build-ups happen (78%), or they do not, with no evident causality for this different pressure response.

3.3 First human skin explant infusions

A few months later, when the sanitary crisis was less acute, we had access to the first human explants of the project. It was the opportunity to test the same protocol upon human samples, with Insulin Aspart U100, a standard insulin analog used for CSII (Figure 18 A and B).

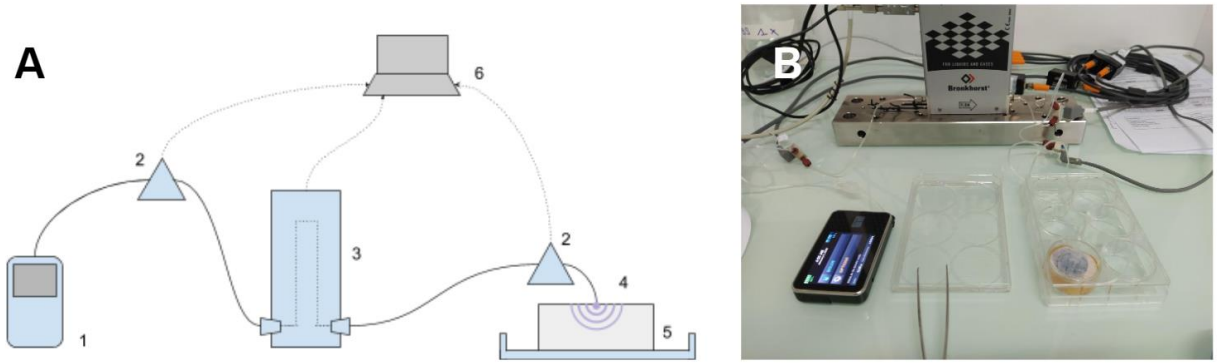

Figure 18: Lab infusion bench setup, with no imaging. A. 1 - Insulin Pump. 2 - Pressure Sensors (upstream and downstream from flowmeter). 3 - Bronkhorst ML120 Flowmeter. 4 - Injection site. 5 - Human skin explant. 6 - Real-time data collection. 7 - Camera (phone)
B. Picture of lab infusion bench during explant infusion.

Infusions were performed on 19 human explants with a basal pump delivery at 2UI/h, 1UI/h, 0.5UI/h and 0.1UI/h (Table 4: Durations observed before a pressure drop occurred in the tubing for infusions performed in 19 human explants.). Pressure data was collected through the sensors with the Elvesys Elveflow software and plotted. A similar phenomenon to pork tail infusion was observed: pressure build-ups were observed, in 52% of infusions. When build-ups were observed, the mean duration before pressure drops was of 18.75 min (minimum of 5 min, maximum of 45 min) for infusions at 1 and 2 UI/h, and of 78 min (minimum of 40 min, maximum of 9h) for infusions at 0.1UI/h. Figure 19 A provides an example of pressure record where no pressure build-up was observed, whereas Figure 19 B displays the pressure record of an infusion where a pressure drop occurred after 25min.

Basal rate (UI/h)	2	1	0.5	0.1
Observed duration before pressure drop (min) for tests performed on 19 different human explants	10	15	0	170
	25	0	0	540
	25	15	0	45
	5	0	0	0
		45		0
		10		

Table 4: Durations observed before a pressure drop occurred in the tubing for infusions performed in 19 human explants.

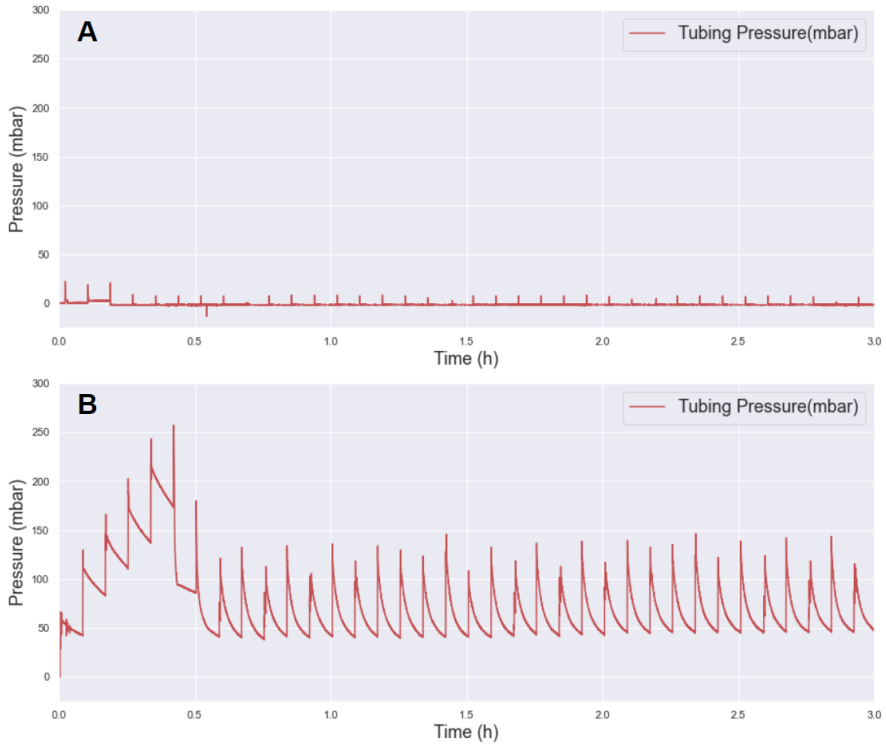

Figure 19: Pressure record of two human explant infusions. A: Delivery at 0.5UI/h, no pressure build-up observed. B: Delivery at 2UI/h, pressure build-up observed until 25min of delivery.

3.4 Hypotheses triggered by pressure build-ups

From these non-systematic pressure build-up observation, and with no imaging opportunity at the time, we built the following **hypothesis**: in a new infusion site, a **local retention of the infused insulin** occurs, with a **pocket of fluid** created within the adipose tissue being progressively filled with the fluid (Figure 20). While the pocket is being filled, pressure increases inside the pocket and therefore, inside the tubing which is directly connected to the pocket via the cannula. Once a

critical pressure is reached, the pocket bursts, and the pressure drops, allowing the insulin to spread further away in the tissue.

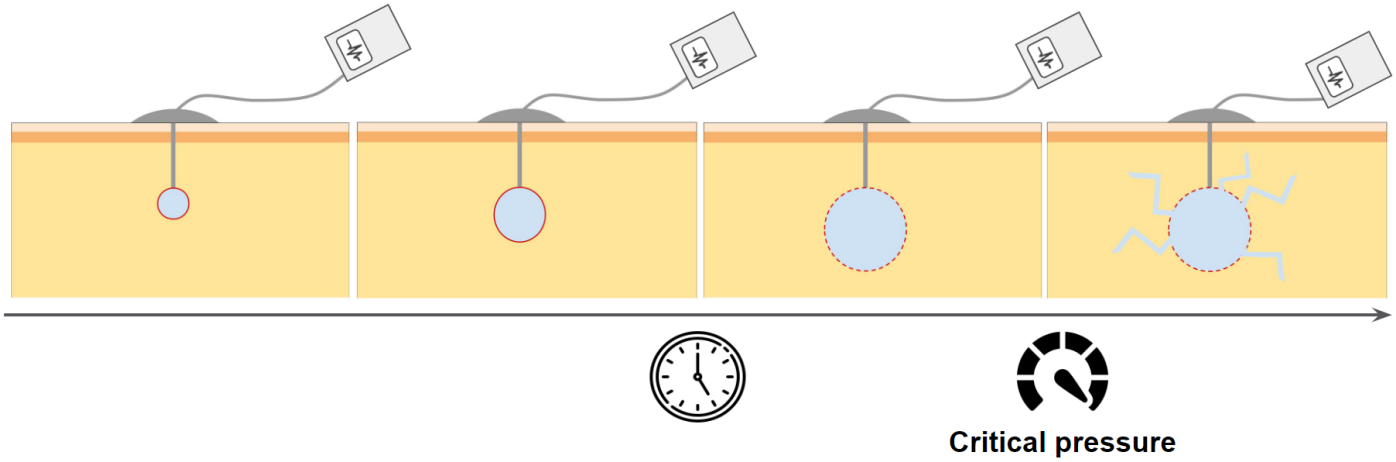

Figure 20: Illustration of the insulin retention hypothesis

This hypothesis would contribute to explaining the pressure build-up observed, **however it does not explain that this observation is not systematic**.

In order to explain the non-systematic pressure build-up, an additional hypothesis was developed upon that first hypothesis. As stated previously, the subcutaneous adipose tissue is constituted of fat lobules that are separated by an interlobular septum mostly formed of collagen. Some studies do suggest that insulin propagates along the path of least resistance in the tissue, which could be this septum [103].

We hypothesise the following: when the cannula is inserted in such a way that the tip of the cannula is at the interlobular septum, insulin propagates immediately when delivered. There is then no retention and no pressure build-up. On the other hand, when the tip of the cannula is inside a lobule, a retention and the associated pressure build-up is observed.

a. *What would be the clinical impact of those hypotheses?*

If a retention occurs at the infusion site, and a pocket of fluid is being progressively filled, then, as long as this pocket has not burst, only the insulin located at the external surface of the pocket is really bioavailable. Hence, the bioavailability of the infused insulin is much more reduced than it should be for one given amount of insulin delivered.

In that context, ruling on such a hypothesis could be especially clinically relevant as the amount of time observed before the pressure drop reaches several hours in some of the infusions.

b. Failure to test the lobule hypothesis

As no imaging was available then, fat lobules were isolated from one another from some explants with the intention of separately infusing them (Figure 21 A). If 100% of the infusions targeting directly the centre of an isolated lobule were associated with a pressure build-up, the hypothesis would be strengthened.

This apparently simple protocol was unfortunately impossible to properly execute for the following reasons:

- Infusions in single lobules were very challenging (Figure 21 B), although solutions were found to prevent movement of both the cannula and the lobule by casting the lobules into gelatine gels (Figure 21 C).
- The mechanical action of detaching the lobules from one another was damaging the lobules, provoking ruptures in the surrounding pellicule of interlobular septum. This undermined the chances of indeed observing pressure build-ups in the case the hypothesis was true.
- One never fully knew if one isolated lobule was not actually several lobules still attached together, and therefore, if no interlobular wall really did not cross the isolated fat pad. Indeed, eye observation was insufficient and lobules dimension did not allow systematic microscopic observation.

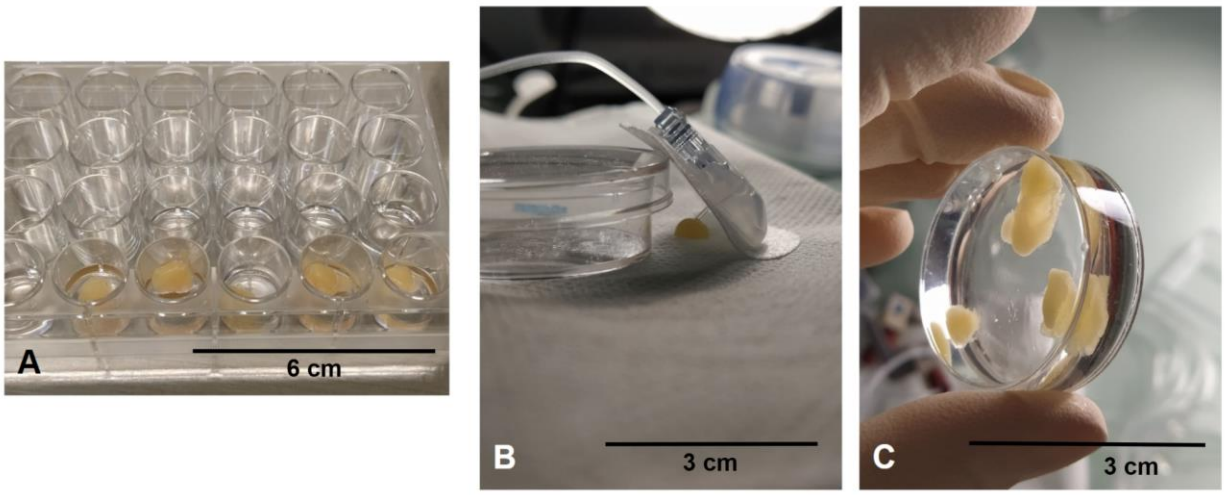

Figure 21: Fat lobules. A. Isolated lobules. B. Struggling to infuse an isolated lobule. C. Three lobules (or sub-groups of lobules) cast into a gel.

3.5 Imaging the tissue

a. Static imaging

One study from Jockel et. al [26] has performed some static ex-vivo imaging of boluses of dyed insulin delivered using a pump in swine tissue (abdominal and kidney regions). They snap-froze

the samples after infusion and performed systematic 20µm cuts in planes parallel to the epidermis. At each slice, and photographed the tissue which displayed the location of the insulin thanks to the dye (Figure 22 A). This allowed them to rebuild rough 3D reconstructions of the insulin depots (Figure 22 B).

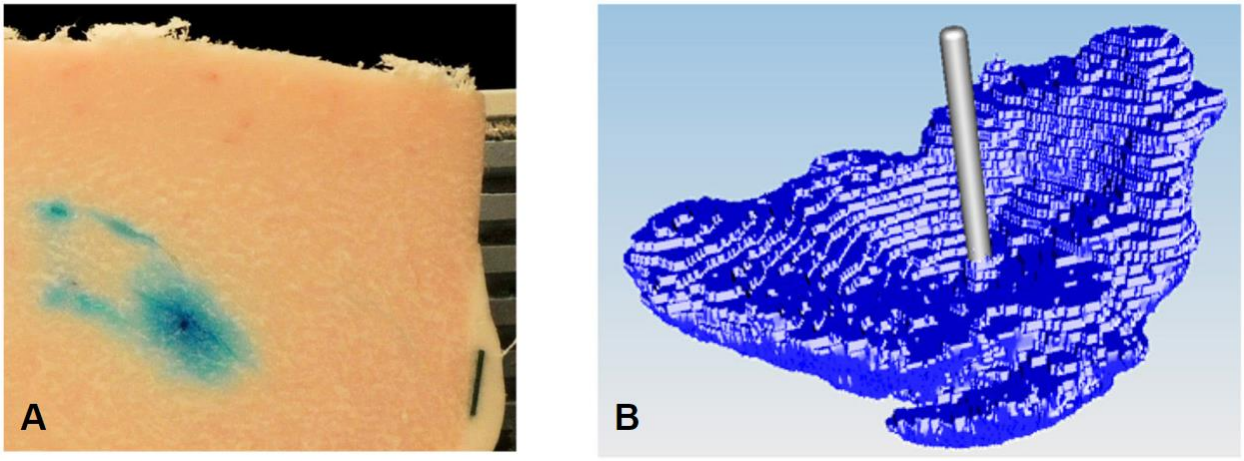

Figure 22: Reconstruction of insulin depot based on frozen cuts photography. Source: Jockel et. al, 2013. A. Photograph of frozen swine sample infused with dyed insulin, sliced in a parallel plane to the epidermis. B. 3D reconstruction of insulin depot based on slices photographs.

In order to have a more precise idea of the shape of an insulin depot after basal delivery, we similarly performed static post-infusion imaging. Although some blue dye was added to the infused insulin Aspart U100 in order to spot the location of the infused region during the cutting process and identify the slices of interest (Figure 23), **we performed insulin identification using fluorescent histological staining**.

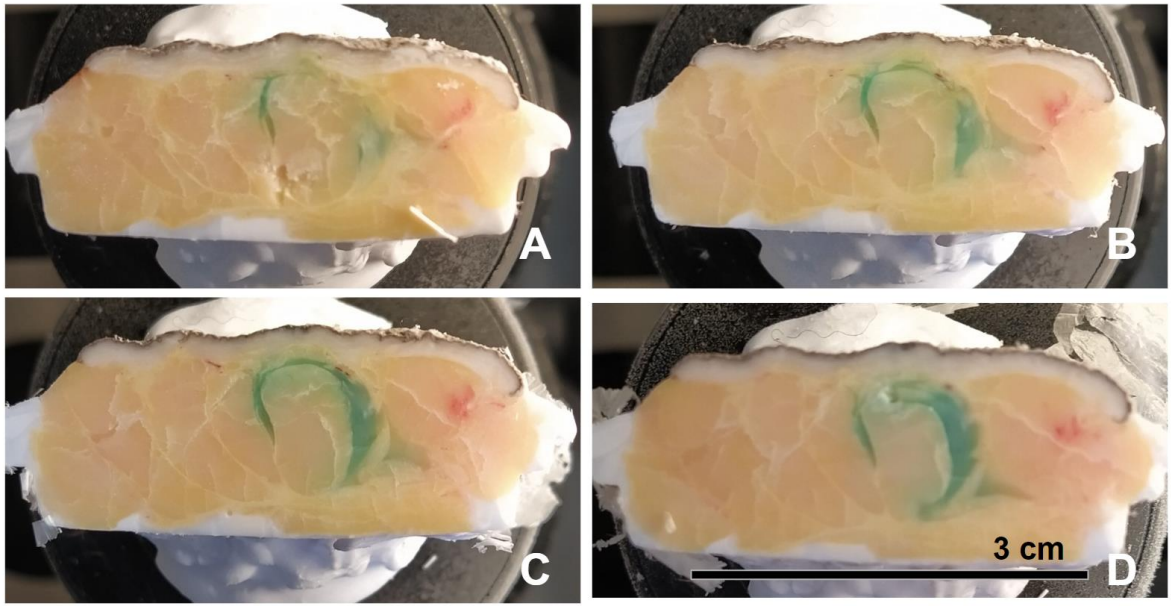

Figure 23: Photographs of snap-frozen human skin explant and infused insulin with blue staining, during the cutting process. Slice plane orthogonal to the epidermis. A, B, C, D: Slices of the same explant, at various depths of the sample.

i. Staining protocol

Explants were embedded within an OCT gel (Q path tissue OCT, ref 00411243, VWR chemicals). Cuts of 8µm were performed at -30°C using a cryostat (Leica CM3050 S). Slides were kept at -80°C before histological processing.

Slides were then put at ambient temperature in 4% formalin (HT501128, Sigma-Aldrich) for 10min. After antigen retrieval, a bovine serum albumin (A2153-100G, Sigma-Aldrich) blocking was performed in PBS with 3% BSA.

The insulin Aspart which was infused in the explants is an insulin analog with slight amino-acid modifications. The antibodies developed for insulin staining are most generally used for endogenous insulin identification. Although the amino-acid change of insulin Aspart is minimal compared to original insulin (aspartic acid replaced by proline in B28 position), not all primary antibodies were efficient. After trying to adapt several protocols with an rabbit-produced C27C9 anti-insulin antibody, we were advised an mouse monoclonal anti-insulin alternative primary antibody (clone K36AC10) [104] which did mark the infused insulin analog successfully.

Slides were incubated with primary antibody (1:1200 in PBS) for 2h and twice rinsed with PBS for 5 min.
Anti-mouse 647nm fluorescent secondary antibody (ab150127, Alexa Fluor® 647, Abcam) incubation (1:200 in PBS) lasted 1h and was twice rinsed with PBS for 5 min.

Counterstaining with Hoechst (Hoechst 33342, Thermoscientific) at 1:10000 was left for incubation for 1 min and was twice rinsed with PBS for 5 min before mounting.

Additionally, on separate slides, picrosirius red was used to stain collagen in the tissue [105]. The Picrosirius red protocol can be found in annex.

ii. Histological images

This allowed to generate images of explants infused with insulin Aspart.

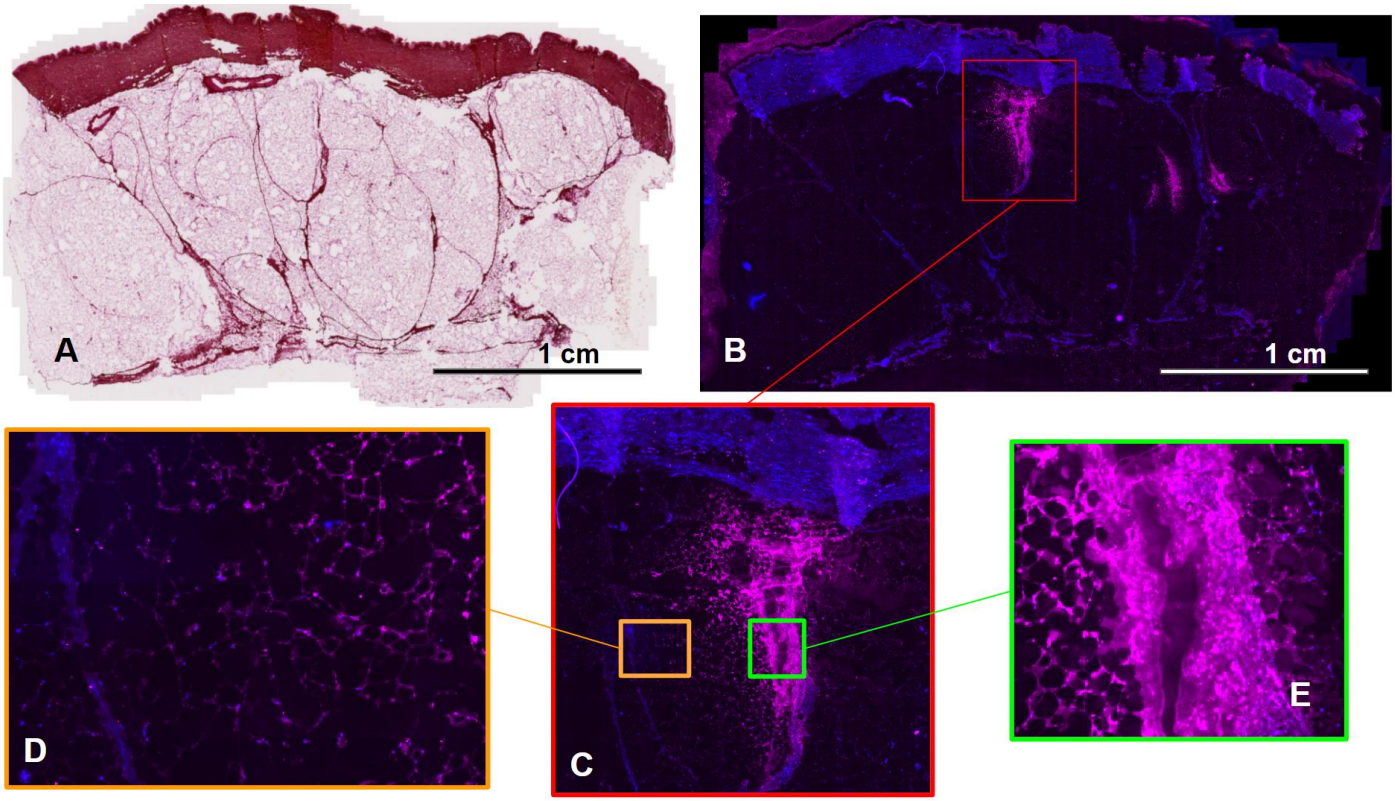

Figure 24: Picrosirius red-stained and immunofluorescent slides of insulin-infused explant. A. Picrosirius red stained slice. B. Immunofluorescence slide of the same explant (647 nm for insulin staining, pink; 457 nm for Hoechst nuclei staining, blue).
C, D, E: Magnifications of B.

These fluorescence and picrosirius red images of the explants **display several features**:

- Picrosirius red staining, which colours collagen, is positive in the dermis and on thin lines which divide the hypodermis in compartments (Figure 24 A). **These lines constitute the interlobular walls** (see structure of the skin tissue, Chapter 1).
  In between these walls, **adipocytes are apparent** (Figure 24 D). Hoechst staining colours all cell nuclei in blue, including adipocytes (Figure 24 D).

- Insulin is visible in pink (647 nm) (Figure 24 B). It is **mostly present in between the lobules, along the septum**. Successive photographs of the slicing process also display a presence of insulin around the lobules (Figure 23). This **suggests a preferred propagation along the interlobular septum**.

- Inside the areas positive for insulin (Figure 24 C) are black areas, with no fluorescent signal (Figure 24 D), including no signal for Hoechst coloration, which displays all cell nuclei. There is therefore no tissue in these regions: **the surrounding tissues were torn**, thus the empty space on the slice. These tearings could either have occurred during the slicing process or during infusion itself, but suggest anyhow a **local mechanical weakening of the tissue in the areas where insulin was infused**.

Despite the quality of the histological images and the precious information collected, these provide **limited information concerning the propagation in the tissue through time**. Therefore, we explored the different imaging technologies available to dynamically follow a basal pump infusion in the tissue.

b. Dynamic imaging

In order to obtain a dynamic follow-up of insulin propagation, three main technologies were considered: **micro magnetic resonance imaging** (µMRI), **micro computed tomography scanner** (µCT), and **ultrasound**. Criteria did not only include the possibility for dynamic imaging, but also the possibility to perform additional measurements such as pressure and/or flowrate measurements upstream from the infusion site. Also, considering the choice to image basal delivery, the insulin volume delivered by one impulsion should be detectable. Indeed, the smallest volume delivered per impulsions at a standard rate of 1UI/h upon all pumps on the French market is 0.83µL (t:slim x2), which corresponds to a spherical volume of radius 0.58mm.

i. µMRI

MRI dimensioned for the imaging of small animals was one of the considered imaging possibilities. In such a case, insulin would have been infused with a gadolinium contrast agent.
However it did not appear achievable to keep the pump at sufficient proximity of the imaging chamber to ensure delivery without **damaging the pump due to the magnetic field**. Similarly, performing additional measurements (pressure and/or flowrate) was **not possible without damaging the measurement equipment**.

ii. Ultrasound

High-resolution ultrasound measurements were discarded because the **required resolution necessary to detect 0.5mm objects could not be reached** for wavelengths within 13 and 50MHz, which are the necessary range of wavelengths to image deeper than 1cm in the tissue [106].

iii. µCT scanner

The µCT scanner we had access to was designed for in vivo imaging [107], and therefore had a chamber protecting the pump from the X-rays and enabling additional measurements.
The adjunction of an iodine-based contrast agent was necessary. **Superposability of iodine contrast agent and insulin subcutaneous depots** in the case of a mixture of insulin and CA injection **has already been demonstrated** [28].
Up to an 9µm resolution is available on this device [107], which is **sufficient to detect the insulin impulsions** at standard BR.

For these reasons, we chose to use a µ-CT scanner. Precisions on the operation principle of this imaging technique will be detailed in *Chapter 4*.

In order to ensure a basal delivery in conditions as close to reality as possible, and due to the small diameter of the delivering cannulas of the pumps, we ensured that viscosity of the contrast agent and insulin mixture that we used was minimally impacting the viscosity of the fluid. These viscosity test results are available in the annex of the article presented in *Chapter 4*.

3.6 Towards synchronised and continuous imaging and pressure recordings of basal CSII delivery in human explants

When the Covid-19 crisis acute phase was over, synchronised access to human explants and to imaging through µCT scanner was finally available.

At this stage, our objectives were clear:

- Using these tools, building a method that would allow to **describe insulin propagation** in skin explants, using both imaging, pressure and maybe flow rate. The intent was to be able to use this method to compare infusions with various infusion parameters (pump model, basal rate, cannula length, shape and material).
- Using this opportunity to **confirm or infirm the retention and the lobule hypothesis**.

Our observations of **pressure build up at the initiation of infusion sites** on one the one hand, and the existence of studies demonstrating **glycemic excursions shortly after catheter change** [33] on the other hand, strengthened the **relevance of such an ex-vivo study in skin tissue that had not previously been infused with insulin**. This was the opportunity to study specifically the

insulin propagation (and potential insulin propagation failures) at the initiation of the new infusion site, likely to affect the efficiency of the administration during the first hours of infusion.

Chapter 4: New ex-vivo method to objectively assess insulin spatial subcutaneous dispersion through time during pump basal administration (including submitted article)

Preliminary experiments described in *Chapter 3* have **strengthened the relevance of studying insulin spatial propagation in the tissue in insulin naive skin samples**. µCT-scanner has been identified as an adapted imaging technique, compatible both with a 3D follow-up of the infusion through time and with additional continuous measurements (pressure and flowrate in the tubing).

The present section first describes the digital image processing that has been performed for the analysis of µCT outputs, as it could only briefly be described in the article. Then, the submitted article "New ex-vivo method to objectively assess insulin spatial subcutaneous dispersion through time during pump basal administration" is displayed.
We will then come back to the retention and lobule hypothesis stated in *Chapter 3*. Finally, we will present the results of some additional experiments that were performed, where two basal rates and another pump were introduced.

4.1 µCT Image processing

In the previous chapters, we described what led us to choose micro-computed tomography (µCT) to image the explants and the contrast agent (CA) and insulin analog infused depot.
A key-endpoint was also identified: the surface-to-volume ratio (STVR) of the insulin depot inside the explant. Therefore, it is critical to be able to identify the location of the insulin depot inside the explant on the µCT images. This step, which consists in differentiating the part of interest in an image from the rest of its content, is called segmentation.

In this section, we will shortly summarise the structure of the data. We will then detail how simple thresholding could not possibly suffice to achieve the computation of STVR. A first segmentation attempt was performed using a region-growing algorithm: we will explain why we chose not to pursue with that method. Then, we will introduce the method on which we settled and develop its main advantages.

We wish to stress the fact that all the processing introduced hereafter had to be very reproducible as it had to be applied identically and automatically upon all explants. Overall, 12 explants were used in developing the method and the image processing. 24 explants were studied as the whole experimental process was set.

a. Brief description of the raw image data

µCT raw data consists of a series of radiological projections. This series then requires tomographic reconstruction to obtain a stack of 2-dimensional cross-sections forming a single 3-dimensional image.

These radiological projections are taken at a fixed rotating angle from the object.
In our setting, 328 radiological images are acquired every 5 minutes (Figure 25), with a tilt rotation angle of 0.6° between two consecutive images. These parameters were chosen specifically to reach a whole-explant acquisition time of 5 minutes.

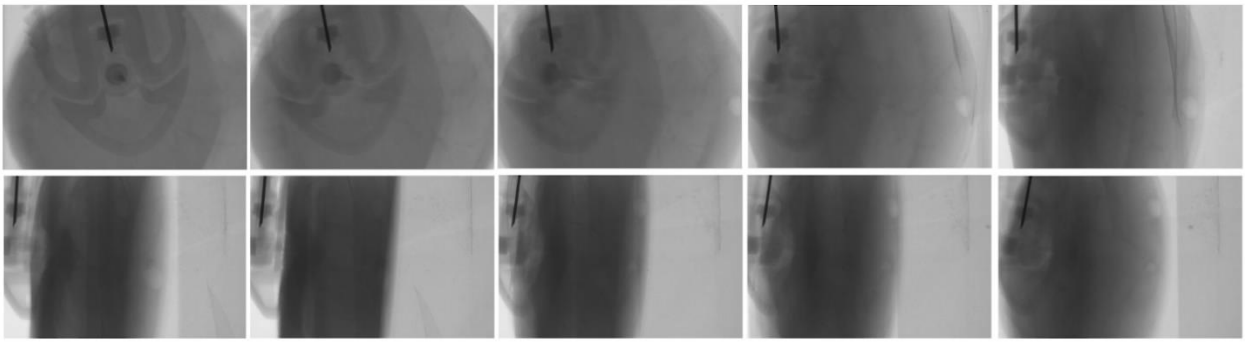

Figure 25: Ten images extracted from a series of radiological projections for one explant

From that series, tomographic reconstruction is performed using the Nrecon software, provided by Brucker (™). The output of reconstruction consists of a 1000-images stack (Figure 26). These 2D cross sections are slices of the 3D image of the explant (Figure 27).
This reconstruction step embeds strong Gaussian smoothing of the images, allowing to drastically limit the noise in them.

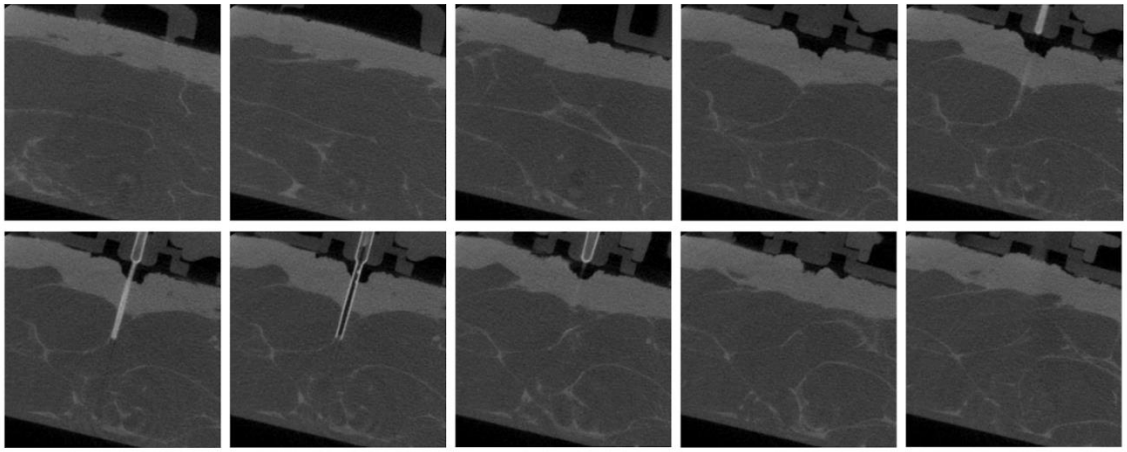

Figure 26: 10 images extracted from the reconstruction stack

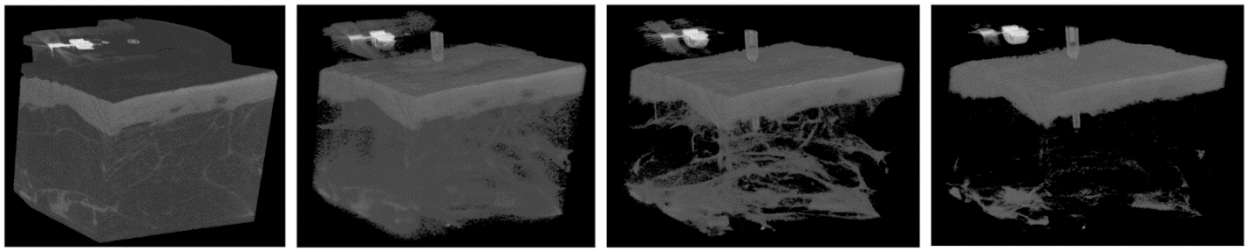

Figure 27: one single 3D-image, displayed from full opacity (left) to increasing levels of transparency for the lightest grey-level, so as to reveal the interlobular structure and the cannula inserted into the tissue.

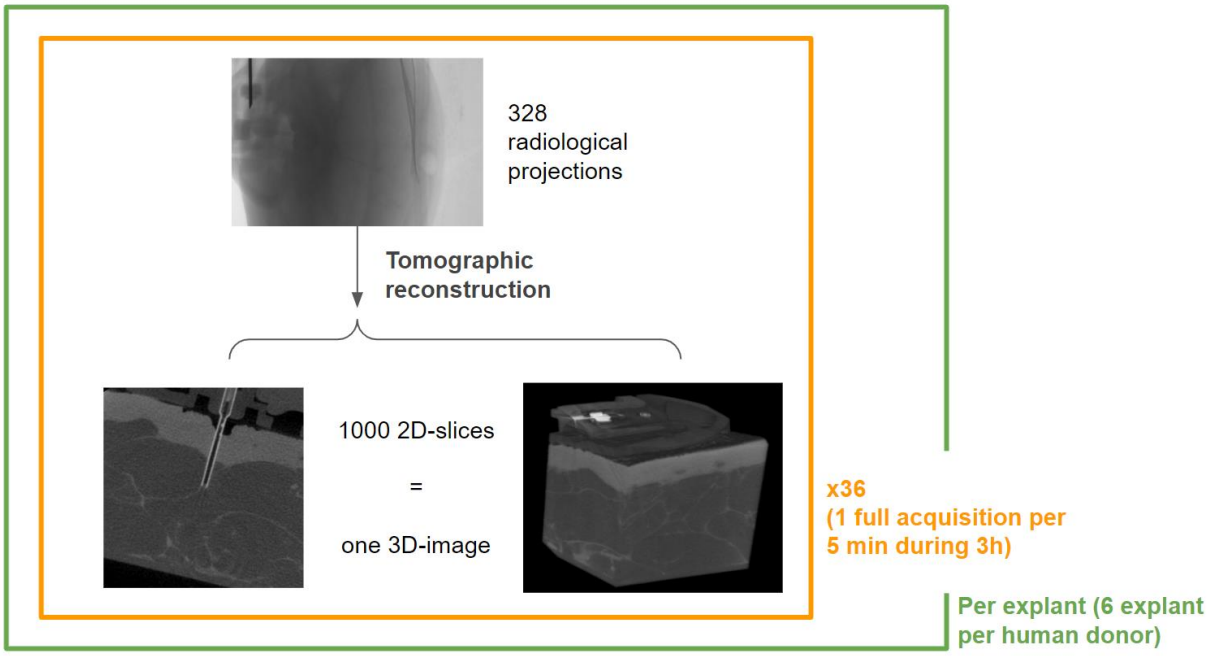

Figure 28: Graphical summary of raw image data structure

From this point on, no more reference will be made to radiological projections and when images are mentioned, the 2D cross-sections are designated (Figure 26), unless specified explicitly.

Visual summary of data structure can be found in Figure 28.

b. Requirements for this segmentation: why is more than thresholding required?

We previously argued that critical morphological endpoints to studying insulin subcutaneous depot were the **volume** and the **surface area** of that depot, from which STVR is computed.

Considering that insulin is associated with CA, the depot is radiopaque, therefore appearing lighter on the images. Each image is a 2-dimensional matrix of pixels containing integer values ranging from 0 (black) to 2^{16} (white).

The histogram below (Figure 29A) shows the repartition of grayscale values for a standard image of an explant after 3h of infusion. Thresholded images are shown Figure 29B-F. It allows one to see that dermis, subcutaneous insulin depot and cannula are visible on Figure 29D but only parts of the cannula, and no insulin depot, are left visible on Figure 29F. One can deduct from those that the insulin depot grayscale values are between 2.2×10^4 and 4×10^4.
A first basic approach would then be to determine one threshold value within that range, above which a pixel is considered to belong to the insulin depot, and below which it does not. The binary object resulting from that operation would then be the insulin depot, from which any morphological characteristic could be computed.

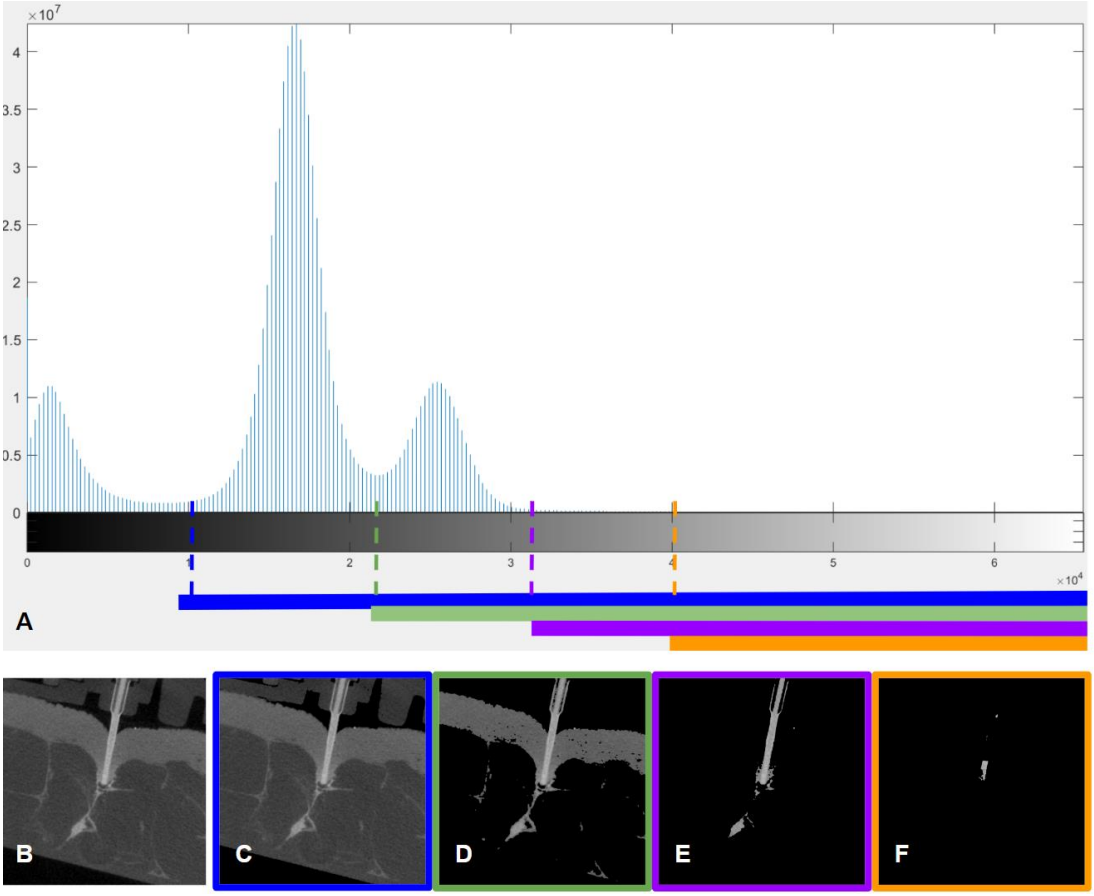

Figure 29: Histogram of a 3D image and illustrating cross-sections
A. Histogram of a 3D image (all 2D cross-sections included) for an explant after 3h of infusion.
B. A 2D cross-section of that 3D image
C. 2D cross-section with all values below 1×10^4 removed (threshold 1×10^4)
D. 2D cross-section with all values below 2.2×10^4 removed (threshold 2.2×10^4)
E. 2D cross-section with all values below 3.1×10^4 removed (threshold 3.1×10^4)
F. 2D cross-section with all values below 4×10^4 removed (threshold 4×10^4)

However, due to noise, but also the fact that reality contains only a continuum of grayscale values rather than strict differences in opacity levels, one would not then obtain a single object that can be identified as the insulin depot, but a multitude of small binary objects. These numerous binary objects can still be located within the insulin depot region, but yet be disconnected from one another. This is illustrated in Table 5: Number of connected components in the binary images of one explant according to the threshold value (18-connectivity), where 10 3D-binary images were generated by thresholding within the previously identified range. The number of connected components inside the binary 3D images is presented according to the threshold value.

Threshold value ($x10^4$)	2.2	2.4	2.6	2.8	3.0	3.2	3.4	3.6	3.8	4.0
Number of connected components in the binary image	6108	3133	10155	14534	3451	360	88	73	86	84

Table 5: Number of connected components in the binary images of one explant according to the threshold value (18-connectivity)

This poses a major issue as to the computation of surface area of the depot, which **artificially increases if the depot is composed of many small binary objects** rather than one connected binary region.

This is why it is essential that the segmentation achieves to isolate a **connected region rather than multiple binary objects**. One could argue that heavy smoothing applied to the images may reduce the probability for a large number of binary objects. However we have not achieved to reach both a smoothing that did not cause excessive information loss, and a satisfactory single-object binarization by thresholding.

c. Of the interest in region-growing algorithm and the limits we met

This criteria for a connected region detection must have been identified also by previous authors studying insulin depots. Indeed, although it is not reported as an issue, Mader et. al [38] explain they have used a region growing algorithm to isolate the insulin depot : from a spot of high intensity, neighbour voxels are aggregated to the region of interest on a decreasing level of intensity criteria. The aggregation process stops when the region of interest reaches the volume known to have been injected.
By construction, this operation guarantees that a single connected object has been segmented.

We did try to perform this strategy in our setting, using a region-growing algorithm available on the Matlab sharing platform [108].
We met two difficulties in the implementation.

The first challenge was met as the algorithm we used did not converge in most of the computations. This was solved by applying a stronger Gaussian filter at the reconstruction step, which reduced the likelihood of growing a region from an exceptionally dark pixel, unrepresentative of its surrounding region.

The second challenge had another cause. In many infusion situations, the tip of the cannula reached a region that was near the dermis (Figure 30: Infused explant with tip of the cannula close to the dermis. Result of the region-growing segmentation numerically identified in green on the second image.), which is denser, and therefore appears whiter than the hypodermis. Such regions are then partially aggregated with no true knowledge of whether CA has infused that dermal region or if part of the dermal region is segmented only due to its lighter shade and proximity to the actually infused region.

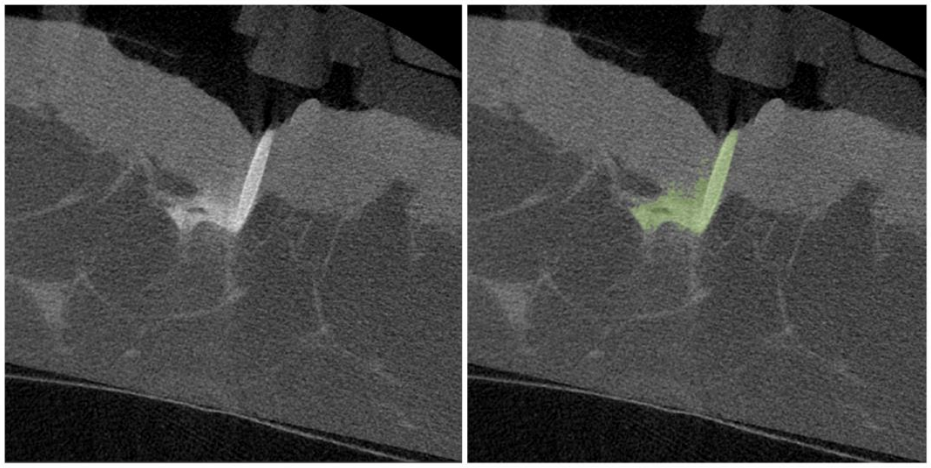

Figure 30: Infused explant with tip of the cannula close to the dermis. Result of the region-growing segmentation numerically identified in green on the second image.

d. Taking advantage of the model: initial image before infusion and subtraction

Imaging throughout the infusion is a specificity of our model. It is a challenge, as keeping acquisition time below 5 minutes comes at the price of reducing image resolution. However, it has one benefit: it is easy to have an image of the explant before infusion has started. Moreover, the explant is submitted to no movement or change in setting position from the beginning to the end of the experiment.

From this acknowledgment came the idea of fully imaging the explant before the infusion and subtracting the insulin-free explant from all the images acquired during the infusion.
This allows to eliminate all the structures that are repeated patterns onto all images: the dermis, the hypodermis, and even the catheter structure which is on the top of the explant, as visible in Figure 31.

If at some point the infused content also reaches the dermis in an experiment, the dermis infused with CA will still be more opaque than the dermis before infusion and the result of the subtraction will show that insulin and CA did reach that area.

After this step, all further processing can be performed on the result of the subtraction (Figure 31C)

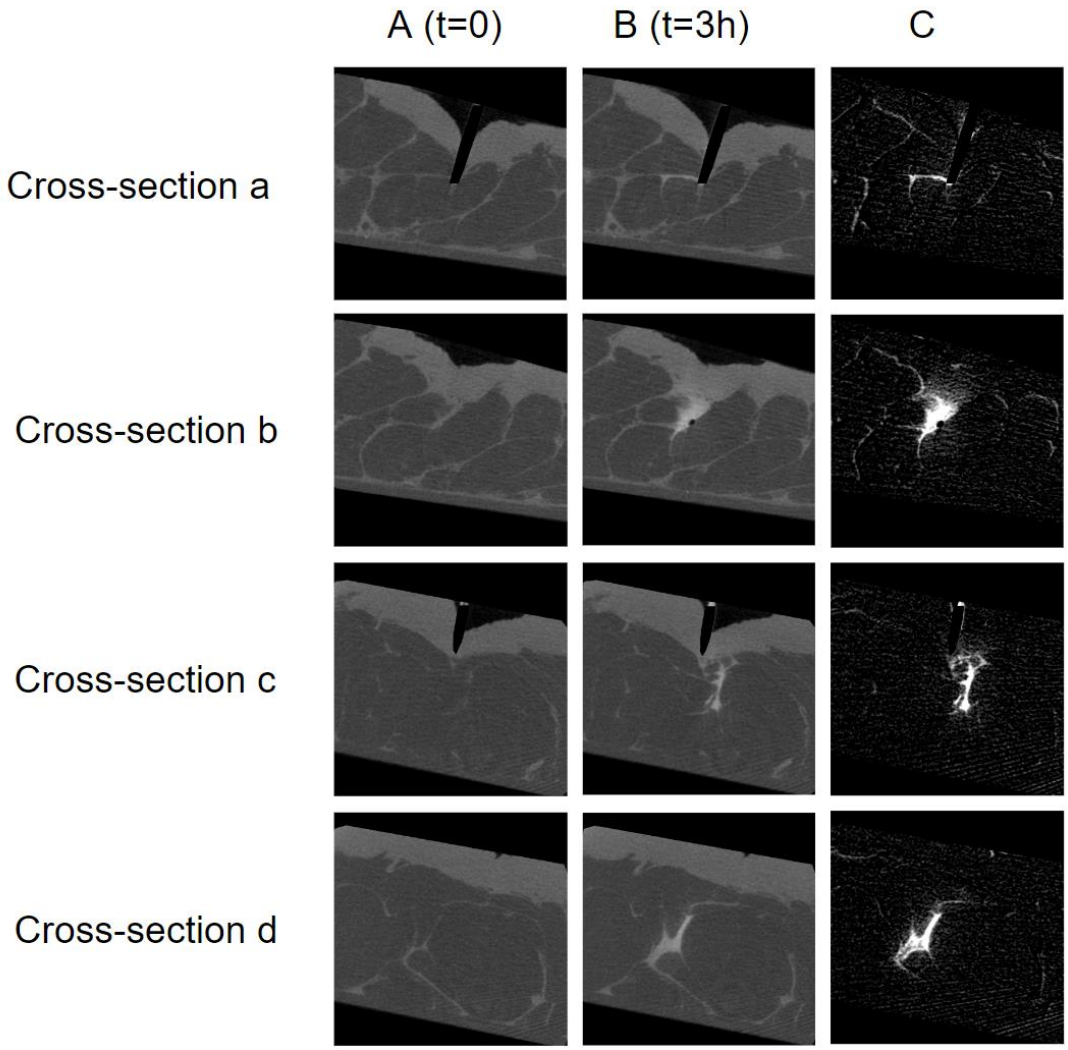

Figure 31: Four cross sections from several explants (cross sections a, b, c, d). Column A: cross sections at t=0. Column B: cross sections at t=3h. Column C: Result of subtraction between B and A.

Side note:
Due to the need to keep acquisition time below 5 minutes, only 180° rotations were performed to acquire each image. Therefore, the X-ray source and receptor would first turn clockwise during the first acquisition, then counter-clockwise for the second, and so on (Figure 32).

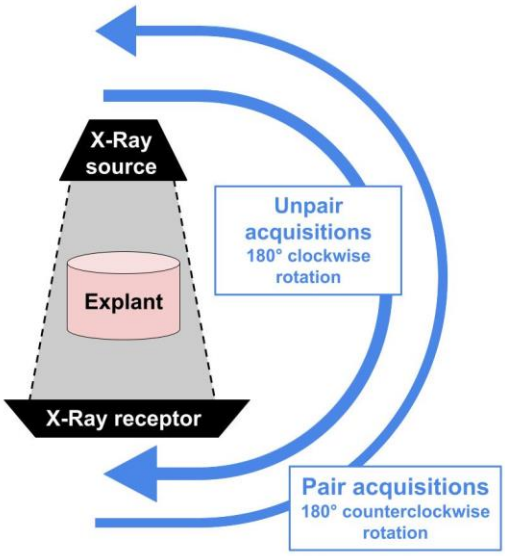

Figure 32: Rotation of X-ray source and receptor according to acquisition timing

The consequence of this is a slight angle tilt between odd and even images.
Therefore, during this subtraction step, image 1 is subtracted from odd images, and image 2 from even images.
It is the reason why two images are acquired before starting pump delivery rather than just one (see acquisition plan, Figure 33)

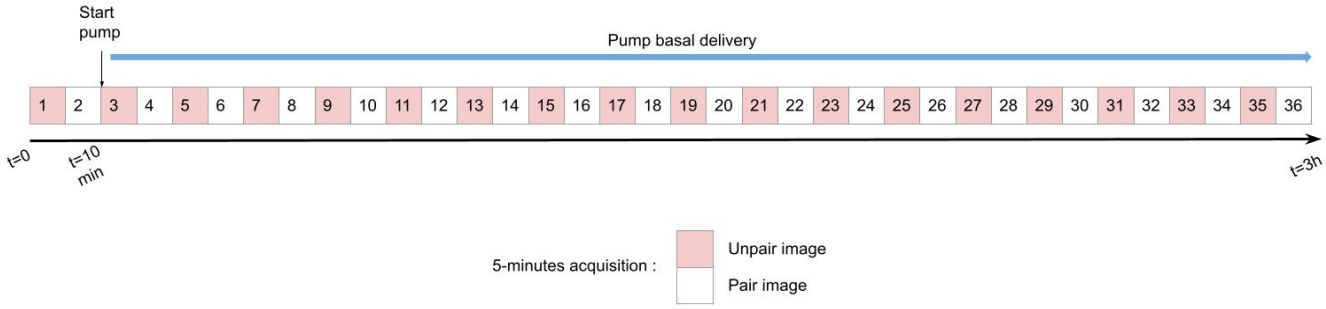

Figure 33: Acquisition timing display

e. Processing the images resulting from subtraction

i. Removing cannula content

Frequent air bubbles were observed inside the cannula inserted into the tissue (Figure 34). As a result, in those images, the cannula did not appear uniformly white (being filled with insulin and CA) but with black patches.

These variations inside the cannula generate artefacts on the result of subtractions. Also, cannula content is of no interest to the morphological study of the insulin depot, therefore cannulas were systematically removed before subtraction, based on a manual selection of the cannula cylinder coordinates on the first image.
Cannula content according to time was however studied by itself, as will be described later.

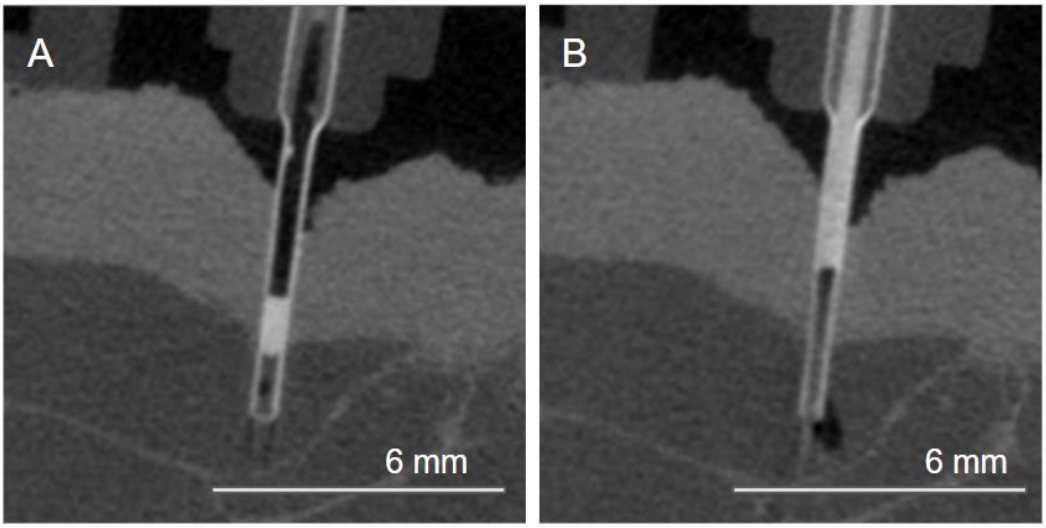

Figure 34: Example of air bubble located inside the cannula during the infusion. A. Before infusion. B. During ongoing air bubble infusion

ii. Linear transformation

As an illustration, a few images from various explants are provided in Figure 31 where an initial cross-section, the corresponding section during the infusion and the result of the subtraction are presented side by side.

The intensity of the signal is reduced due to subtraction. Therefore, a linear transformation was applied to the result of the subtraction. A histogram of the subtraction result for one explant is shown in Figure 35 A. As the maximum values that were observed upon all histograms after 3h of infusion were around 14600, we took a margin and chose 15000 to become the highest pixel value. Therefore, a systematic linear transformation of factor $(10^{16}-1)/15000$ was applied for all explants at this step. Figure 35 B presents the same histogram as Figure 35 A after linear transformation.

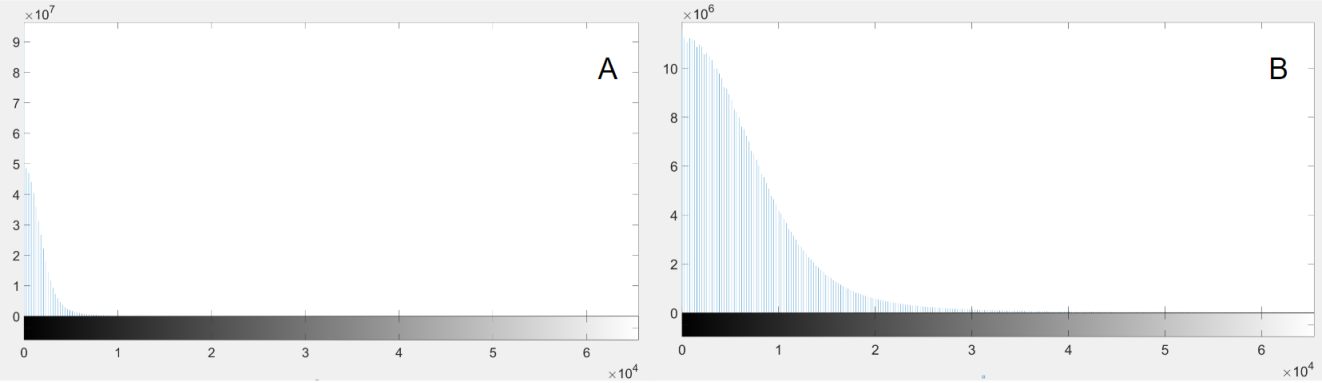

Figure 35: Histogram of explant 3D image after subtraction of initial image (A), and after both subtraction of initial image and linear transformation (B).

Note to the reader: for visibility purposes on this document, it is the results of subtraction once linear transformation was applied that were presented in previously introduced Figure 31 C.

iii. Thresholding

At this point, images are still not binary, as required to compute a volume and a surface area.
A thresholding step is therefore still necessary.

There are slight variations in grayscale values from one explant to the other, although data is rather homogenous. It was necessary to find a threshold criteria applicable for all explants that would make the results comparable from one explant to the other, but would still be adapted to the particularities of each.

At this stage, after subtraction and linear transformation, most of the signal actually visible on the images is the depot. The rest of the signal is a relatively important noise (see Figure 36).

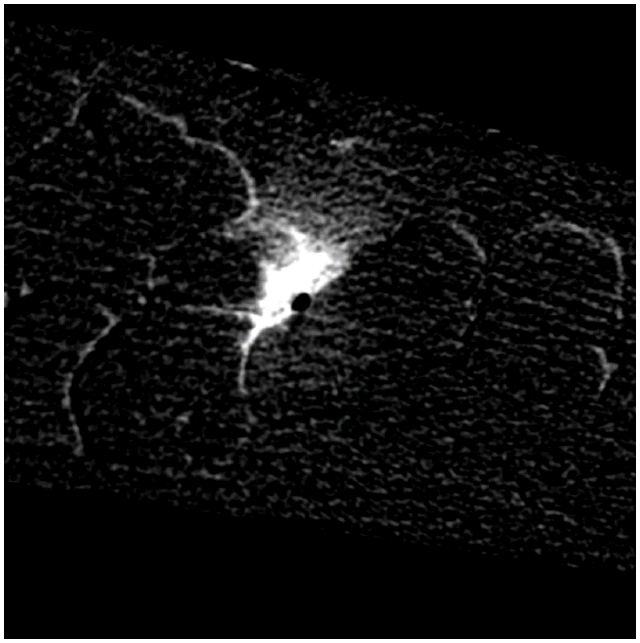

Figure 36: Image after subtraction and linear transformation, to be binarized

We chose a statistical criteria: the threshold would be a certain quantile of the whole grayscale values inside the 3D image of the explant once all the insulin was infused in it.

Which quantile is relevant is an arbitrary choice. But as this thresholding is performed after the subtraction step, we know that the signal is indeed mostly insulin and CA. Therefore, we may perform a sub-selection but not over-select the region of interest. Moreover, by using the same criteria upon all explants, we enable comparison.

After visual observation of the subtraction image and of the corresponding thresholded images for various values of quantile (q), illustrated in Figure 37, our arbitrary choice was q = 0.995.

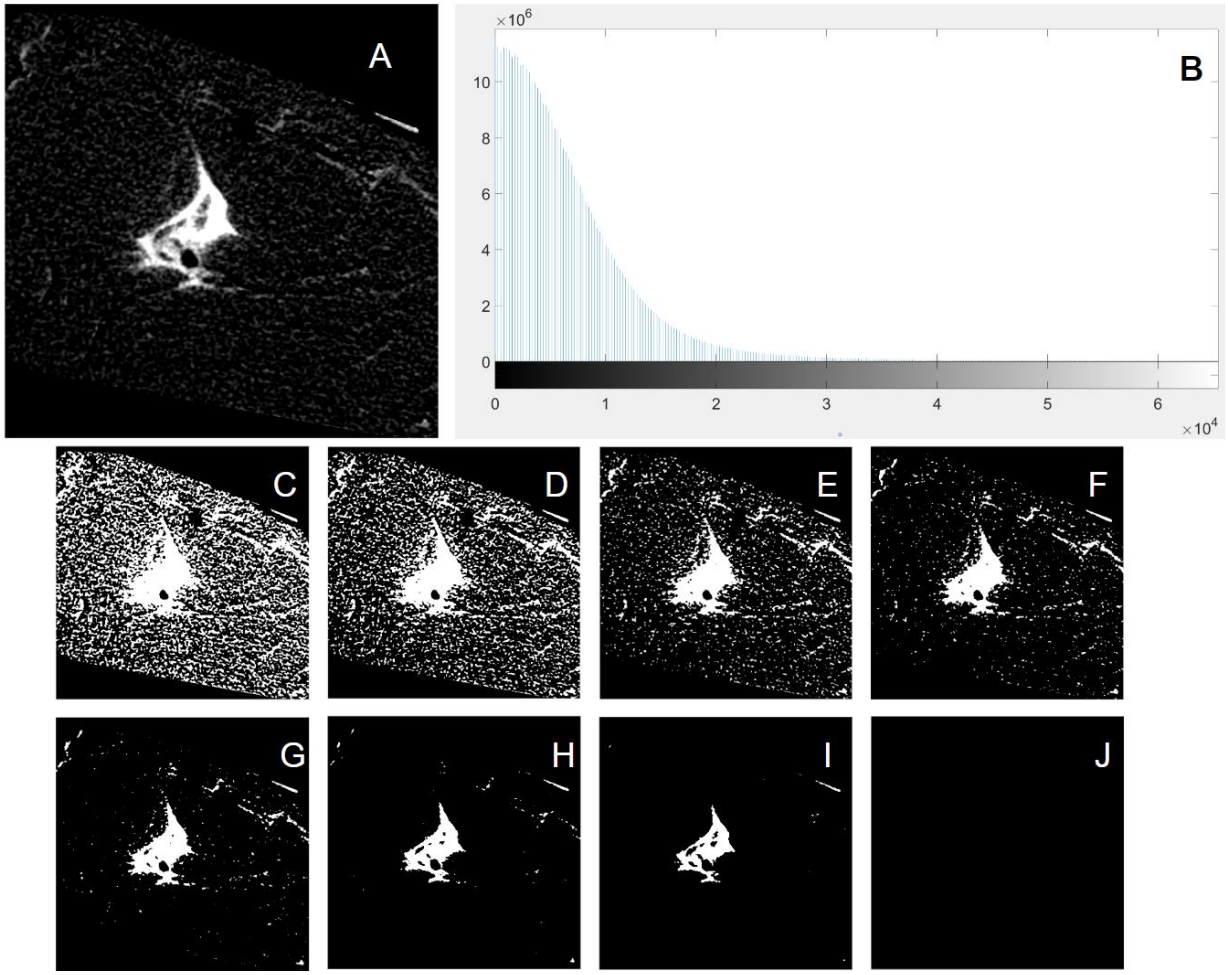

Figure 37: A. Example of subtracted and linear transformed image. B. Histogram for subtracted and linear transformed image. C. Binarised image for q = 0.7. D. Binarised image for q = 0.8. E. Binarised image for q = 0.9. F. Binarised image for q = 0.95. G. Binarised image for q = 0.975. H. Binarised image for q = 0.99. I. Binarised image for q = 0.995. J. Binarised image for q = 0.999.

iv. Labelling

After binarization, due to noise, small objects around the subcutaneous depot may have been selected.
We therefore perform a 3D labelling of the image, which is a step consisting in isolating all objects in the binary image that are disconnected from one another.
Then, we only keep the binary object located at the tip of the cannula (Figure 38)

This allows to have a single-connected component on which surface area computation can be safely performed.

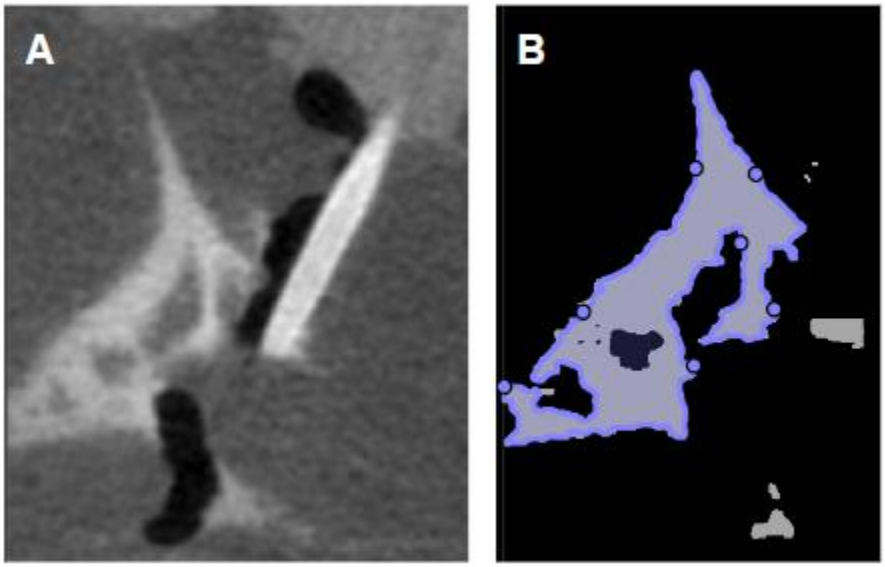

Figure 38: Labelling step illustration. A: original 2D slice. B: After binarization, and labelling, selection of the only labelled region connected to the cannula on that same slice (canula was removed in an earlier step).

These digital image processing steps could only be briefly described in the article which will now be introduced.

4.2 Submitted article (Nature Scientific Reports): New ex vivo method to objectively assess insulin spatial subcutaneous dispersion through time during pump basal-rate based administration

Reference numbering in the article is independent from the rest of this document. References for the article can be found immediately after the main text of the article.

TITLE:
New ex vivo method to objectively assess insulin spatial subcutaneous dispersion through time during pump basal-rate based administration

AUTHORS:

Pauline Jacquemier (1,2), **Yann Retory** (3,4,5), **Clara Virbel-Fleischman** (2), **Alexandra Schmidt** (2), **Agnes Ostertag** (6), **Martine Cohen-Solal** (6,7), **Fawaz Alzaid** (1,8), **Louis Potier** (1,9,10)**, Jean-Baptiste Julla** (1,11,12), **Jean-François Gautier** (1,9,12), **Nicolas Venteclef** (1), **Jean-Pierre Riveline** (1,9,12)

(1) Institut Necker Enfants Malades (INEM), INSERM U1151, Université de Paris Cité, IMMEDIAB Laboratory, Paris, France.
(2) Centre Explor, ALHIST - Air Liquide Healthcare, Bagneux, France
(3) LVL Médical Groupe, Lyon, France
(4) CIAMS, Univ. Paris-Sud, Université Paris-Saclay, 91405 Orsay Cedex, France
(5) CIAMS, Université d'Orléans, 45067, Orléans, France
(6) Université Paris Cité, Inserm U1132 BIOSCAR, F-75010 Paris, France
(7) Service de rhumatologie, Lariboisiere Hospital, AP-HP, F-75010 Paris, France
(8) Dasman Diabetes Institute, Kuwait
(9) Université Paris Cité, UFR de Médecine, Paris, France
(10) Department of Diabetology, Endocrinology and Nutrition, Bichat Hospital, APHP, Paris, France
(11) Sorbonne Université, INSERM, Institut Pierre Louis d'Epidémiologie et de Santé Publique, F75013, Paris, France
(12) Service of Diabetology, Endocrinology and Nutrition, Lariboisiere Hospital, Federation de Diabetologie, AP-HP, F-75010 Paris, France.

CORRESPONDING AUTHOR:
Jean-Pierre Riveline
Service of Diabetology, Endocrinology and Nutrition
Lariboisière Hospital AP-HP,
2 rue Ambroise Paré
75010 Paris, France
+33611416160

jeanpierre.riveline@aphp.fr

3061 words (Abstract and Methods excluded). 7 figures, 0 table

ABSTRACT

Context:
Glycemic variability remains frequent in patients with type 1 diabetes treated with insulin pumps. Heterogeneous spreads of insulin infused by pump in the subcutaneous (SC) tissue are suspected but were barely studied. We propose a new real-time ex-vivo method built by combining high-precision imaging with simultaneous pressure measurements, to obtain a real-time follow-up of insulin subcutaneous propagation.

Method:
Human skin explants from post-bariatric surgery are imaged in a micro-computed tomography scanner, with optimised parameters to reach one 3D image every 5 minutes during 3h of 1UI/h infusion. Pressure inside the tubing is recorded. A new index of dispersion (IoD) is introduced and computed upon the segmented 3D insulin depot per time-step.

Results:
Infusions were hypodermal in 58.3% among 24 assays, others being intradermal or extradermal. Several minor bubbles and one occlusion were observed.
IoD increases with time for all injections. Inter-assay variability is the smallest for hypodermal infusions. Pressure elevations were observed, synchronised with air bubbles arrivals in the tissue.

Conclusion:
A new follow-up method of insulin dispersion evaluation was elaborated. Results encourage the use of this method to compare infusion parameters such as pump model, basal rate, catheter characteristics, infusion site characteristics or patient phenotype.

INTRODUCTION

Patients living with type 1 diabetes are exposed to multiple glycemic disorders, in particular hyperglycemia, hypoglycemia and high glycemic variability (GV) [1,2]. Current innovations focus on increasing time in the target glycemic range, reducing GV, and reducing the number of hypoglycemic events [3]. Among them, insulin pumps or continuous subcutaneous insulin infusion (CSII) are electro-mechanical devices that ensure continuous subcutaneous (SC) delivery of rapid insulin analogs [3,4]. For most patients, CSII largely contribute to reducing GV [5]. CSII are also a major component of closed-loop systems, also sometimes called "artificial pancreas". These systems, which are nowadays reaching an increasing number of patients and will probably become the reference treatment for patients with type 1 diabetes [6], rely on a glucose sensor providing continuous glucose monitoring and a control algorithm to adapt CSII delivery through time according to the patient's specific needs during the day [6].

However in many patients, a high GV remains frequent despite CSII use, without being satisfactorily explained by sporadic copathologies, patient behaviours such as irregular food intakes, irregular physical activities or poor CSII management.
A heterogeneous diffusion of CSII delivered insulin is an often suspected cause for GV although it was not extensively studied. Some studies provide compelling points in favour of the hypothesis that SC insulin absorption variations impact GV. For instance, Luijf et al. observed higher postprandial glycemic excursions immediately after CSII catheter was changed, and thus a new injection site was being used, compared to after 3 days of use [7]. This observation suggests that SC insulin absorption could vary according to catheter age. Famulla et al. demonstrated impaired insulin absorption and higher intra-patient variability for injections in lipodystrophic areas using both a euglycemic clamp study and mixed-meal tolerance tests [8]. Heinemann and Krinelke even describe infusion sets as the "Achilles heel" of CSII delivery [9] , which is conditioned by a reproducible absorption of insulin in the SC tissue [10]. This leads to the hypothesis that inhomogeneous spread of insulin could occur, and highlights the need to increase knowledge of the way insulin spreads into the tissue for basal rate CSII infusion, and in particular in the few hours following a change in catheter [7].
Furthermore, beyond catheter age and lipodystrophies [8,10,11], other factors could alter basal insulin delivery as air bubbles [12], variations in vasculature, or pressure applied to injection site leading to SC insulin underdelivery.

However, although this is the delivery mode in which patients spend the major part of their time, there is currently a lack of method to perform such in depth study of subcutaneous diffusion in basal insulin delivery. Indeed, literature provides multiple examples of bolus delivery studies, either in vivo on swine using imaging [13–15], in vivo in humans using pressure measurement [16,17], or ex vivo using imaging [18–20]. All of these develop indispensable tools and indicators evaluating bolus delivery, and have paved the way to studying basal delivery.

The absence of a method to achieve such analysis of basal rate infused insulin can be explained by the extremely low flow rates and volumes associated with those delivery rates. Indeed, despite insulin pumps being called “continuous infusion” systems, they are built to inject by multiple impulses (or strokes) [21,22]. For instance, a 1 unit of insulin per hour (UI/h) rate will be delivered by a Tandem t:slim® pump through 8.3 µL impulses of insulin delivered every 5 minutes. Volumes of the same order of magnitude would be injected by other manufacturers' insulin pumps. Images of such small infused volumes are challenging to achieve and to our knowledge, not reachable in vivo.

Quantitative description is necessary to enable comparison between CSII infusion parameters in the context of basal delivery. Incidentally, Mader et al.[23] described in 2013 that an increased surface-to-volume ratio (STVR) of the subcutaneous depot increases insulin absorption as it then involves more capillaries, by using a strategy of dispersed bolus injections. Therefore, the imaging method was chosen to enable such computation for small volume injections such as those delivered at each impulsion of a standard rate of basal delivery. The following method is built on the relevance of a high STVR of the insulin depot for optimal insulin bioavailability.

To fill this gap of method to describe insulin propagation in the tissue for the specific context of basal rate delivery, we propose a descriptive, human sample based, ex vivo method linking basal rate insulin delivery and SC spread of insulin using both continuous measurement of catheter pressure, and repeated high-precision 3D imaging using micro-computed tomography (µCT) scans. We obtained new dynamic indicators to describe insulin propagation in the specific case of CSII basal delivery.

RESULTS

Explants infusion sites description

Twenty-four abdominal skin explants were collected from four different human subjects who underwent post-bariatric surgery. They were dimensioned into 3 cm diameter cylinders with a 2 cm thickness so that all three layers of skin tissue (epidermis, dermis, and hypodermis) were present, and infusion catheters were inserted in them. An insulin pump filled with insulin and contrast agent was connected to two microfluidic pressure sensors, and then to the catheter Montage is presented in figure 1.

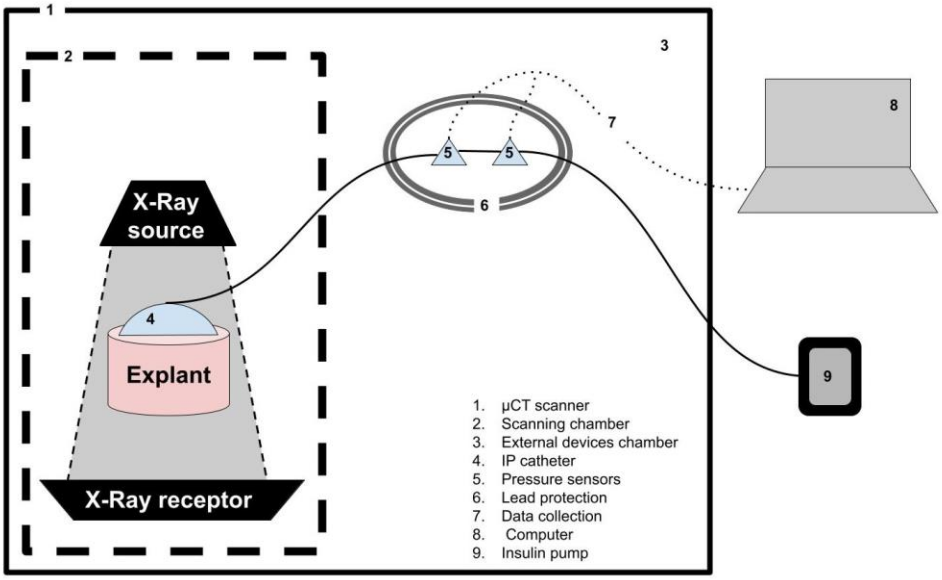

Figure 39: Experimental setting. 1: Micro-CT scanner, 2: Scanning chamber, 3: External devices chamber, 4: CSII catheter, 5: Microfluidic pressure sensors, 6: Lead protection, 7: Data collection wiring, 8: Computer, 9: Insulin pump

Pump was started 10min after initiating the acquisition cascade, so that images before infusion were also available for analysis. For this pilot, a fixed basal rate of 1UI/h during 3h was set. One 3D image was acquired every 5 min during 3h of infusion.

Although CSII catheters target the hypodermis, we observed that hypodermis was reached by the cannula in 58.3% (14/24) of the injections, as depicted in figure 2 A (both in 2D and 3D) where the insulin identified by the segmentation algorithm is numerically coloured in green. The tip of the cannula ended at the limit between dermis and hypodermis in 12.5% (3/24), whereas 20.8% (5/24) of injections were intradermal as in figure 2 B. For one injection, the cannula did not fully pierce the dermis and the injection was hence extra-dermal (figure 2 C). For one injection, images were unexploitable due to an acquisition defect.
During all 5 intradermal injections, insulin spread into the dermis, but in 3/5, it also partly spread in the hypodermis. In the 3 injections where the cannula was at the limit between dermis and hypodermis, in two of them insulin was ultimately found only in hypodermis, whereas in one, it spread both in dermis and hypodermis.

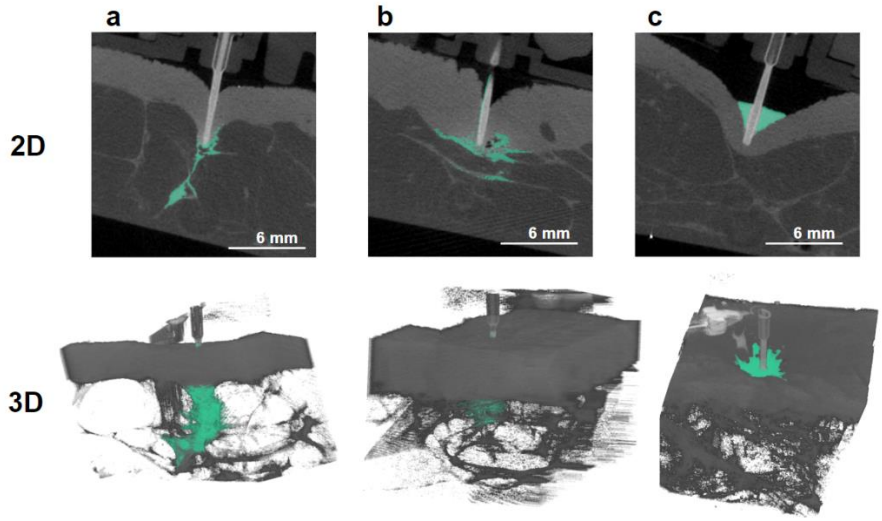

Figure 40: 2D and 3D images of infused explants, with infused insulin and contrast agent numerically identified in green. a: hypodermal infusion, b: intradermal infusion, c: extradermal infusion.

Privileged propagation in interlobular septum in hypodermal injections

Upon all images, the interlobular septum, which divides the subcutaneous tissue into lobules, is clearly visible, as its main component is collagen fibers which are denser than the fat tissue itself. Figure 3 shows extracted slices at various depths in one single explant. The first column is composed of slices extracted from the initial acquisition, when no insulin had yet been delivered. The interlobular walls are visible there.

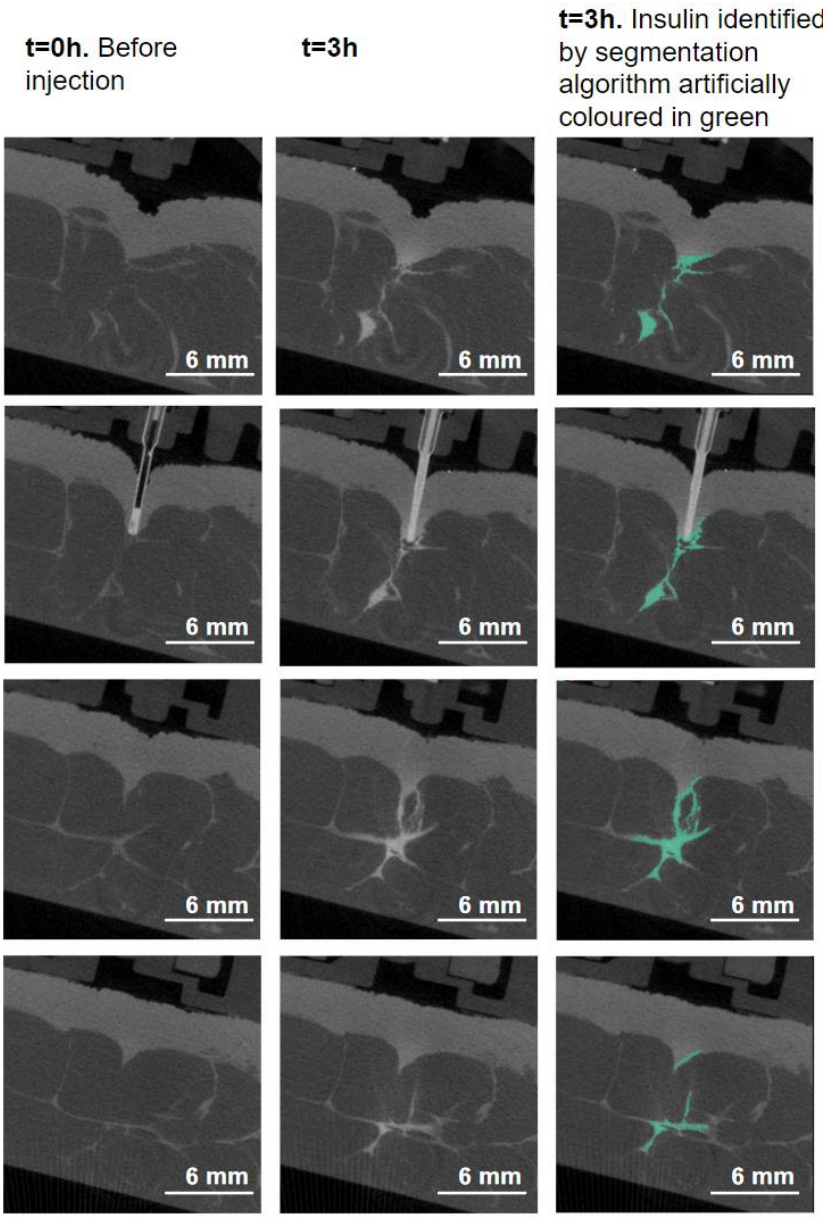

Figure 41: 2D slices of one infused explant. Column 1: slices of the explant before infusion was launched. Column 2: corresponding slices after 3h of insulin infusion. Column 3: corresponding slices after 3h of infusion, where the insulin and contrast agent mixture detected by the algorithm was numerically identified in green.

.

On the corresponding slices after 3h of injection, in the second column, one can see that the white spread of insulin is located along the interlobular walls that had previously been identified. The third column shows which areas of the images were selected by the segmentation algorithm to be insulin and contrast agent (numerically coloured in green).

In the other hypodermal injections, similar visual comparison leads to the same observation: insulin appears to have spread along the interlobular septum.

Some events leading to under-deliveries

Secondly, some under-deliveries were observed: in 18/24 of injections, some minor bubbles were observed at some point in the cannula, leading to the presence of air bubbles imprisoned in the tissue. In one injection, no insulin flow occurred in the cannula during the first hour, as shown by the identical state of the cannula in all of the 13 first 5-minutes acquisitions. Figure 4 displays the content of the cannula for each 5 minutes time slot throughout this particular 3h-test, and in parallel, tubing pressure recorded during that test. A 70 minutes step-wise pressure elevation reaching 557 mBar was associated with this occlusion. This occlusion did not trigger any pump alarm and also happened to occur during the one extra-dermal injection

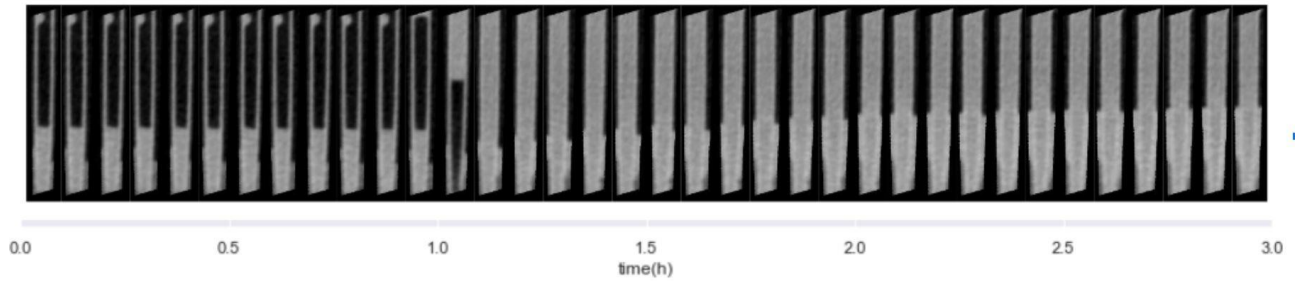

Figure 42: Cannula content during 3h of infusion, during a test where an occlusion occurred.

Introducing a new metric for insulin dispersion: the index of dispersion (IoD)

At each time step, the external surface ($S_{measured}(t)$) and volume ($V_{measured}(t)$ of the insulin depot are computed, allowing to generate the surface-to-volume ratio at each time step.

In order for this ratio to be interpretable, the most minimal surface-to-volume ratio mathematically possible for the given volume of injected insulin is also computed: namely, a spherical volume. To this purpose, the radius $R_{compact}(t)$ of the sphere that would be of the same volume as $V_{measured}(t)$ is first computed as shown in equation (1), leading to the computation of the surface of that theoretical sphere $S_{compact}(t)$ in equation (2).

This corresponds to the theoretical most compact situation where the insulin depot would have a perfect spherical shape, therefore having a minimal amount of capillaries involved in ensuring absorption into the vascular system. It is the less favourable scenario for insulin absorption.

(1)

$$R_{compact} = \left(\frac{3\,V_{measured}(t)}{4\pi}\right)^{\frac{1}{3}}$$

(2)

$$S_{compact} = 4\pi\,R_{compact}(t)^2$$

$$S_{compact} = (4\pi)^{\frac{1}{3}}\,(3V_{measured}(t))^{\frac{2}{3}}$$

We introduce an index of dispersion IoD(t) which is the surface-to-volume measured ratio divided by the corresponding spherical surface-to-volume ratio, as visible in equation (3). It translates how high the surface of contact between the tissue and the insulin depot is, compared to the most compact situation. This index is expressed without unit.

(3)

$$IoD = \frac{Surface\_to\_volume\_ratio_{measured}}{Surface\_to\_volume\_ratio_{compact}}$$

$$IoD(t) = \frac{Surface_{measured}(t)}{Volume_{measured}(t)} \frac{Volume_{compact}(t)}{Surface_{compact}(t)}$$

$$IoD(t) = \frac{Surface_{measured}(t)}{Surface_{compact}(t)} = \frac{Surface_{measured}(t)}{(4\pi)^{\frac{1}{3}} (3V_{measured}(t))^{\frac{2}{3}}}$$

Index of dispersion (IoD) evolution of the SC insulin through time

Upon all injections, the IoD increases with time, as depicted in figure 5A to 5D. Throughout all test duration, median IoDs tend to be comparable from one explant to another and from one patient to another (see figure 5 F). A mean final value of 6.64 is reached after 3h of infusion, when the maximum depot size is reached in our setting. A closer snapshot at IoD values at 3h also shows comparable values, when looking at their distribution classified according to the tissue structure reached by the cannula (figure 6). In addition, there seems to be no major difference in index of dispersion values when one compares intradermal injections versus hypodermal injections. On the other side, the only heterogeneous value of IoD is of 2.62 at 3h (figure 5 E and figure 6 “skin surface”) and corresponds to the only extra-dermal injection, where insulin accumulated at the skin surface, inside a crater formed around the cannula (figure 2 C, both in 2D and 3D).

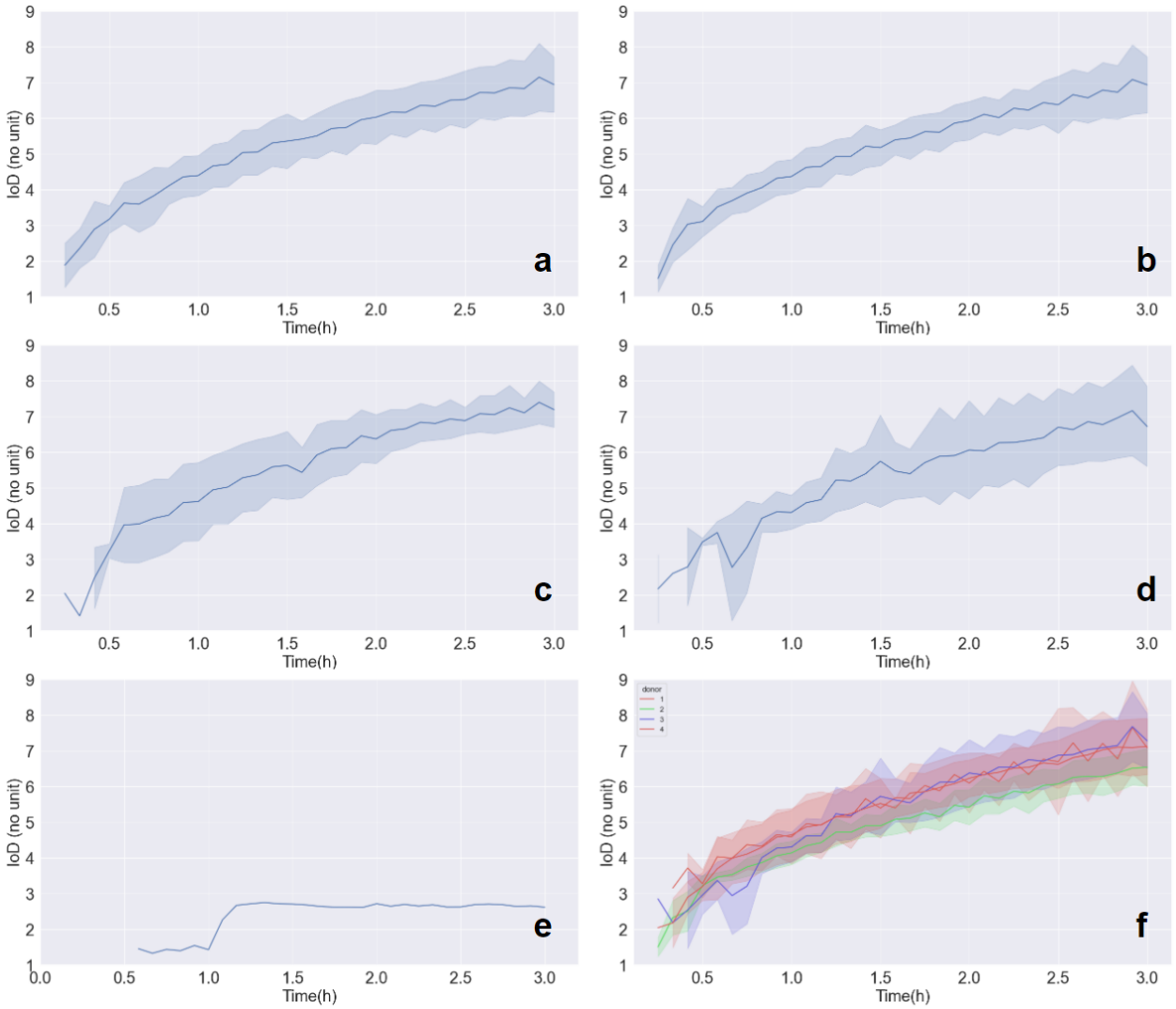

Figure 43: Index of dispersion (IoD) evolution through time, with standard deviation. a: All infusions (N=21), b: Infusions reaching hypodermis (N=13), c: Infusions reaching dermis/hypodermis limit (N=3), d: Infusions reaching dermis (N=4), e: Extradermal infusion (N=1), f: All infusions , aggregated by donor (N=21).

The mean value of standard deviations of IoD computed upon all 5 min intervals was 0.66 when considering all skin-reaching injections. However it was lower (0.55) when only selecting those reaching the hypodermis, than for those reaching the dermis/hypodermis limit (0.62), and the dermal ones (0.83).

When considering explants separately according to the donor as displayed in figure 5 F, standard deviation values across all tissue structures infused, upon all 5 min intervals, are quite similar to the global standard deviation are respectively 0.68, 0.35, 0.77 and 0.58 for donors 1 to 4.

IoD values were left uncomputed for two explants due to unsolvable 3D tomographic reconstruction issues.

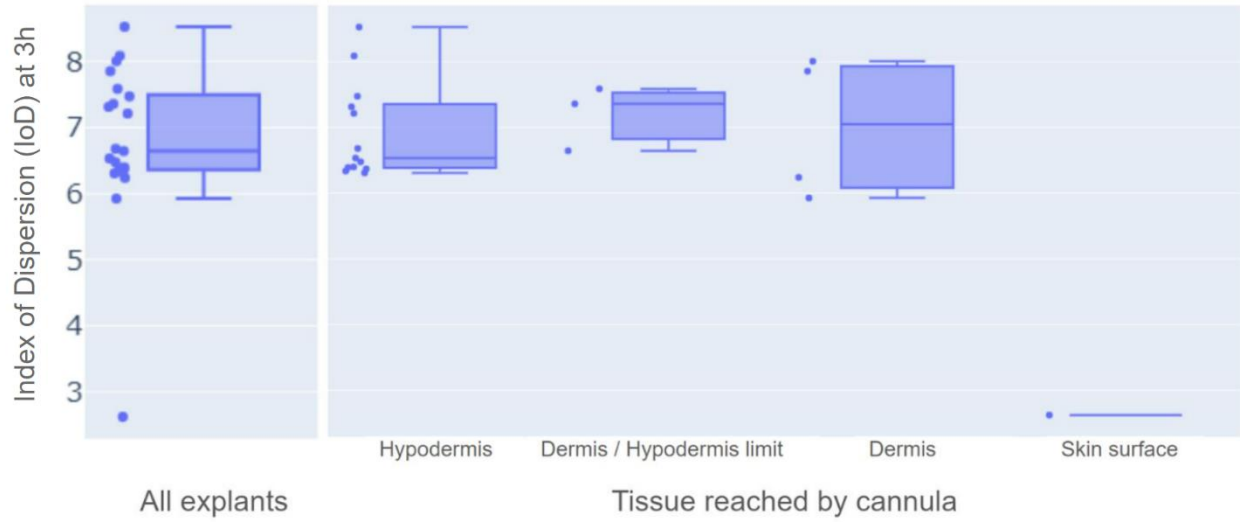

Figure 44: Boxplot of IoD values after 3h of infusion. Classified according to the tissue structure reached by the cannula.

Simultaneous pressure and image observation in case of bubbles in the cannula

As pressure inside the catheter was continuously recorded through the tests, each insulin impulsion was easily identifiable on pressure records (figure 7).

Temporary pressure elevations between impulsions were observed, either at the beginning of the test, or at some point during the infusion. In order to understand the potential cause for these elevations, pressure graphs are juxtaposed to the 2D images of the content of the cannula at the given time-step (figure 7). We observe that pressure elevations appear to match with the presence of an air bubble inside the cannula the 5 minutes before the elevation, suggesting that the pressure step matches with the arrival of the air bubble inside the subcutaneous tissue.

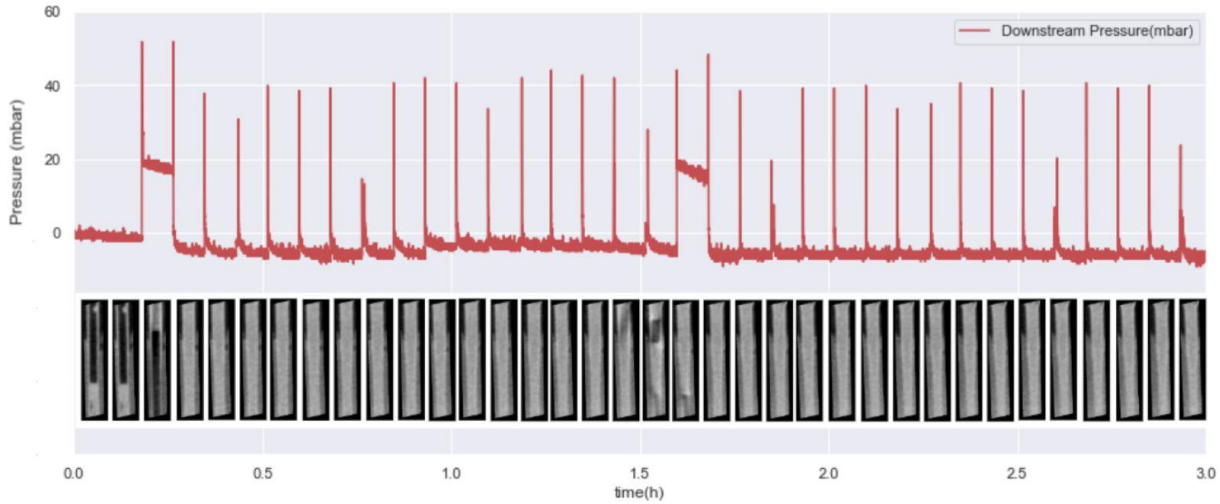

Figure 45: Pressure record and corresponding cannula content for one injection.

DISCUSSION

This study describes a new method which extends previously existing imaging methods, in order to evaluate the insulin spread in the SC tissue continuously during basal CSII administration. It combines imaging with continuous pressure measurement using two different high precision tools: a µCT scanner whose image acquisition was optimised to acquire one 3D image every 5 minutes, and continuous pressure sensors. Each 3D image analysis and continuous pressure records were set with the intention to evaluate SC insulin absorption characteristics, and link morphological events with easily pressure-detectable events.

We introduced an objective new indicator to quantify insulin spread, namely the index of dispersion (IoD). It is related to the surface-to-volume ratio (STVR), therefore it increases with STVR, which was shown to be associated with an increased speed of insulin absorption [23].
Unlike STVR, IoD has the advantage of requiring no comparison with another situation to be interpretable. Indeed, it is built in comparison with the hypothetical case where the insulin depot had a spherical shape, the least favourable situation to diffusion. For instance, an IoD of 7 means that a depot has a surface 7 times higher than the least favourable shape for diffusion. Therefore, one could suppose that the depot has 7 times more probable contacts with capillaries in the SC tissue than it would in the worst-case scenario.

This work is a proof-of-concept aiming to demonstrate feasibility of this method. Therefore, the results demonstrate that IoD, under fixed injection parameters (same pump, same basal rate) and in normal hypodermal infusion, is very reproducible, with a low inter-assay variability (figure 5).

Moreover, some interesting results can be highlighted.
The first one is the observation of a higher variability of IoD during ectopic infusion cases, especially when other anatomical structures than hypodermis are infused such as the dermis or the dermis-hypodermis junction. This happens in our model in about 40% of cases. However the number of injections for which the hypodermis was not reached is higher than the proportions found in-vivo by ultrasound detection of the cannula position [11,24]. This is probably due to our ex-vivo insertion method. Indeed, samples are placed inside small Petri dishes of the exact same dimensions as the explants, providing mechanical support to the samples when the inserter hits the skin surface. The use of an inserter does contribute to a more reproducible insertion of the cannula. But the lack of tension at the surface of the epidermis promotes the possible bending of the epidermis surface, thus limiting the depth reached by the cannula tip. Therefore, our experimental model probably participates in explaining this high percentage. Nonetheless, such ectopic cannula positions are at times observed in patients treated with CSII [24]. We hypothesise that it is indeed possible that such events, where non targeted tissue structures are infused, do play a role in some of the glycemic variability observed in patients in daily practice.
Description of such ectopic infusion is then precious data. In particular, despite higher variability in IoD values when the dermis is infused, it is interesting to notice that the mean IoD is not much

different in the dermis than in the hypodermis. It was otherwise shown that kinetics of insulin action are different in the dermis and in the hypodermis [25,26]. It is therefore likely that this difference is not caused by a different morphology of the insulin depots infused in the dermis versus in the hypodermis, but rather by a different microvascularization of these two skin structures.
A second interesting observation could be mentioned. As a first method to combine pressure data with imaging data, this study also allows to notice the simultaneity of temporary pressure elevations and air bubbles arrival in the tissue, a quite common situation in real life conditions [12] leading to under-delivery. This encourages the development of an air bubble detection system based on finer pressure sensors than those already embarked in pumps.

The low value of variability of the IoD throughout experiments and patients in our fixed setting conditions (same pump, same flowrate, same catheter material, length and insertion angle), in hypodermal injection conditions, makes it a reproducible indicator to compare various injection conditions, such as basal rate, CSII model, cannula characteristics, injection site, lipodystrophic tissue, or patient phenotype, in order to better understand SC insulin infusion characteristics.

Our method does present some limitations. Ex-vivo samples do not benefit from any active microvascularization which would contribute to the active transport of insulin from the SC tissue to the bloodstream [27]. Also, the spread of insulin is likely to be improved in the case of perfused tissue compared to ex-vivo tissue due to this active transport. However, a larger insulin spread in the absence of micro-vascularization is likely to imply a larger spread with active micro-vascularization. In that context, IoD measurements in ex-vivo SC insulin administration can still relevantly be used to compare various injection parameters.

The fact that insulin propagates preferably along the interlobular septum is in accordance with the literature [28,29]. Another limitation must however be acknowledged : our samples come from patients who underwent post-bariatric surgery, and therefore have suffered important weight variations. A known consequence of such weight variations is an irreversible fibrotic adipose tissue [30–33]. Therefore, the interlobular septum of our samples is likely to be thicker and with denser collagen fibres than adipose tissue from patients with type 1 diabetes. Yet such large skin samples from non-obese patients are not easily available for research purposes, for evident ethical reasons. Also, the samples come from female patients only, for during the whole scope of this project, no male tissue was made available to us. This is consistent with the major gender disparity among patients who undergo post-bariatric surgery [34].

Finally, this work stands as a proof of concept of this evaluation method, so that it can be made available and further used to test the impact of various parameters. In order to do so, it was essential that this study was conducted under fixed conditions of pump, catheter model and basal rate of delivery to assess its reproducibility.

This work, which provides tools to identify the sources of variability in insulin SC absorption caused by heterogeneous diffusion or erratic events, is of importance not only in the context of use of CSII alone, but also as closed-loop systems emerge.

METHODS

Human skin explants

This ex-vivo study was performed on 24 abdominal skin explants which were collected from surgical residue of post-bariatric surgery for 4 different human subjects (patient data available in supplemental data S1) in full respect with the Declaration of Helsinki and the article L.1243-4 of the French Public Health Code. BIO-EC Laboratories (Longjumeau, France) possesses an authorization from the Bioethics group of the general director services of the French research and innovation ministry (registered under nDC2008542) to use human skin from surgical waste since 5th May 2010. Explants were dimensioned into 3 cm diameter cylinders with a 2 cm thickness by BIO-EC Laboratories. All 3 layers of skin tissue (epidermis, dermis, hypodermis) were present. From then on, samples were maintained at 37°C in an incubator (5% of CO_2, 95% of humidity) with a survival medium (BEMc solution, BIO-EC Laboratories, Longjumeau) renewed every two days until samples were used for experiment.

Experimental setting description

A Tandem t:slimx2™ insulin pump was connected to two Elveflow™ microfluidic pressure sensors (MPS) manufactured by Elvesys® with ranges of measurement of [-70 mbar ; +70 mbar] and [-340 mbar ; +340 mbar], to ensure the most accurate measurement of a broad scale of pressures. Connections were made using tubing from Autosoft 90 catheters. The second MPS was connected to an Autosoft 90 Catheter with a 6 mm Teflon cannula. Montage is presented in figure 1.

A 15% mass of Iopamiro 200 mg/mL was mixed with insulin Aspart Novorapid U100 and loaded into a t:slim ™ cartridge. Measurements to quantify the impact of contrast agent on insulin Aspart viscosity are available in supplemental data S2.

Tubing and catheters were purged with insulin and contrast agent before insertion of the catheter into the tissue sample.

Radioprotection of the devices

The pump was placed outside of a µCT scanner. The pressure sensors were inside the extended chamber of the µCT, in an area unreachable to X-ray. For full confidence in sensor integrity and measurement, both sensors were surrounded by 3 mm of lead.

Data acquisition and µCT parameters

µCT acquisitions were obtained using a Skyscan 1176 from Brucker® and parameters were optimised to ensure proper imaging of the sample and the insulin depot with a 17 µm resolution while maintaining acquisition time for each 3D image below 5 min. This delay of 5 min was

chosen as it constitutes the delay between two impulsions for a Tandem t:slim x2 [22] and is also to our knowledge the minimum delay between two impulses upon pumps currently on the market.
The X-Ray source was set at (55kV, 455mA) for optimal contrast. A 2mm Aluminium filter was used in order to limit the beam hardening effect. The rotation step was set at 0.6° and exposure time at 0,240 s.
180° acquisitions were conducted. Upon 3h of acquisition, one 3D-image per 5 min interval was collected, leading to an overall collection of 36 3D-images. The first image, the third image, and all "uneven" (respectively "even") 3D images were obtained by clockwise rotation (respectively counterclockwise) of the X-ray source and receptor.

Image processing

3D tomographic reconstruction was achieved using the NRecon® software (Brucker™). Each slice of the 3D-images were loaded into Matlab® (Mathworks™).

The two first 3D-images were acquired while the pump had not started to deliver, so they could be used as reference of a free-from-insulin tissue. The first image was used as reference for all uneven acquired images, and the second for all even images. Indeed, due to the change in rotation direction between even and uneven images, there was a slight angle tilt between even and uneven images.
On these two first 3D-images, the cylindrical volume corresponding to the inserted cannula in the tissue was manually identified. This corresponding volume was then automatically removed on all following images acquired during the injection.

For each processed 3D-image, the 2D-slices were loaded into the Matlab ® environment. The corresponding slices in the free-from-insulin image were subtracted, in order for most of the remaining signal to be the injected insulin and contrast agent mixture.

Then, in order to extract insulin depot properties, a linear transformation was performed and a binary image was obtained by using the 0.95 quantile of pixel values as a threshold, allowing to remove noise due to the previous subtraction. Finally, a unique insulin depot object was selected among this binary stack of images by connected-components labeling : only the connected component to include the tip of the cannula (by 18-connectivity) was kept.

The binary objects obtained during this segmentation step were used to compute the external surface and volume of the insulin depot.

CONCLUSION

A new evaluation method of SC insulin absorption has been elaborated. To this end, a novel objective indicator for insulin spread was proposed, the index of dispersion, IoD. It is therefore now possible to compare various infusion parameters such as basal rate, CSII model, cannula length, material, infusion site, lipodystrophy, on insulin spread in the SC tissue.

REFERENCES:

1. Julla, J.-B. *et al.* Is the Consensual Threshold for Defining High Glucose Variability Implementable in Clinical Practice? *Diabetes Care* **44**, 1722–1725 (2021).
2. Riveline, J.-P. *et al.* Real world hypoglycaemia related to glucose variability and Flash glucose scan frequency assessed from global FreeStyle Libre data. *Diabetes Obes. Metab.* (2022) doi:10.1111/dom.14795.
3. Tauschmann, M. & Hovorka, R. Technology in the management of type 1 diabetes mellitus — current status and future prospects. *Nat. Rev. Endocrinol.* **14**, 464–475 (2018).
4. Berget, C., Messer, L. H. & Forlenza, G. P. A Clinical Overview of Insulin Pump Therapy for the Management of Diabetes: Past, Present, and Future of Intensive Therapy. *Diabetes Spectr. Publ. Am. Diabetes Assoc.* **32**, 194–204 (2019).
5. Pickup, J. C. & Renard, E. Long-Acting Insulin Analogs Versus Insulin Pump Therapy for the Treatment of Type 1 and Type 2 Diabetes. *Diabetes Care* **31**, S140–S145 (2008).
6. Tubiana-Rufi, N. *et al.* Practical implementation of automated closed-loop insulin delivery: A French position statement. *Diabetes Metab.* **47**, 101206 (2021).
7. Luijf, Y. M. *et al.* Patch Pump Versus Conventional Pump: Postprandial Glycemic Excursions and the Influence of Wear Time. *Diabetes Technol. Ther.* **15**, 575–579 (2013).
8. Famulla, S. *et al.* Insulin Injection Into Lipohypertrophic Tissue: Blunted and More Variable Insulin Absorption and Action and Impaired Postprandial Glucose Control. *Diabetes Care* **39**, 1486–1492 (2016).
9. Heinemann, L. & Krinelke, L. Insulin infusion set: the Achilles heel of continuous subcutaneous insulin infusion. *J. Diabetes Sci. Technol.* **6**, 954–964 (2012).
10. Heinemann, L. Insulin Absorption from Lipodystrophic Areas: A (Neglected) Source of Trouble for Insulin Therapy? *J. Diabetes Sci. Technol.* **4**, 750–753 (2010).
11. Abu Ghazaleh, H. *et al.* A Systematic Review of Ultrasound-Detected Lipohypertrophy in Insulin-Exposed People with Diabetes. *Diabetes Ther.* **9**, 1741–1756 (2018).
12. Knoll, M. M., Vazifedan, T. & Gyuricsko, E. Air occlusion in insulin pumps of children and adolescents with type 1 diabetes. *J. Pediatr. Endocrinol. Metab.* **33**, 179–184 (2020).
13. Hauzenberger, J. R. *et al.* Detailed Analysis of Insulin Absorption Variability and the Tissue Response to Continuous Subcutaneous Insulin Infusion Catheter Implantation in Swine. *Diabetes Technol. Ther.* **19**, 641–

650 (2017).

14. Hauzenberger, J. R. *et al.* Systematic in vivo evaluation of the time-dependent inflammatory response to steel and Teflon insulin infusion catheters. *Sci. Rep.* **8**, 1132 (2018).
15. Eisler, G. *et al.* In vivo investigation of the tissue response to commercial Teflon insulin infusion sets in large swine for 14 days: the effect of angle of insertion on tissue histology and insulin spread within the subcutaneous tissue. *BMJ Open Diabetes Res. Care* **7**, e000881 (2019).
16. Patte, C. *et al.* Effect of infusion rate and indwelling time on tissue resistance pressure in small-volume subcutaneous infusion like in continuous subcutaneous insulin infusion. *Diabetes Technol. Ther.* **15**, 289–294 (2013).
17. Regittnig, W. *et al.* Insulin induces a progressive increase in the resistance of subcutaneous tissue to fluid flow: Implications for insulin pump therapy. *Diabetes Obes. Metab.* **24**, 455–464 (2022).
18. Jockel, J. P. L., Roebrock, P. & Shergold, O. A. Insulin depot formation in subcutaneoue tissue. *J. Diabetes Sci. Technol.* **7**, 227–237 (2013).
19. Thomsen, M. *et al.* Visualization of subcutaneous insulin injections by x-ray computed tomography. *Phys. Med. Biol.* **57**, 7191–7203 (2012).
20. Kim, H., Park, H. & Lee, S. J. Effective method for drug injection into subcutaneous tissue. *Sci. Rep.* **7**, 9613 (2017).
21. Girardot, S. *et al.* Kalman filter-based novel methodology to assess insulin pump accuracy. *Diabetes Technol. Ther.* (2019) doi:10.1089/dia.2019.0147.
22. Girardot, S. *et al.* All Insulin Pumps Are Not Equivalent: A Bench Test Assessment for Several Basal Rates. *Diabetes Technol. Ther.* (2020) doi:10.1089/dia.2019.0486.
23. Mader, J. K. *et al.* Enhanced absorption of insulin aspart as the result of a dispersed injection strategy tested in a randomized trial in type 1 diabetic patients. *Diabetes Care* **36**, 780–785 (2013).
24. Hofman, P. L. *et al.* Defining the ideal injection techniques when using 5-mm needles in children and adults. *Diabetes Care* **33**, 1940–1944 (2010).
25. McVey, E., Keith, S., Herr, J. K., Sutter, D. & Pettis, R. J. Evaluation of Intradermal and Subcutaneous Infusion Set Performance Under 24-Hour Basal and Bolus Conditions. *J. Diabetes Sci. Technol.* **9**, 1282–1291 (2015).
26. Pettis, R. J. *et al.* Intradermal microneedle delivery of insulin lispro achieves faster insulin absorption and

insulin action than subcutaneous injection. *Diabetes Technol. Ther.* **13**, 435–442 (2011).

27. Hildebrandt, P. & Birch, K. Basal rate subcutaneous insulin infusion: absorption kinetics and relation to local blood flow. *Diabet. Med. J. Br. Diabet. Assoc.* **5**, 434–440 (1988).
28. Richter, W. F., Bhansali, S. G. & Morris, M. E. Mechanistic Determinants of Biotherapeutics Absorption Following SC Administration. *AAPS J.* **14**, 559–570 (2012).
29. Richter, W. F. & Jacobsen, B. Subcutaneous Absorption of Biotherapeutics: Knowns and Unknowns. *Drug Metab. Dispos.* **42**, 1881–1889 (2014).
30. Henegar, C. *et al.* Adipose tissue transcriptomic signature highlights the pathological relevance of extracellular matrix in human obesity. *Genome Biol.* **9**, R14 (2008).
31. Tordjman, J. Histologie du tissu adipeux blanc normal et pathologique. *Obésité* **8**, 228–233 (2013).
32. Divoux, A. *et al.* Fibrosis in human adipose tissue: composition, distribution, and link with lipid metabolism and fat mass loss. *Diabetes* **59**, 2817–2825 (2010).
33. Marcelin, G. & Clément, K. La fibrose du tissu adipeux: Un facteur aggravant de l'obésité. *médecine/sciences* **34**, 424–431 (2018).
34. Sun, S., Borisenko, O., Spelman, T. & Ahmed, A. R. Patient Characteristics, Procedural and Safety Outcomes of Bariatric Surgery in England: a Retrospective Cohort Study-2006-2012. *Obes. Surg.* **28**, 1098–1108 (2018).

ACKNOWLEDGMENTS

We deeply thank Bio-EC Laboratories for their adaptability in providing skin samples adapted to our needs. We thank Loïc Anderlesse for the help in optimising micro-CT parameters, and IMOSAR Lab and Christine Chappard for the help with micro-CT use.
Finally, we thank Fawaz Alzaid for the English language review.

AUTHORS CONTRIBUTIONS

P.J.: Conceptualization, Methodology, Software, Formal analysis, Investigation, Data curation, Writing (Original Draft), Visualisation
Y.R.: Project administration, Conceptualization, Methodology, Supervision
C.V-F.: Formal Analysis, Writing (Review and Editing), Supervision
A.S.: Funding acquisition, Resources
A.O.: Resources, Software
M.C-S.: Resources, Software
F.A.: Writing (Review and Editing)
L.P.: Writing (Review and Editing)
J-B.J.: Writing (Review and Editing)
J-F.G.: Resources, Writing (Review and Editing)
N.V.: Resources, Writing (Review and Editing)

J-P.R.: Conceptualization, Methodology, Writing (Original Article), Writing (Review and Editing), Supervision, Project administration, Funding acquisition

DATA AVAILABILITY STATEMENT

The datasets generated during the current study are not publicly available due to the heavy numerical size of the µ-CT 3D images (390 Go of image data for each of the 24 explants) but are available from the corresponding author on reasonable request.

ADDITIONAL INFORMATIONS

Competing interest statement:
P.J.,Y.R., C.V.-F., A.S. are employees of Air Liquide Healthcare.
J.-P.R. is an advisory panel member for Sanofi,MSD,Eli Lilly, Novo Nordisk, AstraZeneca, Abbott, Dexcom, Alphadiab, and Medtronic; and has received research funding and provided research support to Abbott, Air Liquide Healthcare, Sanofi, and Novo Nordisk.

Funding:
P.J. is a recipient of a CIFRE doctoral fellowship (CIFRE: Conventions Industrielles de Formation par la Recherche) from Association Nationale de la Recherche et de la Technologie (ANRT, Paris, France).

End of the article

The supplemental data section of this article is available in the annex section of this document.

4.3 Coming back to the retention hypothesis

The preliminary experiments (including on human explants) in *Chapter 3* lead us to the hypothesis of a frequent **insulin retention phenomena at the initiation of infusion sites**, associated with **temporary pressure build-ups in the tubing**.

In those previous experiments, the rate of appearance of these build-ups was a little above 50% for human explants. However in the experiments conducted in the scope of the article, **only one pressure build-up** upon 24 infusions was observed, which was **associated with an extradermal deposit of insulin**.

The imaging technology is not invasive and the **only notable difference** between those experiments was in the **procedure to insert the cannula in the explant**. Up until the µCT imaging, catheter and cannula insertions were performed by **pinching the superior skin layers with tweezers** with one hand, and inserting the cannula with the insertion needle within it, into the skin (Figure 46 A and B), with the other hand. Then, the insertion needle was removed and the skin superior layers unpinched.

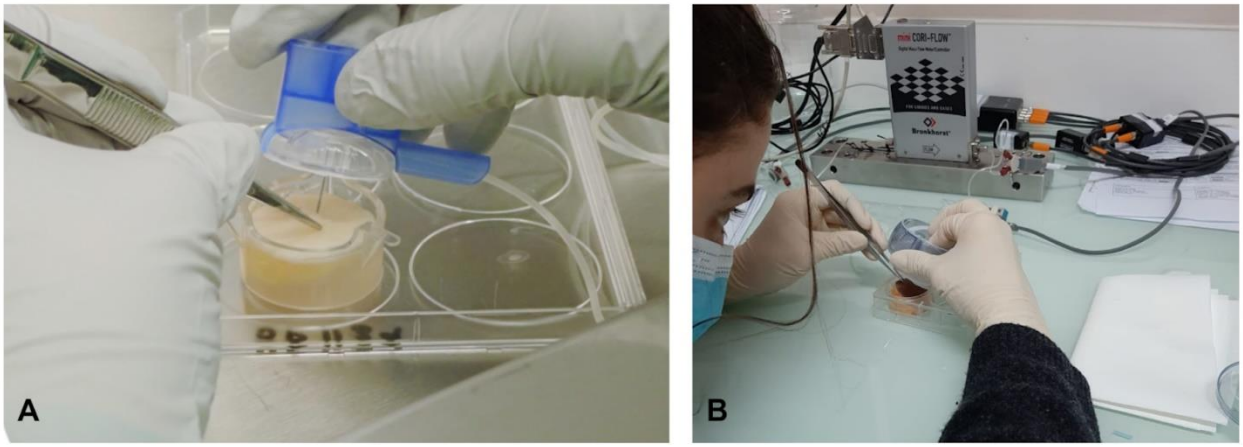

Figure 46: Insertions of catheter illustrations. A. Manual insertion of Medtronic Quick-set (™) catheter, with no inserter. B. Manual insertion of Tandem Autosoft 90 (™) catheter, without using the inserter function.

For the µCT imaging, skin explants were placed into small petri dishes of diameter 2.8cm. The mechanical support provided by those allowed to use the inserters provided by the manufacturers. For the tests of the article, the insertion system of the Tandem Autosoft 90 (™) was used (Figure 47 A), allowing an insertion of the cannula by conferring a high impact speed of the insertion needle onto the skin.
For the tests with the Medtronic 780G pump, presented in the next paragraph, insertions relied on the Minimed (™) Mio (™) Advance technology (Figure 47 B), which also confers an elevated impact speed of the insertion needle.

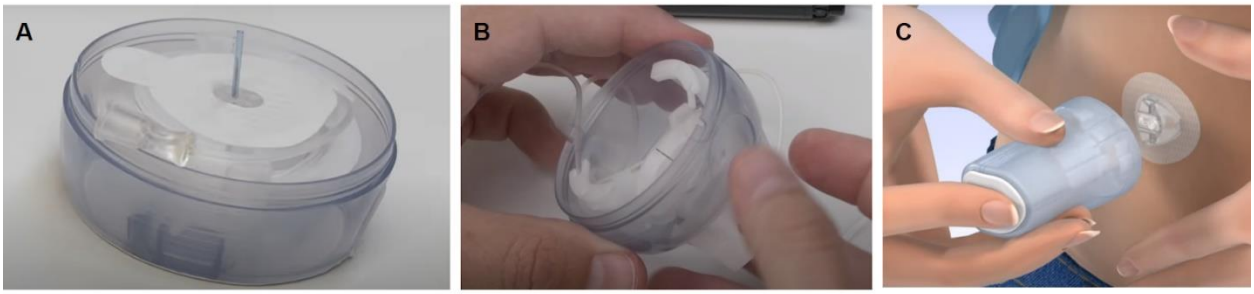

Figure 47: Tandem and Medtronic inserters. A: Tandem Autosoft 90 inserter as it is initially. B: Tandem Autosoft 90 as it is when prepared for insertion. Source: official Tandem video for inserter use. C: Display of Medtronic inserter after insertion. Source: official Medtronic video for inserter use.

Then, **an improper insertion of the catheter** when insertion is performed in the initial way could have led to these build-ups, either because this manual **insertion process triggered an obstruction** of the cannula, or because **this insertion process is more likely lead to extradermal infusions** like the one of the article, where the cannula did not fully pierce the epidermis.

The hypothesis of a different behaviour when the tip of the cannula is inserted inside a lobule or in between lobules remains partially relevant, even in the absence of pressure build-ups. The results of the article describe indeed a **favoured propagation of the insulin in the interlobular septum**, which **could cause a facilitated dispersion of the insulin when the tip of the cannula is already within the path of least resistance**.

4.4 Testing infusions with alternative basal rate and pump

The article presented above introduces a method for comparison of insulin propagation in pump basal delivery. It was used under fixed conditions: one pump (a Tandem (™) t:slim x2), at one flowrate (1UI/h) with one catheter model (Autosoft 90 inserter, Tandem (™)). The intent was to describe the method as a proof of concept to then gather data about the impact of various infusion parameters upon the insulin propagation in the tissue. This part introduces a few tests where other infusion parameters were explored.

Little data was collected on alternative BR and pumps within the scope of this work. Therefore, it does not allow to draw conclusions but only to state a few first observations. These experiments constitute a first step towards applying this method to study BR and pump impact of insulin subcutaneous propagation.

Due to µCT scanner defect, within the scope of this project, few tests could be performed and only the following test results are available:

- 3 explants at 0.5UI/h using a Tandem (™) t:slim x2 pump (*)

- 2 explants at 1UI/h using a Medtronic (™) 780G pump (**) with a 6mm Mio Advance 90 catheter (non-angled, 6mm long, Teflon catheter)
- 2 explants at 0.5UI/h using a Medtronic (™) 780G pump with a 6mm Mio Advance 90 catheter (non-angled, 6mm long, Teflon catheter)

(*) same pump as the one used in the article above
(**) same BR as the one used in the article above

Also, for the Medtronic tests, two more tests were launched, one at 1UI/h and one at 0.5UI/h. However due to a leak at the connection between the tubing and the tubing pressure recording device, none of the insulin was delivered to the tissue. This data was therefore not exploitable for insulin propagation. Yet the images of the explants and the cannula inserted within them were still available to us.

a. General comments about infusions

All infusions but one reached the target tissue, the hypodermis. One reached in the dermis, with the tip of the cannula inserted in the inferior part of the dermis, rather than the hypodermis. For this explant (one of the Tandem infusions), insulin propagated in the dermis, the epidermis and some insulin was also found at the epidermal surface (Figure 48 A, red circle). For that specific explant, the insulin initially found atop of the skin appeared to have dried by the end of 3h of test, resulting in a concentrated (and thus very radio-opaque) pellicle of insulin at the top of the epidermis (Figure 48 B, red circle).

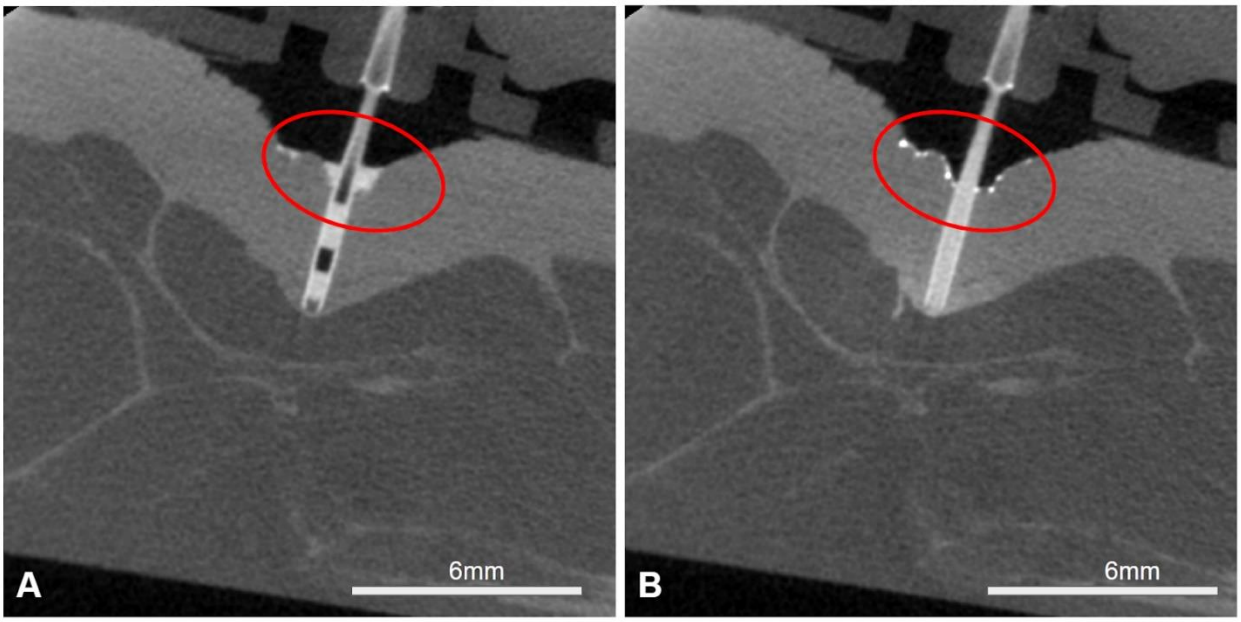

Figure 48: Explant with dermal infusion with Tandem t:slim x2 at 0.5UI/h. A. Before the delivery starts. B. After 3h of infusion

On all but two the tests performed with the Tandem t:slim x2 pump and the associated Autosoft 90 catheter, including those of the article, **a bending of the dermis was observed around the spot where the cannula was inserted** (Figure 49 A). That represents 25/27, or 92% of Tandem tests. Besides, as reported in the article, **only in 14/24 of the tests did the tip of the cannula actually reach the hypodermis due to this bedding effect**, which corresponds to 58% of the infusions. And again, one in three of the infusions performed at 0.5UI/h with the Tandem pump reached the junction between the dermis and the hypodermis rather than only the latter.
On the other hand, **6/6 insertions performed with the Medtronic pump and its associated Mio Advance inserter did reach the hypodermis**. Also, **no bending at all was observed** around the spot where the cannula had been inserted (Figure 49 B).

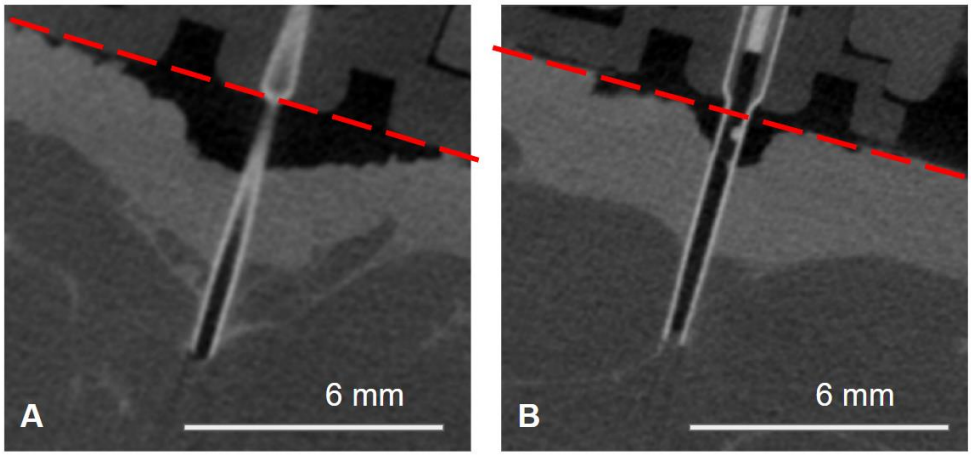

Figure 49: Illustration of a situation where the skin bent around the cannula insertion spot (A) compared to one where it did not (B). Red dotted lines show plane of skin surface around.

Air bubbles were observed in all tests.

The Medtronic insertion system requires inserting the cannula before filling it with insulin. On the other hand, the Tandem cannula is already filled with insulin when inserted. As a consequence, during a catheter change process, there is the possibility for Medtronic 780G users to trigger a small delivery of insulin to fill the cannula. This step was only performed in one of the tests performed with the Medtronic pump (Explant 1, infused at 1UI/h). This is likely to explain why, even before initiation of basal delivery, in that specific explant, some insulin (and air) had already been delivered into the tissue in this one explant (Figure 50). This is also likely to explain some differences observed in DI graphs, which are presented hereafter.

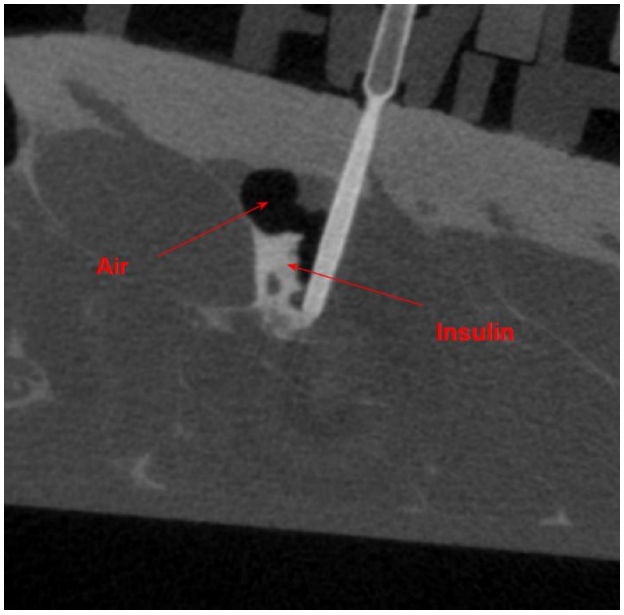

Figure 50: Explant with a Medtronic Mio Advance 90 (6mm) inserted, before the BR delivery was started. Some insulin and air are already in the tissue.

b. Dispersion index for infusions with the Tandem t:slim x2 at 0.5UI/h

The dispersion index (DI) for the three explants infused with a Tandem t:slim x2 at 0.5UI/h was of 6.32, 6.05 and 7.36 after 3h. The evolution of the DI through time for these explants resembles the general evolution at 1UI/h (Figure 51). The explant n°2 (darker green line, Figure 51) is the one intradermal infusion (Figure 48).

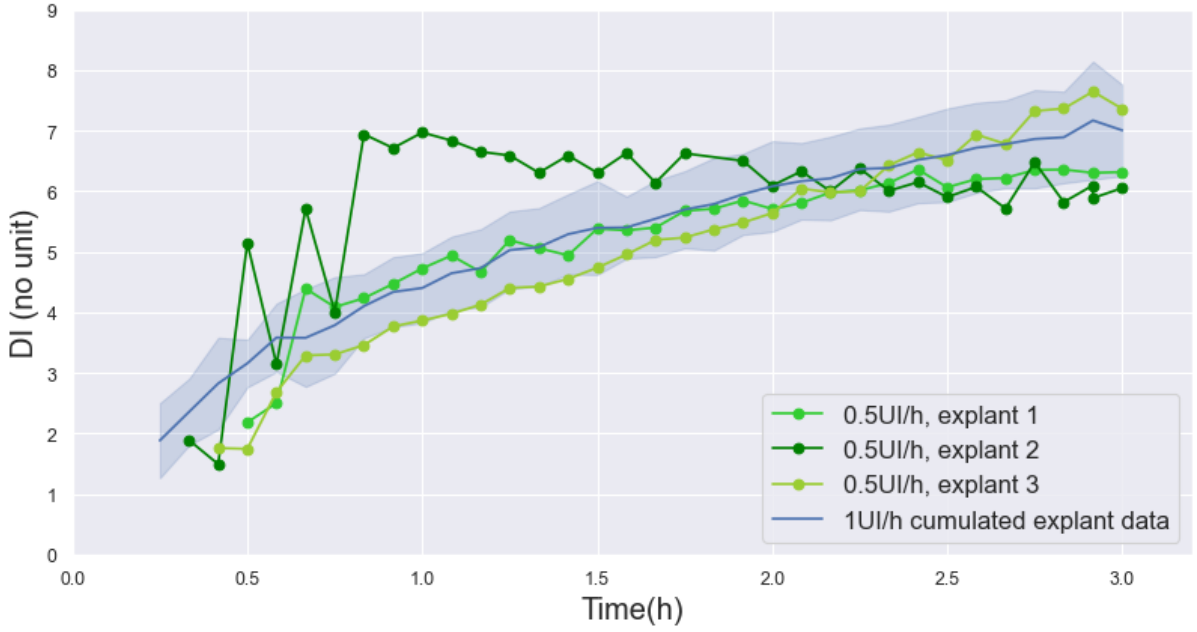

Figure 51: Dispersion index of the three explants infused with a Tandem t:slim x2 at 0.5UI/h. Mean and standard deviation of aggregated data for 1UI/h infused explants are presented in blue.

As an indicator, the volume (quantified in number of voxels) was also plotted (Figure 52).
As expected, the delivered volume was lower for 0.5UI/h than for 1UI/h infusions, while DI values are similar between 0.5 and 1UI/h. This observation strongly suggests that DI is indeed an objective evaluation of bioavailability independently from BR.

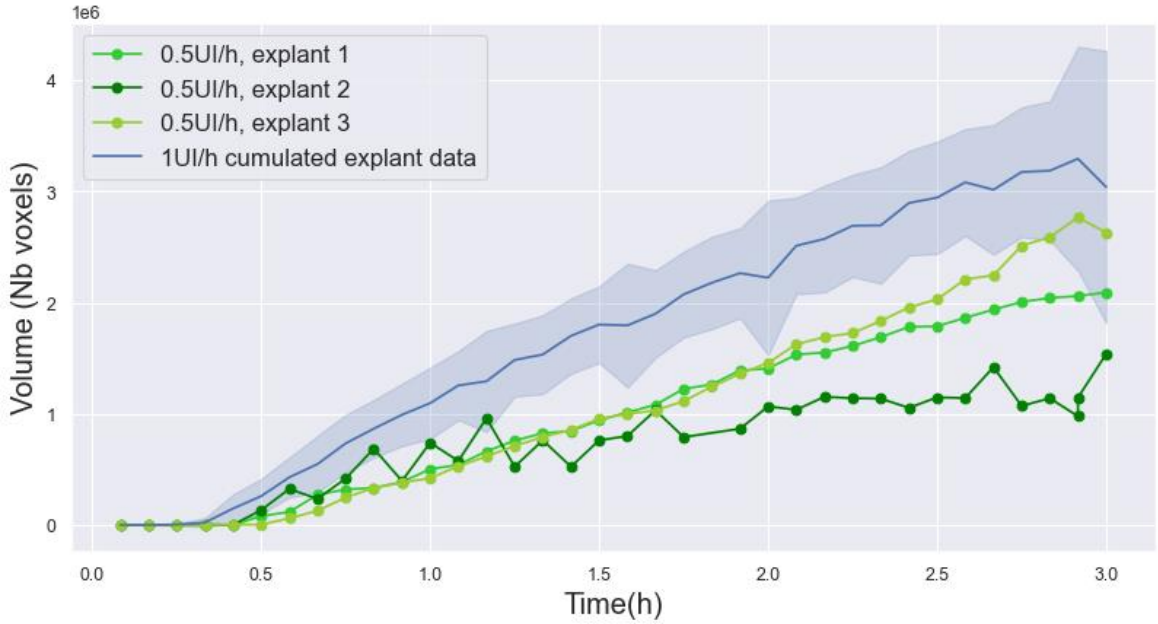

Figure 52: Volume of the zone identified as insulin for the three explants infused with a Tandem t:slim x2 at 0.5UI/h. Mean and standard deviation of aggregated data for 1UI/h infused explants are presented in blue.

c. Dispersion index for infusions with the Medtronic 780G at 1UI/h and 0.5UI/h

For the two infusions with the Medtronic at 0.5UI/h, insulin depots were only detectable from the 10th image (after 50 min), and for one of the infusions at 1UI/h, only from the 14th image (70 min). This can be seen on the DI graph (Figure 20) where the lines associated with 3 of the 4 explants only start around 1h. This is likely to be explained by the fact that no filling of the cannula post-insertion was executed.

In tests with the Medtronic pump, DI increases with time and follows a curve of similar shape to the ones of the tests performed in the article, with a Tandem pump (Figure 53). However, Medtronic infusions at 0.5UI/h have a DI value after 3h of respectively 5.48 and 5.94, and are therefore lower than the mean value observed for infusions performed with a Tandem pump both at 0.5UI/h (DI_{mean} = 6.57) and at 1UI/h (DI_{mean} = 7.02).

A notable difference can be observed between the two infusions at 1UI/h. DI values of the first explant are about 2 points higher than DI values of the other, at any time point. It is to be noticed

that the explant 1 is the one depicted in Figure 50, where some insulin was already in the tissue before delivery was started due to filling the cannula.

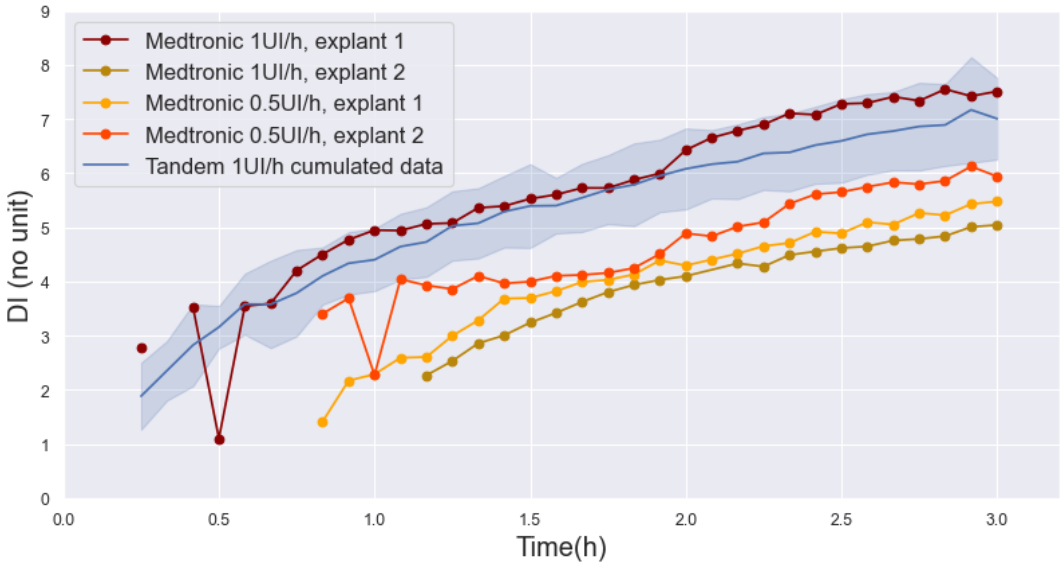

Figure 53: Dispersion index of the four explants infused with a Medtronic 780G. Mean and standard deviation of aggregated data of explants infused at 1UI/h with a Tandem t:slim x2 are presented in blue.

Comparison of volume of detected insulin depot between those infusions still show that the total amount delivered in both explants at 1UI/h is higher than the volume delivered for 0.5UI/h (Figure 54).

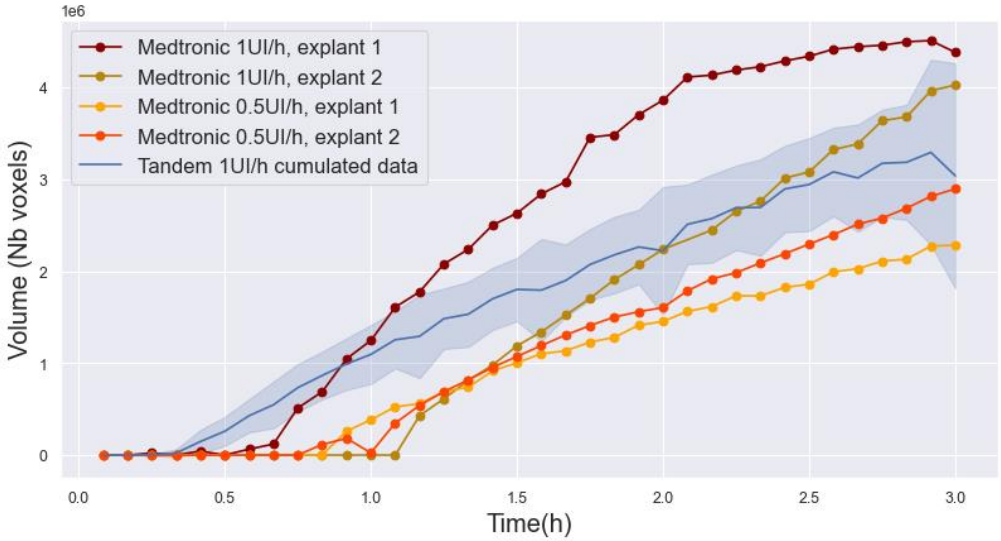

Figure 54: Volume of the zone identified as insulin for the explants infused with a Medtronic 780G. Mean and standard deviation of aggregated data for explants infused at 1UI/h with a Tandem t:slim x2 are presented in blue.

Also, one can notice that the **late detectability of the insulin depot**, which causes a belated start of the curve of the DI graphs in three out of four Medtronic infusions, i**s associated with a prolonged period of time with air in the cannula** and a **pressure profile with a slightly superior value while no insulin is detected than once some insulin is detectable in the tissue** (Figure 55, B to D). On the contrary, in the one infusion where insulin can be detected from the start, the cannula contains insulin from the beginning (Figure 55 A).

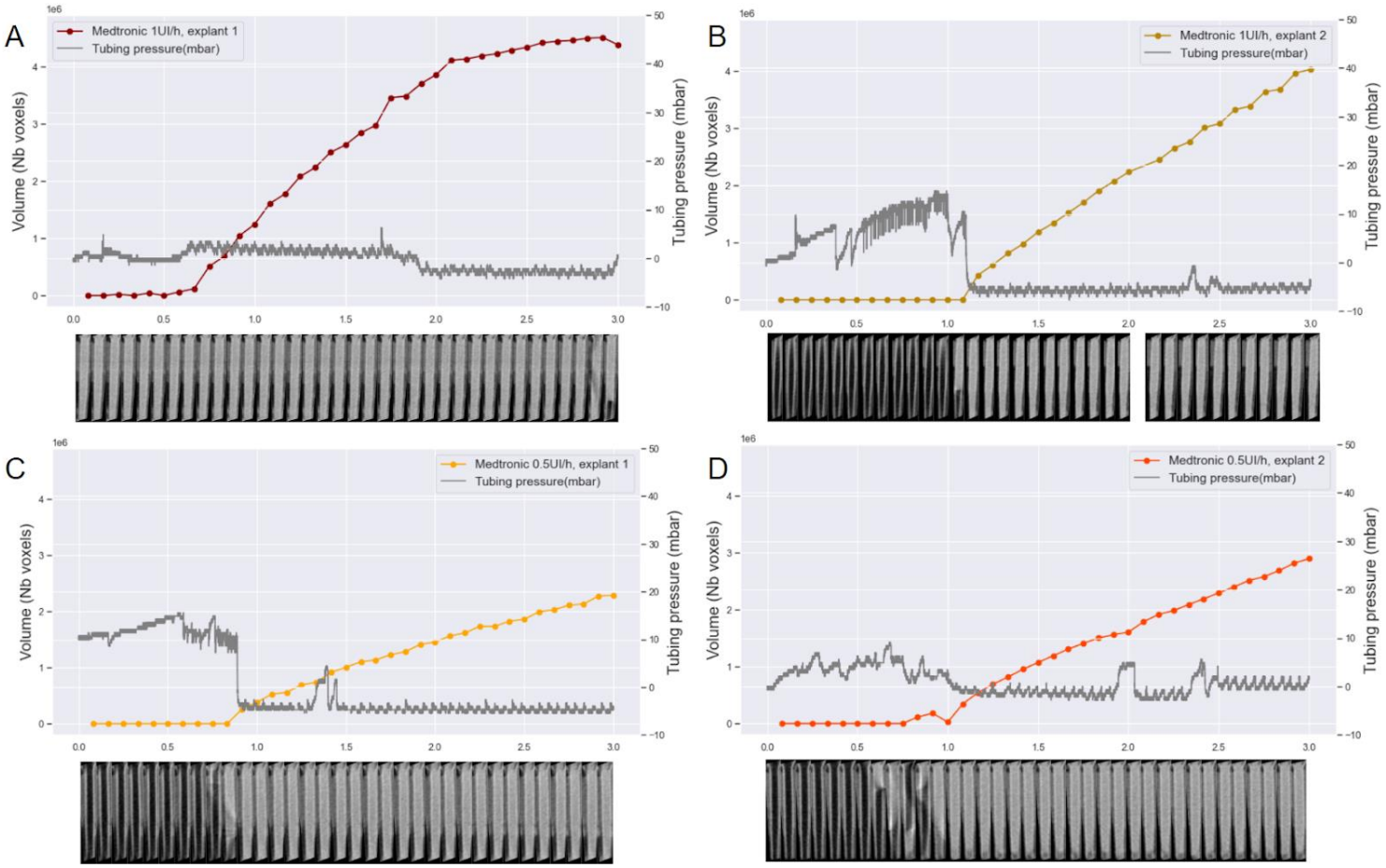

Figure 55: Volume of insulin depot, tubing pressure, and cannula content evolution through time for 4 infusions with a Medtronic 780G. A. Medtronic 780G at 1UI/h, explant 1. B. Medtronic 780G at 1UI/h, explant 2. C. Medtronic 780G at 0.5UI/h, explant 1. D. Medtronic 780G at 0.5UI/h, explant 2

Conclusions on alternative basal rate and pump infusions

Two main ideas are suggested by this series of tests:

- In Tandem t:slim x2 tests performed with 0.5UI/h, the DI evolution through time appears to be similar to the ones of 1UI/h despite the 50% reduction in BR. This suggests that the DI is not sensitive to the volume infused, which is consistent considering its mathematical construction (ultimately, a ratio of areas).

- Most Medtronic infusions have a DI value after 3h inferior to the ones of the Tandem t:slim x2. This is most likely due to a delayed infusion of the insulin due to air in the cannula in 3 out of 4 explants.

More tests should be performed to describe potential differences between these pumps and flowrates. However two structural differences between the Tandem and the Medtronic system could enlighten these first results.

First, the difference in catheter insertion system is most likely bringing differences in the observed insulin propagation upon 3 hours. For proper comparison with Tandem tests, more Medtronic tests with cannula filling should be performed.

The second difference which could introduce differences is the speed of impact of the insertion needle onto the skin. In the Tandem system, insertion speed is acquired by slight deformation and release of a flexible plastic element, and is smoother than the insertion from the Medtronic system that relies on a spring. This could lead to differences in the occurrence of a bending of the dermis during the impact, which happened a lot in infusions with the Tandem t:slim, thus participating in frequent infusions of the dermis rather than infusion at the intended depth, into the hypodermis.

General conclusion on Chapter 4

This experimental method describes insulin propagation in the tissue. It is a tool to explore the influence of various infusion parameters upon insulin propagation and thus insulin absorption, especially at initiation of delivery in a new infusion site. However such an ex-vivo method can only partially describe the clinical impact of insulin propagation in the tissue during delivery in new infusion sites.
The next part is a step further towards understanding insulin absorption in new infusion sites, based on in-vivo clinical evidence.

Chapter 5: the IMPLIQUE-KT study

The experimental work of this project has consisted in describing insulin propagation in the tissue in new infusion sites, based on the hypothesis that the mechanical spread of insulin in the tissue plays an essential role in the efficiency of absorption. This assumption relies both on results demonstrating links between the shape of the insulin depot and the speed of absorption [38], and on the observation of higher postprandial glucose excursions after catheter (KT) change compared to the third day of KT wear [33].

However, these observations come mainly from ex vivo experimentation or during meal tests. The existence of post-catheter change glycemic excursions must be confirmed in real life conditions. In addition, insulin pumps are being increasingly associated with both CGMs and control algorithms into hybrid closed-loop systems, which automate and adjust insulin delivery up to every 5 min according to a patient's need.
In that context:

- Can one observe **in real-life** the existence of glycemic excursions after KT change, like those observed in a clinical setting by Luijf et al [33], suggesting a **slower insulin absorption in the hours following KT change**?
- If this result is confirmed, **are these glucose excursions compensated under closed-loop systems**, when insulin administration is adapted every 5 min to the patient's needs?

The IMPLIQUE study (NCT04939766) is an observational longitudinal study that initially aimed at describing the impact of a closed-loop system upon the patient's quality of life and on the burden associated with the disease [109]. An **ancillary study named IMPLIQUE-KT** was designed in order to answer the questions stated above. Its aim was indeed to **compare real-life glycemic profiles after KT change, to those of 24 and 48h later, both in open-loop (OL) (with no control algorithm) and closed-loop (CL)**.

5.1 Method

a. Inclusion criteria

Inclusion criteria were the same as the main IMPLIQUE study. They included:

- Patients with T1D aged 13 to 18 years old or adults with an insulin pump for at least 6 months including at least 4 months with the Tandem t:slim x2 pump.
- Patients using a CGM system for at least 6 months including at least 4 months with a Dexcom G6 system.
- Patients for whom the use of a CL system is compliant with the Francophone Diabetes Society (SFD) recommendations [110]
- Patients consenting in having their clinical data collected in the scope of this study
- Patients with internet access.

Similarly to the main IMPLIQUE study, exclusion criteria were:

- Patients with HbA1c at inclusion above 11%.
- Patients with ongoing or planned pregnancy during the study
- Patients with altered glucose metabolism due to a treatment or a pathology.
- Patients with an evolutive diabetic retinopathy requiring laser treatment.
- Patients included in another clinical trial in diabetology in the month prior to inclusion.

b. Population

257 patients from 59 different centres were included in the main IMPLIQUE study from which this ancillary study was drawn. After inclusion visit (V0), they spent 20 days wearing a Tandem t:slim x2 insulin pump and a Dexcom G6 CGM sensor, in an OL setting. On their second visit (V1), the CL was activated. Three months later, there was a follow-up visit (V5) (Figure 56).

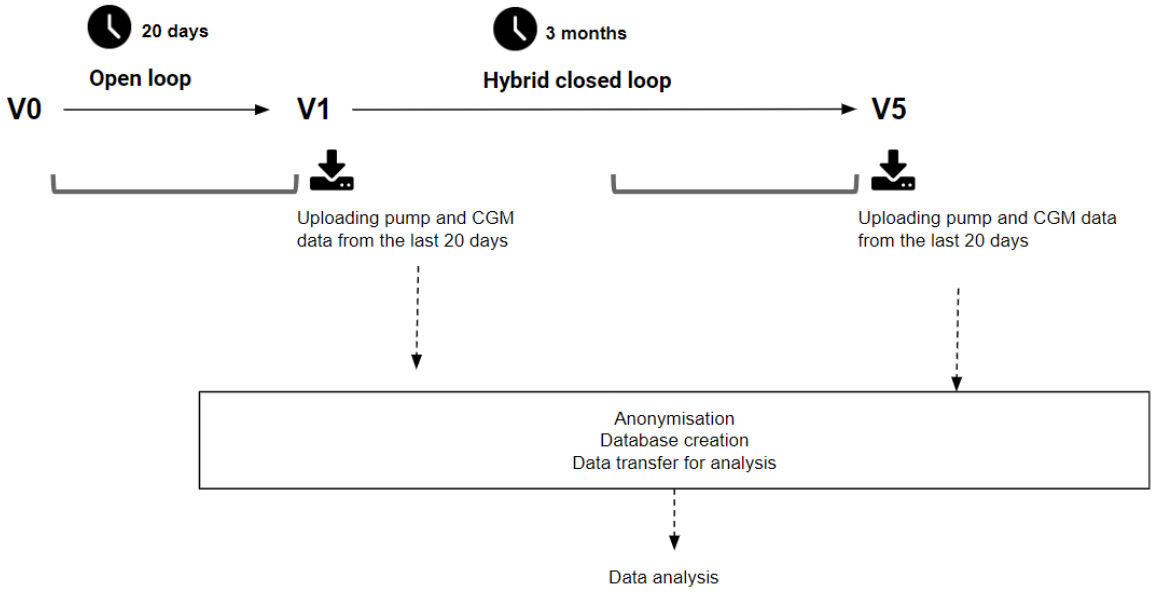

Figure 56: Graphic summary of the IMPLIQUE ancillary study protocol

The data from the pump and from the CGM were gathered either in the *MyDiabby Healthcare* app or the *Diasend* app (which had become *Glooko* by the end of the study). At V1 and V5, pump and CGM data were downloaded from the app platform and uploaded to the clinical study platform (e-CRF) by the clinician.

c. Description of the data collected via app downloads

Only the data from the *Mydiabby* app were analysed. Data from the 20 OL days and the 20 last days of the CL record were analysed. They contained:

- All pump events and their timestamps: pump interruptions, low battery alarms, low insulin alarms, occlusion alarms, and **reservoir changes.**
- All infused insulin information: **basal rates**, **bolus**, and **automatic boluses** (triggered by the control algorithm) and their timestamps.
- Glucose measurements every 5 minutes.

Recommendation is that reservoir changes are performed at the same time as KT changes. In the t:slim x2 pump, it is tricky to do one without the other. Moreover, several educational nurses confirmed to us that changing the KT at another time than the reservoir is a marginal behaviour in patients, that nurses rarely meet in their practice. Also, participants had been reminded of the importance of doing both changes at the same time and knew their data was recorded, which is an additional influence to behave in accordance with the practitioner's recommendations.
Therefore, **we will further refer to "reservoir changes" as the same event as a KT changes**.

d. Endpoints computations

For each KT change of each patient, the percentage of time spent in hyperglycemia (above 180 mg/dL) (%TA180) in the 2h that follow KT change was computed, and compared to the %TA180 at the same time of day 24h and 48h later.

Other variables were also computed, upon 2h time intervals after KT change, and the corresponding time intervals (same time of day) 24h and 48h later. They are listed, with their description, in Table 6. "Event" refers to either a KT change, or to the same time of days 24 or 48h later.

Variable abbreviation	Variable description
%TA180	Percentage of time spent at glycemia above 180 mg/dL in the 2h following the event
Cat_bolus	Bolus location category. See next section "adjustments" and Figure 2.
sum_bolus	Total bolus volume sent in the 2h before and the 2h after the event
sum_bolus_auto_2h	Total volume of automatic boluses (triggered by the algorithm) sent in the 2h after the event
last_gly_before_change	Last punctual value of glycemia before KT change
%TA180 (2/4/6h before change)	Percentage of time spent at glycemia above 180 mg/dL in the 2h before KT change
complete_change_cycle_3days	**True**: if the patient changed his/her KT at least after 3 days of wear-time. **False**: if the patient changed his/her KT before 3 days of wear-time.
SDw_2h	Standard deviation of glycemia in the 2h following the event

Mean_2h	Mean glycemia in the 2h following the event
Max_2h	Maximum of glycemia in the 2h following the event
Min_2h	Minimum of glycemia in the 2h following the event
TA180	Time spent at glycemia above 180 mg/dL in the 2h following the event
TA250	Time spent at glycemia above 250 mg/dL in the 2h following the event
TB070	Time spent at glycemia below 70 mg/dL in the 2h following the event
TA180 (2h before change)	Time spent at glycemia above 180 mg/dL in the 2h before the event
TIR_2h	Time spent in the target glycemic range in the 2h following the event
SD_day	Standard deviation of glycemia on the day of the event
Mean_day	Mean glycemia on the day of the event
Max_day	Maximum glycemia on the day of the event
Min_day	Minimum glycemia on the day of the event
TA180_day	Time spent at glycemia above 180 mg/dL on the day of the event
TA250_day	Time spent at glycemia above 250 mg/dL on the day of the event
TB70_day	Time spent at glycemia below 70 mg/dL on the day of the event
TIR_day	Time spent in the target glycemic range on the day of the event
%TA180_day	Percentage of time spent at glycemia above 180 mg/dL on the day of the event
%TA250_day	Percentage of time spent at glycemia above 250 mg/dL on the day of the event
%TB070_day	Percentage of time spent at glycemia below 70 mg/dL on the day of the event

Table 6: All extracted and computed data from patient's pump and CGM logs.

e. Pump or CGM data interruptions management

Regarding pump or CGM interruptions, any time interval of interest where the pump or the CGM data collection was interrupted for more than 10% of the time interval **was discarded and not considered for the analysis**. If the interruption occurred in the time window that immediately followed a KT change, the corresponding time intervals 24 and 48h later were also discarded and not considered in the analysis.

f. Statistical adjustments

All statistical analysis were performed by a statistician. Data was adjusted for age, sex, glycated haemoglobin (HbA1c), body mass index (BMI) and %TA180 in the 2h previous to KT change.

g. Analysis by bolus timing categories

Data was additionally analysed separately according to when a bolus is triggered relatively to the time of KT change (Figure 57):
Category A: One or several boluses were infused both in the 2h before and the 2h after KT change.
Category B: One or several boluses were infused in the 2h before the KT change only.
Category C: One or several boluses were infused in the 2h after the KT change only.
Category D: No bolus was infused in the 2h before or after KT change

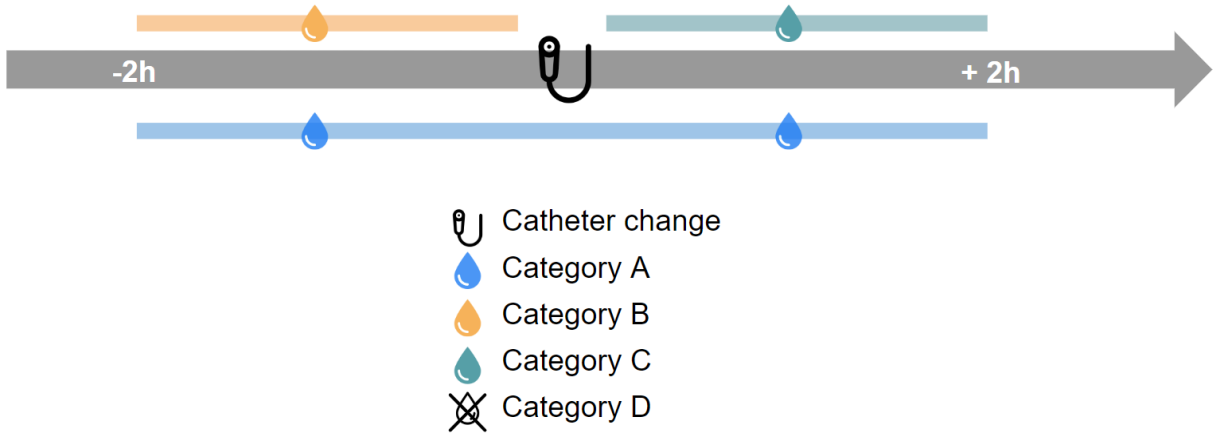

Figure 57: Graphical summary of categories for adjustment according to bolus localisation

5.2 Results

134 patients logs were properly uploaded from *MyDiabby* to the electronic case report form (e-CRF), with both the OL and the closed-loop data. In total, 5360 days were scanned, and 1636 KT changes were analysed (847 in open loop and 789 in closed loop).
Among them were 72 women, mean age was 35.6 (+/- 15.7) years old, BMI 25.2 kg/m² (+/- 4.7), HbA1c 7.48 % (+/-0.82).

343 KT changes occurred before 3 days of wear (174 in open loop and 169 in closed loop).

In OL, the mean value of %TA180 in the 2h following KT change was of 58.7%, and was significantly reduced to 44.2% 24h later ($p<0.0001$) and to 41.2% 48h later ($p<0.0001$) (Figure 58 A). Also, %TA180 in the 2h before KT change was 51.3% which was significantly lower than in the 2h after KT change ($p<0.01$).

As for OL, in hybrid CL, the mean value of %TA180 in the 2h following KT change was of 49.3% and was significantly reduced to 31.2% 24h later ($p<0.0001$) and to 33.2% 48h later ($p<0.0001$)

(Figure 58 B). %TA180 in the 2h before KT change was 33.2% which was significantly lower than in the 2h after KT change (p<0.0001).

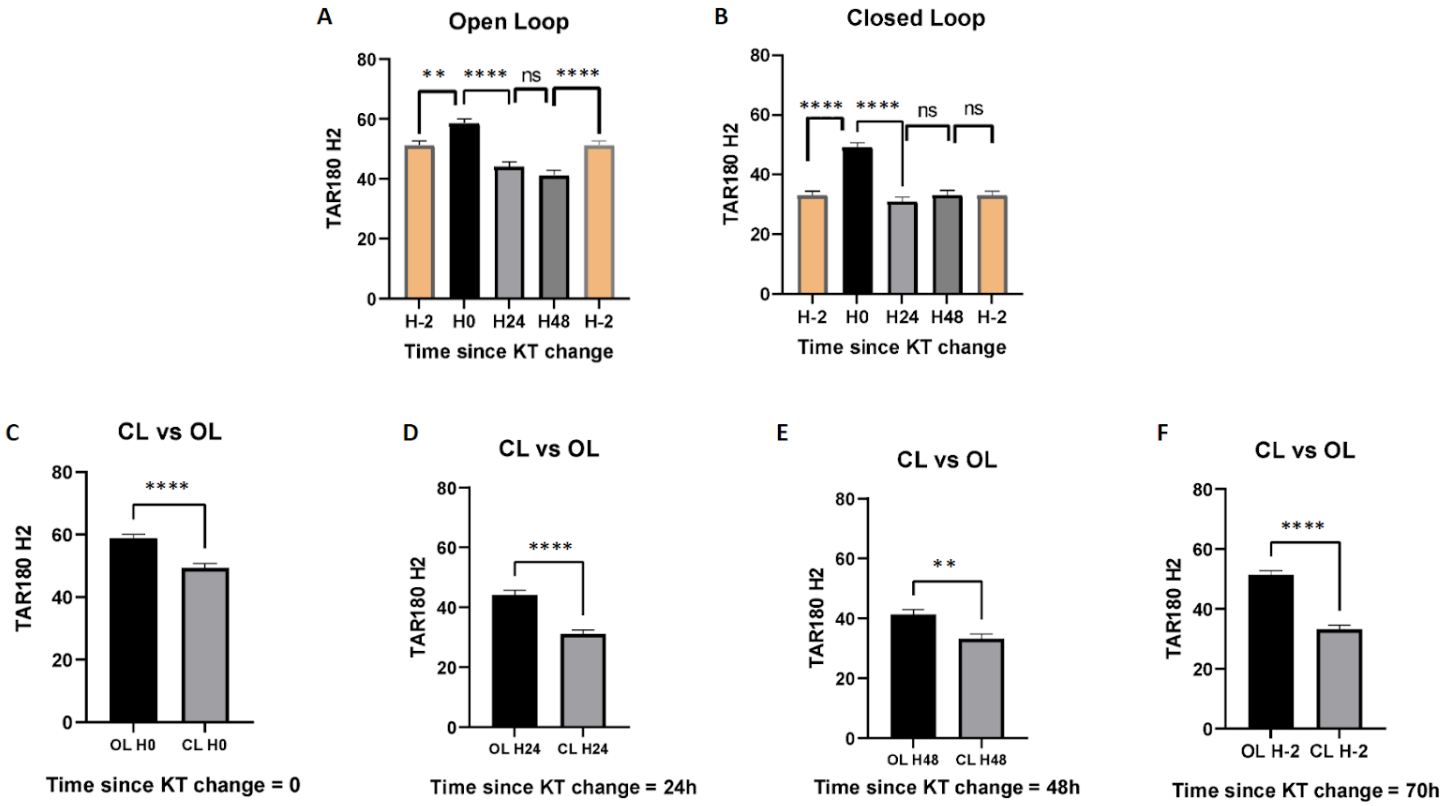

Figure 58: Boxplot of %TA180 for 2h time windows. ** = p<0.01. **** = p<0.0001.

A. In OL, % of time above 180 mg/dL in the two hours before KT change (H-2), in the two hours after KT change (H0), in the 2h-window 24h later (H24) and in the 2h-window 48h later (H48).

B. In CL, % of time above 180 mg/dL in the two hours before KT change (H-2), in the two hours after KT change (H0), in the 2h-window 24h later (H24) and in the 2h-window 48h later (H48).

C. % of time above 180 mg/dL in the two hours after KT change, in open-loop (OLH0) versus closed-loop (CLH0)

D. % of time above 180 mg/dL in the 2h-window located 24h after KT change, in open-loop (OLH24) versus closed-loop (CLH24)

E. % of time above 180 mg/dL in the 2h-window located 24h after KT change, in open-loop (OLH48) versus closed-loop (CLH48)

F. % of time above 180 mg/dL in the two hours before KT change, in open-loop (OLH-2) versus closed-loop (CLH-2)

There was a significant reduction (p<0.0001) in %TA180 in the 2h following KT change in CL compared to OL (Figure 58 C). A significant reduction was also found in CL compared to OL for the 2h time windows located 24h after a KT change (p<0.0001) (Figure 58 D), and the reduction in %TA180 was less, but still significant (p<0.01) for 2h time windows located 48h after KT

change (Figure 58 E). In the 2h prior to KT change, a significant reduction in %TA180 was also observed from OL to CL ($p<0.0001$).

	Parameter estimates	Variable	Estimate	95% CI (asymptotic)	P value
Open Loop Delta D0-D1	β0	Intercept	47,33	4,186 to 90,46	0,0316
	β1	Sex	-2,93	-10,68 to 4,820	0,4581
	β2	BMI (kg/m²)	-0,08669	-0,9347 to 0,7613	0,841
	β3	HbA1c (%)	-2,515	-7,513 to 2,483	0,3235
	β4	Age (years old)	-0,3986	-0,6612 to -0,1360	0,003
	β5	% Time Above 180 mg/dl during the 2 hours before the change	0,08736	-0,006350 to 0,1811	0,0676

Table 7: Multivariate analysis of the difference in % of time spent above 180 mg/dL between the first day of KT wear (D0) and the next day (D1), according to sex, age, BMI, HbA1c, and the % of time spent above 180 mg/dL in the 2h prior to the event, during the OL period.

	Parameter estimates	Variable	Estimate	95% CI (asymptotic)	P value
Close Loop Delta D0-D1	β0	Intercept	-4,451	-46,39 to 37,49	0,835
	β1	Sex	-1,804	-9,403 to 5,796	0,6413
	β2	BMI (kg/m²)	0,4124	-0,3851 to 1,210	0,3102
	β3	HbA1c (%)	3,443	-1,359 to 8,244	0,1596
	β4	Age (years old)	-0,4162	-0,6712 to -0,1611	0,0014
	β5	% Time Above 180 mg/dl during the 2 hours before the change	0,09099	-0,006794 to 0,1888	0,0681

Table 8: Multivariate analysis of the difference in % of time spent above 180 mg/dL between the first day of KT wear (D0) and the next day (D1), according to sex, age, BMI, HbA1c, and the % of time spent above 180 mg/dL in the 2h prior to the event, during the CL period.

Multivariate analysis shows that both in OL (Table 7) and CL (Table 8), the significant delta observed between day 0 and day 1 was affected (negatively) by age only ($p<0.05$). It was not affected by BMI or HbA1c, nor by the %TA180 in the 2h prior to KT change.

Also, the delta values between %TA180 on day 0 and day 1 were not significantly impacted by the change from OL to CL (Figure 59). Neither were the delta values between %TA180 on day 0 and day 2, or between day 1 and day 2 (Figure 59).

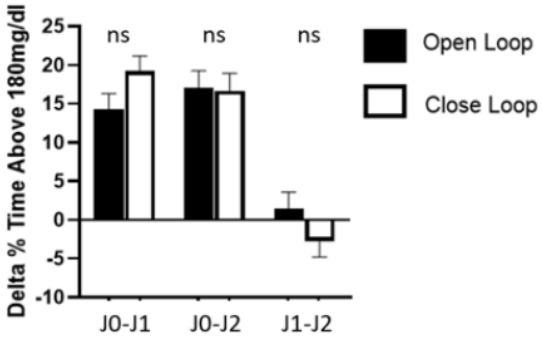

Figure 59: Delta values between %TA180 in the 2h following KT change and 24h later (J0-J1), in the 2h following KT change and 48h later (J0-J2), and between the 2h located 24h and 48h after KT change (J1-J2).

All KT changes were sorted according to the localisation of the near boluses between categories A, B, C or D (see *5.1 Method* section for category definitions). Repartition of KT changes between the categories is presented in Table 9.

	n
BF	789
A	209
B	194
C	261
D	125

	n
BO	847
A	236
B	194
C	324
D	93

	n
Total	1636
A	445
B	388
C	585
D	218

Table 9: Repartition of KT changes according to their bolus category

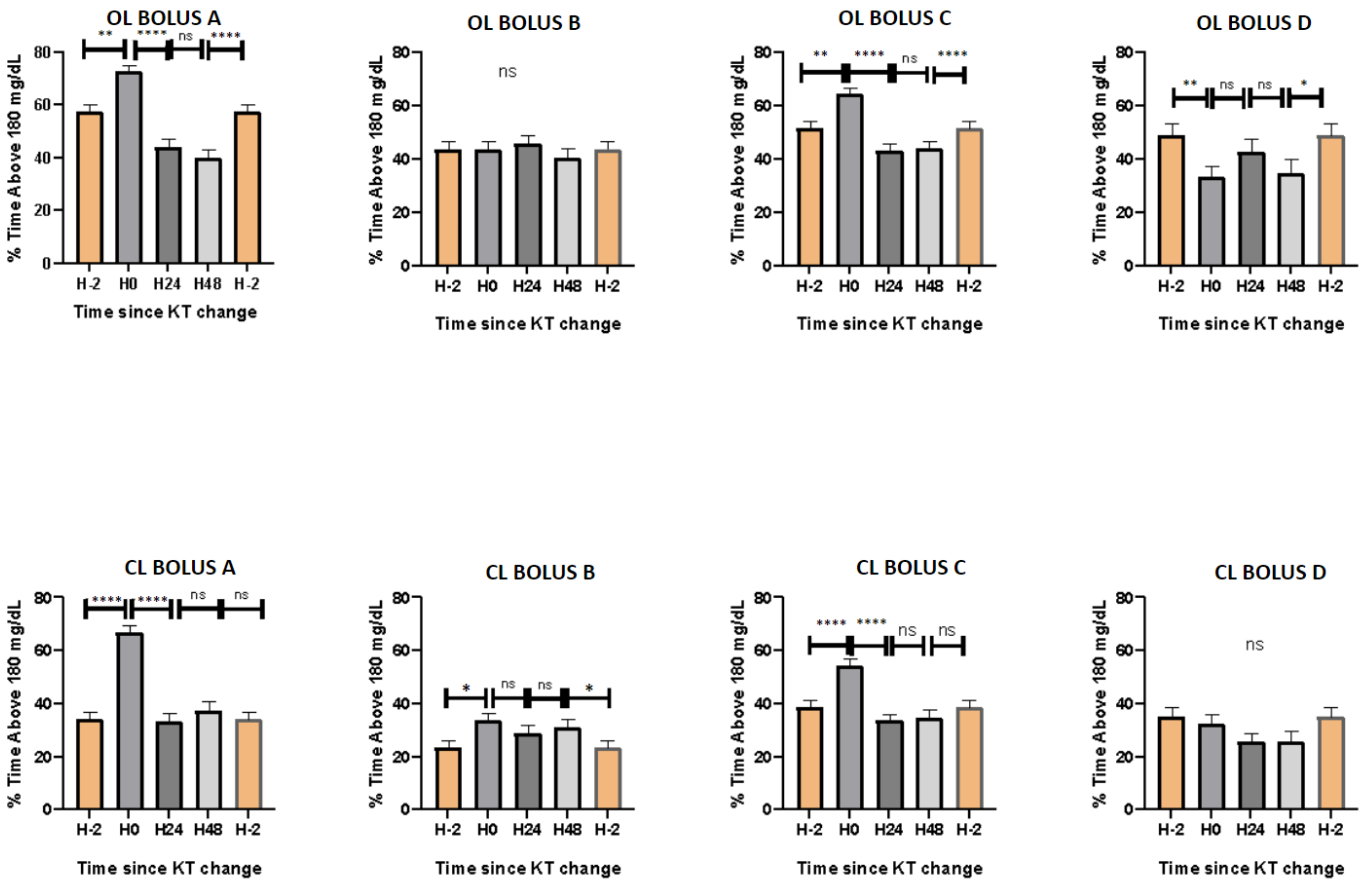

Figure 60: %TA180 in the 2h prior to KT change (H-2), 2h following KT change (H0), 24h (H24) and 48h after KT change (H48), according to bolus category, in open-loop (OL) and in closed-loop (CL).

In the situations where some bolus were infused both before and after KT change (category A), %TA180 were found significantly higher in the 2h following KT change than before KT change ($p<0.01$ in OL and $p<0.0001$ in CL) and also than 24 and 48h later ($p<0.0001$ in OL and CL) (Figure 60: %TA180 in the 2h prior to KT change (H-2), 2h following KT change (H0), 24h (H24) and 48h after KT change (H48), according to bolus category, in open-loop (OL) and in closed-loop (CL).).

Similar results were found when a bolus was infused only after KT change.

However when a bolus was infused before KT change, no difference in %TA180 could be found in all these time slots in OL, and in CL, %TA180 was found significantly higher to the 2h before KT change only ($p<0.01$).

Finally when no bolus at all were infused either before or after KT change, the tendency in OL was found different than in the previous situations, for indeed, the %TA180 in the 2h prior to KT change was higher than immediately after KT change ($p<0.001$). No significant observations could be made when no bolus was infused in CL.

5.3 Discussion

In this work, real life glycemic data was collected in 134 patients with T1D under OL and CL system, and the glycemic state following KT changes was studied compared to other moments in the course of the insulinotherapy. Results depict significant glycemic excursions in the 2h that follow KT change compared to 24h and 48h later, both in OL and in CL. This result is independent from glycemic status in the 2h before KT change, as shown by the $p>0.05$ associated with %TA180 in the 2h prior to KT change (β_5 parameter, Table 2 and 3).

To our knowledge, these are the first results which observe glycemic excursions after KT change in real life conditions. The 2013 study from Luijf et al [33] observed this effect in a very strict clinical setting with a test meal. Moreover, these results bring new critical information compared to 2013: these frequent glycemic excursions after KT change are mostly maintained under a CL system.

When patients bolused only before the KT change, rather than only after, they do not seem to have experienced a glycemic excursion. On the other hand, those who perform boluses after catheter change do experience such excursions. This suggests that the moment of the bolus may have an incidence on the excursions. However in order to confirm a causal relationship between these observations, a crossover randomised study would be required to see whether timing bolusing before a KT change could indeed prevent (or limit) such excursions.

CL systems can drastically increase the time spent in the glycemic range (TIR) of patients, but despite this effective technology, TIR appears to reach a structural limit at 70%. On the other hand, KT changes are frequent (every 3 days), and were here demonstrated to be critical moments in the insulinotherapy, including when using a CL system. In that context, identifying this moment of weakness in the efficiency of the therapy is highly relevant, for indeed, reducing this post-KT change effect could constitute a leverage in order to reach another level of TIR in patients with T1D.

A clear strength of this study is the high number of patients (134), and additionally, the high number of KT changes which could be observed per patient (12.3 changes in average per patient). It is also the first study to observe KT change effect on glycemia both in OL and in CL.

However one can acknowledge a few limitations to this study. It would have been highly interesting to also have access to which infusion site the patient was using (thigh, abdomen, arm or buttocks) for each KT change, and to study the potential impact of those locations on the glycemic excursions observed. Collecting data on whether or not the infusion site bore a lipodystrophy before and/or after infusion site use would also have been interesting.

Further crossover randomised study is needed to answer how bolusing behaviour affects glycemic excursions after KT changes, from which very simple recommendations could be built to patients in order to improve their glycemic control in the hours after KT change. If such a study is conclusive, patient education could then indeed include anticipation of the post-KT change glycemic excursion by timing the KT change after a meal bolus.

Chapter 6: Discussion

This multidisciplinary project aimed at studying insulin subcutaneous propagation and absorption in the specific case of an insulin pump basal rate delivery, as a potential cause for glycemic variability. It mainly interrogates insulin propagation in the tissue during the first hours in infusion, when a "naive" infusion site is being infused, first from an ex-vivo point of view, then using a clinical approach.

6.1 Summary of the results of the ex-vivo study

A first ex-vivo part consisted in building a method to study the mechanical propagation of insulin in human subcutaneous tissue. This method is the first method to combine 3D imaging of the insulin depot and pressure measurements, in a time-dependent analysis. It is the first, to our knowledge, to be precise enough to observe basal rate delivered-insulin, while being performed upon human tissue.

This method was the occasion to introduce a reproducible metric, the dispersion index (DI), to describe insulin propagation. DI is interpretable for itself. A DI value of 7 means that the contact area of the insulin depot is 7 times higher than it would be in the least favourable situation to absorption. In that sense, might be understood as an indirect indicator of the bioavailability of the infused insulin, among other tools.

During the first implementation of this method, a single set of infusion conditions were used: one unique pump was used, and it was set to a unique basal rate to deliver through one model of KT. We observed that the actually infused tissue (whether hypodermis, dermis, or dermis-hypodermis junction) strongly impacts the evolution of DI with time. Also, for a quite important amount of these infusions (9/24, which were performed with a Tandem t:slim x2 pump and Autosoft 90 catheters, the cannula ended up inserted in an untargeted tissue (dermis or dermis-hypodermis junction). We hypothesised that this was partly due to our setting, for it is tricky to operate an insertion on an isolated explant that has no superficial skin tension, without having the skin surface bend during the insertion process. However, it is possible that such ectopic catheter insertion could also happen in real life clinical situations.

This method was then employed upon a limited number of explants with other infusion conditions, introducing a new pump (the Medtronic 780G) and a new basal rate (0.5UI/h).
These results tended to confirm that DI is independent from the volume delivered, which is consistent with its mathematical construction. The use of a different pump does seem to slightly affect DI, although due to the very limited number of experiments, it is not possible to determine whether this is due to the infusion rate profiles, which differs between the two pumps, or to the

insertion process of the cannula, as both pumps use different inserters with very different characteristics.

Yet, it may be noted that no skin bending was observed in the tests performed with the Medtronic Mio advance inserter. As a consequence, cannulas were inserted inside the hypodermis in all experiments. Based on our previous result concluding on different DI behaviours according to which tissue structure is infused, this would at least tend to confirm the suspicion of a critical role of the inserter, although more tests would be required to draw such a conclusion.

Finally in all test conditions, infusion of air bubbles which constitute an under delivery of insulin, were associated with pressure build-ups or elevation of tubing pressure.

6.2 Perspectives on the ex-vivo study

These results highlight the need for further application of this method to conclude on various comparisons on infusion parameters. More tests with various pumps could be performed, including at various basal rates. Indeed, although DI is independent from the volume delivered, pumps do not all have the same strategies to modulate their flowrate. Some modulate the frequency of their impulsions, others the volume of impulsion [9,94], and this is likely to affect the characteristics of the spread of insulin in the tissue.

But also, as previously mentioned in this work, many more infusion parameters are likely to affect insulin propagation. Insertion system, cannula length, material, shape or angle of insertion, are relevant parameters to study. Parameters which do not depend on the technology, but rather on the patient, could also be explored. Studying infusions in explants sampled from various body locations would contribute to answer an often repeated interrogation of the literature on the impact of these body locations [24,34]. In such a perspective, studying insulin propagation in a sample bearing lipodystrophies would be also highly relevant, although access to such tissue is rare, which is why such an experiment would be difficult to plan. As lipodystrophies modify the mechanical characteristics of the tissue, one could hypothesise that DI behaviour with time would then be significantly affected. Finally the impact of other variables could be explored, such as insulin type, demographic characteristics of the patient (sex, phototype, age), BMI, skin temperature during delivery…

In the scope of this work, only deliveries at fixed BR were studied. However in the context of the generalisation of CL systems, BR will less and less be stable, but rather change up to every 5 min according to the patients' needs. One could therefore relevantly study how insulin propagation is affected by brutal changes in basal rates throughout the delivery.
Similarly, studying how insulin propagates in BR delivery after a bolus was released would be relevant data to increase knowledge on both OL and CL delivery modes.

Also, delivering a BR of insulin for several days in a given explant, then imaging the propagation of a CA and insulin mixture in the explant would be a way of studying some of the effects of wear time of an infusion site. One must stress that in an ex-vivo context, this would only be an opportunity to observe whether mechanical propagation is eased in a tissue infused for a long time compared to the initiation of infusion. It would not, however, allow to see the impact of inflammation of the tissue like it would be in an in-vivo experimentation [95].

Finally, the observed increases in tubing pressure suggest that **detection of events regarding insulin delivery, such as air infusion**, would be possible if some **finer pressure sensors were integrated to the pumps**. Indeed, although we observed increases in tubing pressure when air bubbles were infused, no occlusion alarm was ever triggered during any of our experiments.

6.3 Summary and perspectives of the clinical study

The IMPLIQUE-KT protocol aimed at confirming the existence of post-KT change hyperglycemia in real-life and evaluating the effect of a CL system upon this phenomenon.

Results do describe significant hyperglycemic events after KT changes, which persist under CL. This is the confirmation of a variability of insulin absorption associated with KT wear-time that had been observed in a clinical setting by Luijf et. al [33].

Also, a significant association between this increase of time above range and bolus timing was found. Bolusing before KT change was found to be associated with a disappearance of this phenomenon. Yet, a causal relationship between bolusing before the KT change, and the reduction of the time above range must be confirmed during a dedicated study.

One could imagine that bolusing before KT change allows one to benefit from the insulin from the previous infusion site while the new infusion site is being initiated. We indeed know from the first experimental work on human explants that during the first hours in that new infusion site, DI of the insulin depot progressively increases. As a consequence, a given amount of insulin delivered benefits from a reduced contact area with the tissue compared to a few hours later, thus limiting initial absorption speed.

One could also have formed the hypothesis that delivering a bolus immediately after the KT change could participate in mechanically initiating the infusion site, opening channels in the subcutaneous tissue for the insulin to spread into. This would then allow the insulin newly delivered into this site, at a basal delivery rate, to be absorbed more rapidly, and therefore closer to how it would be in a site that had already been used for a few hours. Our results do not appear to support this hypothesis. However, our study does not allow methodologically to state on this matter. Indeed, in the IMPLIQUE setting, the post-KT change boluses are delivered at the initiative of the patient,

because they see a need for it. This constitutes a bias compared to a setting where bolus would systematically be delivered after catheter change. However, Luijf et. al [33] observe higher glycemic excursions on day 1 than on day 3 of KT in a context where the bolus is delivered after KT change, which does not support this hypothesis.

To definitely state on this matter, and on a positive effect of a pre-KT change bolus, a randomised crossover study would be relevant. It would indeed allow to see if a bolusing behaviour that includes anticipation of KTC could improve time-in-range (whether in OL or CL), and if so, which behaviour exactly.

Such study could be built in such a way: patients' pump and CGM data would be collected the same way as in IMPLIQUE. However, for each new KT change, they would be given an instruction on whether to time a bolus immediately before, or immediately after, they carry out the change, independently from their current glycemia.
In order not to expose patients to a risk of hypoglycemia, the instruction would be to associate these KT changes (whether effected before or after a bolus) with mealtimes and therefore, with **meal bolus which would have to be infused anyway** to compensate for a meal.

One could imagine including prevention of hyperglycemia after KT change into CL algorithms, based on the announcement of the imminent KT change event. However our results show that this hyperglycemia phenomenon, although existent and significant, is not systematic. Therefore, it could also be dangerous to include an extra delivery of insulin associated with KT changes in a CL algorithm. In that context, if one was to fully demonstrate the causality between such a bolusing behaviour and avoiding the post-KT change hyperglycemic events, then this behaviour could easily be included in patients' education. Besides, this would constitute a frugal solution to post-KT change hyperglycemia instead of heavy technological development.

These results also speak in favour of the ongoing development of KT of extended wear-time. All major infusion set manufacturers are indeed currently developing such KT with 7-days wear-time [59,111,112], and to date, one of those has reached the market (Medtronic Extended). Indeed, long-wearing time KT would reduce the frequency at which patients are exposed to this KT-change hyperglycemia. However several studies alert on the decline of infusion set efficiency after 3 days [22,76,79]. Some of the long KT wear time issues identified in the literature could potentially be improved on: skin reactions (itching, bruising, swelling and/or pain) [113] could potentially be resolved by changes in the materials used. However, an increase in daily blood glucose was observed with wear-time as well [76], which appears to be harder to resolve. In that context, resolving the post-KT change effect by a specific bolusing behaviour could be a privileged strategy compared to a reduction of KT frequency of use.

General conclusion

This work is **an appraisal for the inclusion of a mechanical approach** to better understand the differences in insulin subcutaneous absorption. Its intent was to provide **new data, tools and reflexions to nurture research on insulin subcutaneous diffusion**. It resulted in the **technological proposition of a time-dependent follow up of insulin basal delivery**, on **its proof of concept**, and led to the **introduction of a new interpretable metric to characterise insulin subcutaneous propagation**. The IMPLIQUE-KT study is the demonstration that improvement of our understanding of subcutaneous propagation in the hours that follow KT change **is still relevant in the context of the new technological therapeutic approach that are CL systems**.

Annex

Annex 1 – Supplemental data S1 to the submitted article

S1. Patients data

Samples provided by Bio-EC laboratories

All samples were collected on patients who underwent post-bariatric surgery.

	Age	Gender	Phototype (Fitzpatrick scale)	Sampling site
Donor 1	**55**	**F**	**III**	**abdomen**
Donor 2	**57**	**F**	**II**	**abdomen**
Donor 3	**43**	**F**	**V**	**abdomen**
Donor 4	**51**	**F**	**II**	**abdomen**

Annex 2 – Supplemental data S2 to the submitted article

S2. Viscosity of insulin Aspart Novorapid U100 and Iopamiro 200 contrast agent mixture

A 15% mass of Iopamiro 200mg/mL was mixed with insulin Aspart Novorapid U100 and loaded into a t:slim ™ cartridge. This concentration results from the comparison between the µCT detectability of a low volume depot for a 10% mass concentration of CA, in accordance with another example in the literature (Mader et al, 2013) and a 15% mass concentration of CA. The increase in viscosity was measured using a Brookfield DV2T viscometer, and found negligible (2% - see further viscosity measurements in figure S1, supplemental data) against the improvement in depot detectability.

Concentration CA (% of mass)	Viscosity (cP)	% increase of viscosity compared to pure Insulin Aspart U100
0	1.41	0
5	1.42	0.71
10*	1.47	4.26
15**	**1.50**	**6.38**
17.5	1.53	8.51
20	1.57	11.35
22.5	1.58	12.06
25	1.59	12.77

* value of CA concentration available in Mader et al, 2013
** value of CA concentration used in this study

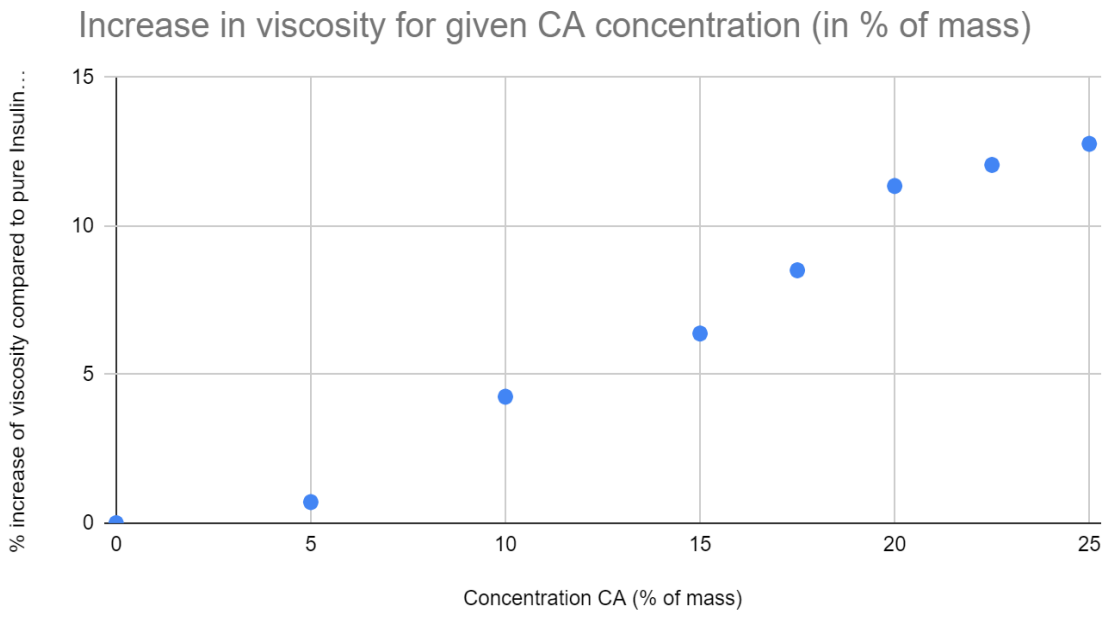

Annex 3 - Picrosirius red staining protocol on frozen slides

- Take frozen slides out of -80°C freezer and leave 1h in 0.1% Picrosirius red staining solution
- Rinse picrosirius red with deionised water
- Leave for twice 30” in deionised water and acetic acid (5‰)
- Rinse in deionised water and remove the excess of water
- Immediately transfer into 3 successive 100% ethanol baths of 1min for dehydration
- Mount with hydrophobic mounting agent

References

1. Nakhleh A, Shehadeh N. Hypoglycemia in diabetes: An update on pathophysiology, treatment, and prevention. World J Diabetes 2021;12(12):2036–2049; doi: 10.4239/wjd.v12.i12.2036.

2. Julla J-B, Jacquemier P, Fagherazzi G, et al. Is the Consensual Threshold for Defining High Glucose Variability Implementable in Clinical Practice? Diabetes Care 2021;44(7):1722–1725; doi: 10.2337/dc20-1847.

3. Riveline J-P, Wojtusciszyn A, Guerci B, et al. Real world hypoglycaemia related to glucose variability and Flash glucose scan frequency assessed from global FreeStyle Libre data. Diabetes Obes Metab 2022; doi: 10.1111/dom.14795.

4. Kovatchev B. Glycemic Variability: Risk Factors, Assessment, and Control. J Diabetes Sci Technol 2019;13(4):627–635; doi: 10.1177/1932296819826111.

5. Anonymous. The Effect of Intensive Treatment of Diabetes on the Development and Progression of Long-Term Complications in Insulin-Dependent Diabetes Mellitus. N Engl J Med 1993;329(14):977–986; doi: 10.1056/NEJM199309303291401.

6. Anonymous. Intensive blood-glucose control with sulphonylureas or insulin compared with conventional treatment and risk of complications in patients with type 2 diabetes (UKPDS 33). UK Prospective Diabetes Study (UKPDS) Group. Lancet Lond Engl 1998;352(9131):837–853.

7. Anonymous. The Effect Produced on Diabetes by Extracts of Pancreas | The Discovery and Early Development of Insulin. n.d. Available from: https://insulin.library.utoronto.ca/islandora/object/insulin%3AT10010 [Last accessed: 2/8/2023].

8. Hartman I. Insulin Analogs: Impact on Treatment Success, Satisfaction, Quality of Life, and Adherence. Clin Med Res 2008;6(2):54–67; doi: 10.3121/cmr.2008.793.

9. Girardot S, Jacquemier P, Mousin F, et al. All Insulin Pumps Are Not Equivalent: A Bench Test Assessment for Several Basal Rates. Diabetes Technol Ther 2020; doi: 10.1089/dia.2019.0486.

10. Foster NC, Beck RW, Miller KM, et al. State of Type 1 Diabetes Management and Outcomes from the T1D Exchange in 2016-2018. Diabetes Technol Ther 2019;21(2):66–72; doi: 10.1089/dia.2018.0384.

11. Benkhadra K, Alahdab F, Tamhane SU, et al. Continuous subcutaneous insulin infusion versus multiple daily injections in individuals with type 1 diabetes: a systematic review and meta-analysis. Endocrine 2017;55(1):77–84; doi: 10.1007/s12020-016-1039-x.

12. Misso ML, Egberts KJ, Page M, et al. Continuous subcutaneous insulin infusion (CSII) versus multiple insulin injections for type 1 diabetes mellitus. Cochrane Database Syst Rev 2010;(1):CD005103; doi: 10.1002/14651858.CD005103.pub2.

13. Rys PM, Ludwig-Slomczynska AH, Cyganek K, et al. Continuous subcutaneous insulin infusion vs multiple daily injections in pregnant women with type 1 diabetes mellitus: a systematic review and meta-analysis of randomised controlled trials and observational studies. Eur J Endocrinol 2018;178(5):545–563; doi: 10.1530/EJE-17-0804.

14. Pańkowska E, Błazik M, Dziechciarz P, et al. Continuous subcutaneous insulin infusion vs. multiple daily injections in children with type 1 diabetes: a systematic review and meta-analysis of randomized control trials. Pediatr Diabetes 2009;10(1):52–58; doi: 10.1111/j.1399-5448.2008.00440.x.

15. Jeitler K, Horvath K, Berghold A, et al. Continuous subcutaneous insulin infusion versus multiple daily insulin injections in patients with diabetes mellitus: systematic review and meta-analysis. Diabetologia 2008;51(6):941–951; doi: 10.1007/s00125-008-0974-3.

16. van Duinkerken E, Snoek FJ, de Wit M. The cognitive and psychological effects of living with type 1 diabetes: a narrative review. Diabet Med 2020;37(4):555–563; doi: 10.1111/dme.14216.

17. Hirsch IB, Gaudiani LM. A new look at brittle diabetes. J Diabetes Complications 2021;35(1):107646; doi: 10.1016/j.jdiacomp.2020.107646.

18. Toni G, Berioli MG, Cerquiglini L, et al. Eating Disorders and Disordered Eating Symptoms in Adolescents with Type 1 Diabetes. Nutrients 2017;9(8):906; doi: 10.3390/nu9080906.

19. Franklin V. Influences on Technology Use and Efficacy in Type 1 Diabetes. J Diabetes Sci Technol 2016;10(3):647–655; doi: 10.1177/1932296816639315.

20. Klonoff DC, Reyes JS. Insulin Pump Safety Meeting: Summary Report. J Diabetes Sci Technol 2009;3(2):396–402.

21. Deiss D, Adolfsson P, Alkemade-van Zomeren M, et al. Insulin Infusion Set Use: European Perspectives and Recommendations. Diabetes Technol Ther 2016;18(9):517–524; doi: 10.1089/dia.2016.07281.sf.

22. Pfützner A, Sachsenheimer D, Grenningloh M, et al. Using Insulin Infusion Sets in CSII for Longer Than the Recommended Usage Time Leads to a High Risk for Adverse Events. J Diabetes Sci Technol 2015;9(6):1292–1298; doi: 10.1177/1932296815604438.

23. Heinemann L. Insulin Absorption from Lipodystrophic Areas: A (Neglected) Source of Trouble for Insulin Therapy? J Diabetes Sci Technol 2010;4(3):750–753.

24. Heinemann L, Krinelke L. Insulin infusion set: the Achilles heel of continuous subcutaneous insulin infusion. J Diabetes Sci Technol 2012;6(4):954–964; doi: 10.1177/193229681200600429.

25. Kim H, Park H, Lee SJ. Effective method for drug injection into subcutaneous tissue. Sci Rep 2017;7(1):9613; doi: 10.1038/s41598-017-10110-w.

26. Jockel JPL, Roebrock P, Shergold OA. Insulin depot formation in subcutaneoue tissue. J Diabetes Sci Technol 2013;7(1):227–237; doi: 10.1177/193229681300700128.

27. Thomsen M, Hernandez-Garcia A, Mathiesen J, et al. Model Study of the Pressure Build-Up during Subcutaneous Injection. PLOS ONE 2014;9(8):e104054; doi: 10.1371/journal.pone.0104054.

28. Thomsen M, Poulsen M, Bech M, et al. Visualization of subcutaneous insulin injections by x-ray computed tomography. Phys Med Biol 2012;57(21):7191–7203; doi: 10.1088/0031-9155/57/21/7191.

29. Thomsen M, Rasmussen CH, Refsgaard HHF, et al. Spatial distribution of soluble insulin in pig subcutaneous tissue: Effect of needle length, injection speed and injected volume. Eur J Pharm Sci Off J Eur Fed Pharm Sci 2015;79:96–101; doi: 10.1016/j.ejps.2015.08.012.

30. Eisler G, Kastner JR, Torjman MC, et al. In vivo investigation of the tissue response to commercial Teflon insulin infusion sets in large swine for 14 days: the effect of angle of insertion on tissue histology and insulin spread within the subcutaneous tissue. BMJ Open Diabetes Res Care 2019;7(1); doi: 10.1136/bmjdrc-2019-000881.

31. Hauzenberger JR, Hipszer BR, Loeum C, et al. Detailed Analysis of Insulin Absorption Variability and the Tissue Response to Continuous Subcutaneous Insulin Infusion Catheter Implantation in Swine. Diabetes Technol Ther 2017;19(11):641–650; doi: 10.1089/dia.2017.0175.

32. Hauzenberger JR, Münzker J, Kotzbeck P, et al. Systematic in vivo evaluation of the time-dependent inflammatory response to steel and Teflon insulin infusion catheters. Sci Rep 2018;8(1):1132; doi: 10.1038/s41598-017-18790-0.

33. Luijf YM, Arnolds S, Avogaro A, et al. Patch Pump Versus Conventional Pump: Postprandial Glycemic Excursions and the Influence of Wear Time. Diabetes Technol Ther 2013;15(7):575–579; doi: 10.1089/dia.2013.0016.

34. Heinemann L. Variability of insulin absorption and insulin action. Diabetes Technol Ther 2002;4(5):673–682; doi: 10.1089/152091502320798312.

35. Knoll MM, Vazifedan T, Gyuricsko E. Air occlusion in insulin pumps of children and adolescents with type 1 diabetes. J Pediatr Endocrinol Metab 2020;33(2):179–184; doi: 10.1515/jpem-2019-0358.

36. James DE, Jenkins AB, Kraegen EW, et al. Insulin precipitation in artificial infusion devices. Diabetologia 1981;21(6):554–557; doi: 10.1007/BF00281548.

37. Wolpert HA, Faradji RN, Bonner-Weir S, et al. Metabolic decompensation in pump users due to lispro insulin precipitation. BMJ 2002;324(7348):1253.

38. Mader JK, Birngruber T, Korsatko S, et al. Enhanced absorption of insulin aspart as the result of a dispersed injection strategy tested in a randomized trial in type 1 diabetic patients. Diabetes Care 2013;36(4):780–785; doi: 10.2337/dc12-1319.

39. Tran HV. Caractérisation des propriétés mécaniques de la peau humaine in vivo via l'IRM. n.d.;174.

40. Reilly DM, Lozano J. Skin collagen through the lifestages: importance for skin health and beauty. Plast Aesthetic Res 2021;8:2; doi: 10.20517/2347-9264.2020.153.

41. Kim JY, Dao H. Physiology, Integument. In: StatPearls StatPearls Publishing: Treasure Island (FL); 2022.

42. Estève D, Boulet N, Belles C, et al. Lobular architecture of human adipose tissue defines the niche and fate of progenitor cells. Nat Commun 2019;10; doi: 10.1038/s41467-019-09992-3.

43. Comley K. A micromechanical model for the Young's modulus of adipose tissue. Int J Solids Struct 2010;9.

44. Zhang Y, Yu J, Kahkoska AR, et al. Advances in transdermal insulin delivery. Adv Drug Deliv Rev 2019;139:51–70; doi: 10.1016/j.addr.2018.12.006.

45. Ryan TJ. The blood vessels of the skin. J Invest Dermatol 1976;67(1):110–118.

46. Kølendorf K, Bojsen J, Nielsen SL. Adipose tissue blood flow and insulin disappearance from subcutaneous tissue. Clin Pharmacol Ther 1979;25(5part1):598–604; doi: 10.1002/cpt1979255part1598.

47. Braverman IM. Ultrastructure and organization of the cutaneous microvasculature in normal and pathologic states. J Invest Dermatol 1989;93(2 Suppl):2S-9S; doi: 10.1111/1523-1747.ep12580893.

48. Nucci G, Cobelli C. Models of subcutaneous insulin kinetics. A critical review. Comput Methods Programs Biomed 2000;62(3):249–257.

49. Lauritzen T, Pramming S, Deckert T, et al. Pharmacokinetics of continuous subcutaneous insulin infusion. Diabetologia 1983;24(5):326–329.

50. Young RJ, Hannan WJ, Frier BM, et al. Diabetic Lipohypertrophy Delays Insulin Absorption. Diabetes Care 1984;7(5):479–480; doi: 10.2337/diacare.7.5.479.

51. Vora JP, Burch A, Peters JR, et al. Absorption of radiolabelled soluble insulin in type 1 (insulin-dependent) diabetes: influence of subcutaneous blood flow and anthropometry. Diabet Med J Br Diabet Assoc 1993;10(8):736–743.

52. Patte C, Pleus S, Wiegel C, et al. Effect of infusion rate and indwelling time on tissue resistance pressure in small-volume subcutaneous infusion like in continuous subcutaneous insulin infusion. Diabetes Technol Ther 2013;15(4):289–294; doi: 10.1089/dia.2012.0319.

53. Regittnig W, Tschaikner M, Tuca A, et al. Insulin induces a progressive increase in the resistance of subcutaneous tissue to fluid flow: Implications for insulin pump therapy. Diabetes Obes Metab 2022;24(3):455–464; doi: 10.1111/dom.14594.

54. Kildegaard J, Christensen TF, Hejlesen OK. Sources of Glycemic Variability—What Type of Technology is Needed? J Diabetes Sci Technol Online 2009;3(4):986–991.

55. DeFronzo RA, Tobin JD, Andres R. Glucose clamp technique: a method for quantifying insulin secretion and resistance. Am J Physiol 1979;237(3):E214-223; doi: 10.1152/ajpendo.1979.237.3.E214.

56. Rini CJ, McVey E, Sutter D, et al. Intradermal insulin infusion achieves faster insulin action than subcutaneous infusion for 3-day wear. Drug Deliv Transl Res 2015;5(4):332–345; doi: 10.1007/s13346-015-0239-x.

57. Raz I, Weiss R, Yegorchikov Y, et al. Effect of a local heating device on insulin and glucose pharmacokinetic profiles in an open-label, randomized, two-period, one-way crossover study in patients with type 1 diabetes using continuous subcutaneous insulin infusion. Clin Ther 2009;31(5):980–987; doi: 10.1016/j.clinthera.2009.05.010.

58. Cengiz E, Weinzimer SA, Sherr JL, et al. Acceleration of insulin pharmacodynamic profile by a novel insulin infusion site warming device. Pediatr Diabetes 2013;14(3):168–173; doi: 10.1111/pedi.12001.

59. Simic A, Schøndorff PK, Stumpe T, et al. Survival assessment of the extended-wear insulin infusion set featuring lantern technology in adults with type 1 diabetes by the glucose clamp technique. Diabetes Obes Metab 2021;23(6):1402–1408; doi: 10.1111/dom.14337.

60. Mudaliar SR, Lindberg FA, Joyce M, et al. Insulin aspart (B28 asp-insulin): a fast-acting analog of human insulin: absorption kinetics and action profile compared with regular human insulin in healthy nondiabetic subjects. Diabetes Care 1999;22(9):1501–1506; doi: 10.2337/diacare.22.9.1501.

61. Sandby-Møller J, Poulsen T, Wulf HC. Epidermal thickness at different body sites: relationship to age, gender, pigmentation, blood content, skin type and smoking habits. Acta Derm Venereol 2003;83(6):410–413; doi: 10.1080/00015550310015419.

62. Shuster S, Bottoms E. SENILE DEGENERATION OF SKIN COLLAGEN. Clin Sci 1963;25:487–491.

63. Anonymous. Vogel, H.G. (1987) Age Dependence of Mechanical and Biochemical Properties of Human Skin. Part I Stress-Strain Experiments, Skin Thickness and Biochemical Analysis. Bioengineering and the Skin, 3, 67-91. - References - Scientific Research Publishing. n.d. Available from: https://www.scirp.org/(S(351jmbntvnsjt1aadkposzje))/reference/ReferencesPapers.aspx?ReferenceID=2134931 [Last accessed: 2/20/2023].

64. Mencel J, Jaskólska A, Marusiak J, et al. Effect of gender, muscle type and skinfold thickness on myometric parameters in young people. PeerJ 2021;9:e12367; doi: 10.7717/peerj.12367.

65. Shuster S, Black MM, McVitie E. The influence of age and sex on skin thickness, skin collagen and density. Br J Dermatol 1975;93(6):639–643; doi: 10.1111/j.1365-2133.1975.tb05113.x.

66. Wesley NO, Maibach HI. Racial (ethnic) differences in skin properties: the objective data. Am J Clin Dermatol 2003;4(12):843–860; doi: 10.2165/00128071-200304120-00004.

67. Yazdanparast T, Hassanzadeh H, Nasrollahi SA, et al. Cigarettes Smoking and Skin: A Comparison Study of the Biophysical Properties of Skin in Smokers and Non-Smokers. Tanaffos 2019;18(2):163–168.

68. Morita A. Tobacco smoke causes premature skin aging. J Dermatol Sci 2007;48(3):169–175; doi: 10.1016/j.jdermsci.2007.06.015.

69. Klemp P, Staberg B, Madsbad S, et al. Smoking reduces insulin absorption from subcutaneous tissue. Br Med J Clin Res Ed 1982;284(6311):237; doi: 10.1136/bmj.284.6311.237.

70. Sugihara T, Ohura T, Homma K, et al. The extensibility in human skin: variation according to age and site. Br J Plast Surg 1991;44(6):418–422; doi: 10.1016/0007-1226(91)90199-t.

71. Galloway JA, Spradlin CT, Nelson RL, et al. Factors influencing the absorption, serum insulin concentration, and blood glucose responses after injections of regular insulin and various insulin mixtures. Diabetes Care 1981;4(3):366–376; doi: 10.2337/diacare.4.3.366.

72. Bantle JP, Neal L, Frankamp LM. Effects of the anatomical region used for insulin injections on glycemia in type I diabetes subjects. Diabetes Care 1993;16(12):1592–1597; doi: 10.2337/diacare.16.12.1592.

73. Henriksen JE, Djurhuus MS, Vaag A, et al. Impact of injection sites for soluble insulin on glycaemic control in type 1 (insulin-dependent) diabetic patients treated with a multiple insulin injection regimen. Diabetologia 1993;36(8):752–758; doi: 10.1007/BF00401147.

74. Owens DR, Coates PA, Luzio SD, et al. Pharmacokinetics of 125I-labeled insulin glargine (HOE 901) in healthy men: comparison with NPH insulin and the influence of different subcutaneous injection sites. Diabetes Care 2000;23(6):813–819; doi: 10.2337/diacare.23.6.813.

75. Kwa T, Zhang G, Shepard K, et al. The improved survival rate and cost-effectiveness of a 7-day continuous subcutaneous insulin infusion set. J Med Econ 2021;24(1):837–845; doi: 10.1080/13696998.2021.1945784.

76. Schmid V, Hohberg C, Borchert M, et al. Pilot study for assessment of optimal frequency for changing catheters in insulin pump therapy-trouble starts on day 3. J Diabetes Sci Technol 2010;4(4):976–982; doi: 10.1177/193229681000400429.

77. Swan KL, Dziura JD, Steil GM, et al. Effect of Age of Infusion Site and Type of Rapid-Acting Analog on Pharmacodynamic Parameters of Insulin Boluses in Youth With Type 1 Diabetes Receiving Insulin Pump Therapy. Diabetes Care 2009;32(2):240–244; doi: 10.2337/dc08-0595.

78. Karlin AW, Ly TT, Pyle L, et al. Duration of Infusion Set Survival in Lipohypertrophy Versus Nonlipohypertrophied Tissue in Patients with Type 1 Diabetes. Diabetes Technol Ther 2016;18(7):429–435; doi: 10.1089/dia.2015.0432.

79. Sampson Perrin AJ, Guzzetta RC, Miller KM, et al. A web-based study of the relationship of duration of insulin pump infusion set use and fasting blood glucose level in adults with type 1 diabetes. Diabetes Technol Ther 2015;17(5):307–310; doi: 10.1089/dia.2014.0336.

80. Hildebrandt P, Birch K. Basal rate subcutaneous insulin infusion: absorption kinetics and relation to local blood flow. Diabet Med J Br Diabet Assoc 1988;5(5):434–440.

81. Jp V, A B, Jr P, et al. Relationship between absorption of radiolabeled soluble insulin, subcutaneous blood flow, and anthropometry. Diabetes Care 1992;15(11); doi: 10.2337/diacare.15.11.1484.

82. Wu Y, Nieuwenhoff MD, Huygen FJPM, et al. Characterizing human skin blood flow regulation in response to different local skin temperature perturbations. Microvasc Res 2017;111:96–102; doi: 10.1016/j.mvr.2016.12.007.

83. Nieuwenhoff MD, Wu Y, Huygen FJPM, et al. Reproducibility of axon reflex-related vasodilation assessed by dynamic thermal imaging in healthy subjects. Microvasc Res 2016;106:1–7; doi: 10.1016/j.mvr.2016.03.001.

84. Wong BJ, Hollowed CG. Current concepts of active vasodilation in human skin. Temp Multidiscip Biomed J 2016;4(1):41–59; doi: 10.1080/23328940.2016.1200203.

85. Gradel AKJ, Porsgaard T, Lykkesfeldt J, et al. Factors Affecting the Absorption of Subcutaneously Administered Insulin: Effect on Variability. Research article. 2018.; doi: 10.1155/2018/1205121.

86. Heimhalt-El Hamriti M, Schreiver C, Noerenberg A, et al. Impaired skin microcirculation in paediatric patients with type 1 diabetes mellitus. Cardiovasc Diabetol 2013;12(1):115; doi: 10.1186/1475-2840-12-115.

87. Dillon RS. Improved serum insulin profiles in diabetic individuals who massaged their insulin injection sites. Diabetes Care 1983;6(4):399–401; doi: 10.2337/diacare.6.4.399.

88. Hauner H, Stockamp B, Haastert B. Prevalence of lipohypertrophy in insulin-treated diabetic patients and predisposing factors. Exp Clin Endocrinol Diabetes Off J Ger Soc Endocrinol Ger Diabetes Assoc 1996;104(2):106–110; doi: 10.1055/s-0029-1211431.

89. Richardson T, Kerr D. Skin-Related Complications of Insulin Therapy. Am J Clin Dermatol 2003;4(10):661–667; doi: 10.2165/00128071-200304100-00001.

90. Thethi TK, Rao A, Kawji H, et al. Consequences of delayed pump infusion line change in patients with type 1 diabetes mellitus treated with continuous subcutaneous insulin infusion. J Diabetes Complications 2010;24(2):73–78; doi: 10.1016/j.jdiacomp.2009.03.002.

91. Ta C, V E. Poor glycaemic control caused by insulin induced lipohypertrophy. BMJ 2003;327(7411); doi: 10.1136/bmj.327.7411.383.

92. Johansson U-B, Amsberg S, Hannerz L, et al. Impaired absorption of insulin aspart from lipohypertrophic injection sites. Diabetes Care 2005;28(8):2025–2027; doi: 10.2337/diacare.28.8.2025.

93. Girardot S, Mousin F, Vezinet J, et al. Kalman filter-based novel methodology to assess insulin pump accuracy. Diabetes Technol Ther 2019; doi: 10.1089/dia.2019.0147.

94. Girardot S. In Vitro and in Silico Approach of Continuous Subcutaneous Insulin Infusion System Reliability. These de doctorat. Sorbonne université; 2020.

95. Kalus A, Shinohara M, Wang R, et al. The DERMIS Study: Evaluation of Insulin Pump Infusion Sites in Type 1 Diabete. 2023; doi: 10.2139/ssrn.4345818.

96. Anonymous. Regulation (EC) No 1223/2009 of the European Parliament and of the Council of 30 November 2009 on Cosmetic Products (Recast) (Text with EEA Relevance). 2009.

97. Yoon T-J, Lei TC, Yamaguchi Y, et al. Reconstituted 3-dimensional human skin of various ethnic origins as an in vitro model for studies of pigmentation. Anal Biochem 2003;318(2):260–269; doi: 10.1016/s0003-2697(03)00172-6.

98. Chadebech P, Goidin D, Jacquet C, et al. Use of human reconstructed epidermis to analyze the regulation of beta-defensin hBD-1, hBD-2, and hBD-3 expression in response to LPS. Cell Biol Toxicol 2003;19(5):313–324; doi: 10.1023/b:cbto.0000004975.36521.c8.

99. Pourchet LJ, Thepot A, Albouy M, et al. Human Skin 3D Bioprinting Using Scaffold-Free Approach. Adv Healthc Mater 2017;6(4); doi: 10.1002/adhm.201601101.

100. Peno-Mazzarino Laurent, Percoco Giuseppe, Almeida Scalvino Stéphanie, et al. Chapitre 10, Modèles Pour l'évaluation Des Produits Cosmétiques. In: Modèle d'explants de Peau Humaine n.d.; pp. 159–185.

101. Ward WH, Lambreton F, Goel N, et al. TABLE 1, Fitzpatrick Classification of Skin Types I through VI. Text. Codon Publications; 2017. Available from: https://www.ncbi.nlm.nih.gov/books/NBK481857/table/chapter6.t1/ [Last accessed: 3/7/2023].

102. Marcelin G, Clément K. La fibrose du tissu adipeux: Un facteur aggravant de l'obésité. médecine/sciences 2018;34(5):424–431; doi: 10.1051/medsci/20183405015.

103. Comley K, Fleck N. Deep penetration and liquid injection into adipose tissue. J Mech Mater Struct 2011;6(1):127–140; doi: 10.2140/jomms.2011.6.127.

104. Anonymous. Insulin monoclonal antibody Insulin Antibody. n.d. Available from: http://www.sigmaaldrich.com/ [Last accessed: 3/13/2023].

105. R L, R Y, D L, et al. Picrosirius red staining: a useful tool to appraise collagen networks in normal and pathological tissues. J Histochem Cytochem Off J Histochem Soc 2014;62(10); doi: 10.1369/0022155414545787.

106. Lim STJ, Hui YCA, Lim PK, et al. Ultrasound-guided measurement of skin and subcutaneous tissue thickness in children with diabetes and recommendations for giving insulin injections. J Clin Transl Endocrinol 2018;12:26–35; doi: 10.1016/j.jcte.2018.04.004.

107. Anonymous. Scanner in vivo : SKYSCAN 1176. n.d. Available from: https://www.imosar.cnrs.fr/equipements-de-la-plateforme-imosar/skyscan-1176/ [Last accessed: 4/15/2023].

108. Anonymous. Region Growing (2D/3D Grayscale) - File Exchange - MATLAB Central. n.d. Available from: https://fr.mathworks.com/matlabcentral/fileexchange/32532-region-growing-2d-3d-grayscale [Last accessed: 3/16/2023].

109. VitalAire. Impact of the Use of a Closed-Loop Insulin Therapy on the Burden of the Diabetes and the Quality of Life in Type 1 Diabetic Patients With Continuous Glucose Monitoring (CGM). Clinical trial registration. clinicaltrials.gov; 2021.

110. Franc S, Schaepelynck P, Tubiana-Rufi N, et al. Mise en place de l'insulinothérapie automatisée en boucle fermée : position d'experts français. Médecine Mal Métaboliques 2020;14(5, Supplement):S1–S40; doi: 10.1016/S1957-2557(20)30003-1.

111. Kastner JR, Venkatesh N, Brown K, et al. Feasibility study of a prototype extended-wear insulin infusion set in adults with type 1 diabetes. Diabetes Obes Metab 2022;24(6):1143–1149; doi: 10.1111/dom.14685.

112. Brazg R, Garg SK, Bhargava A, et al. Evaluation of Extended Infusion Set Performance in Adults with Type 1 Diabetes: Infusion Set Survival Rate and Glycemic Outcomes from a Pivotal Trial. Diabetes Technol Ther 2022;24(8):535–543; doi: 10.1089/dia.2021.0540.

113. Diedisheim M, Pecquet C, Julla J-B, et al. Prevalence and Description of the Skin Reactions Associated with Adhesives in Diabetes Technology Devices in an Adult Population: Results of the CUTADIAB Study. Diabetes Technol Ther 2023;25(4):279–286; doi: 10.1089/dia.2022.0513.